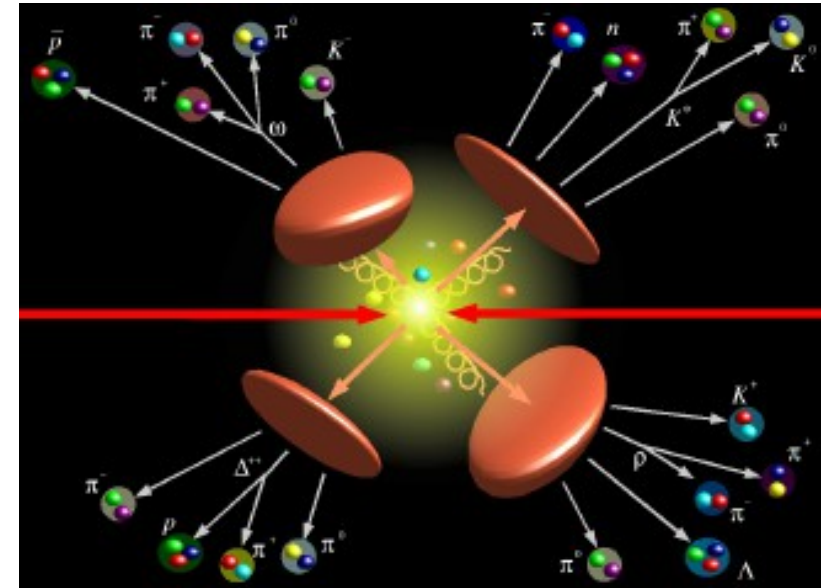
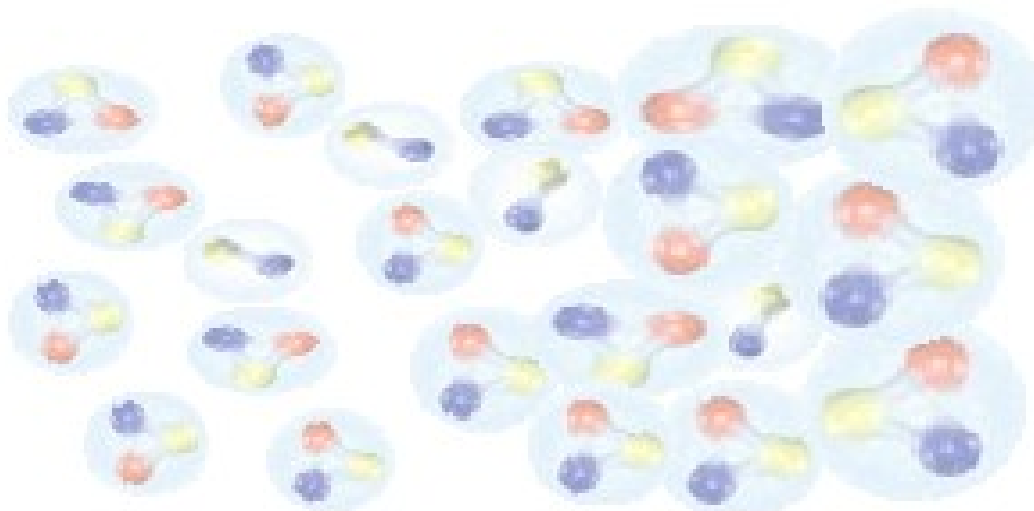


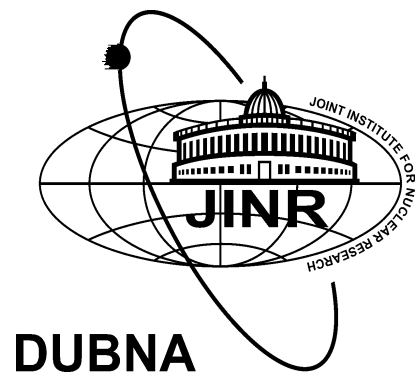
Boiling dense QCD – Theory and event simulation for collisions at NICA and FAIR energies

David Blaschke

University of Wroclaw, Poland & JINR Dubna & MEPhI Moscow, Russia



Association of Young Scientists and Specialists, JINR Dubna, 15.03.2016



Helmholtz International Center

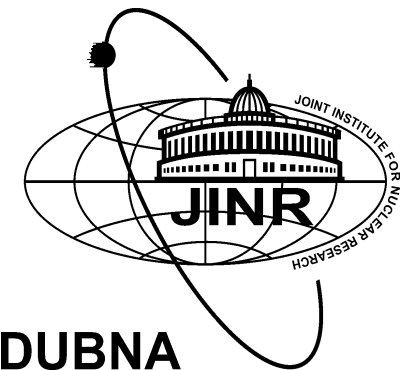
Boiling dense QCD – Theory and event simulation for collisions at NICA and FAIR energies

David Blaschke

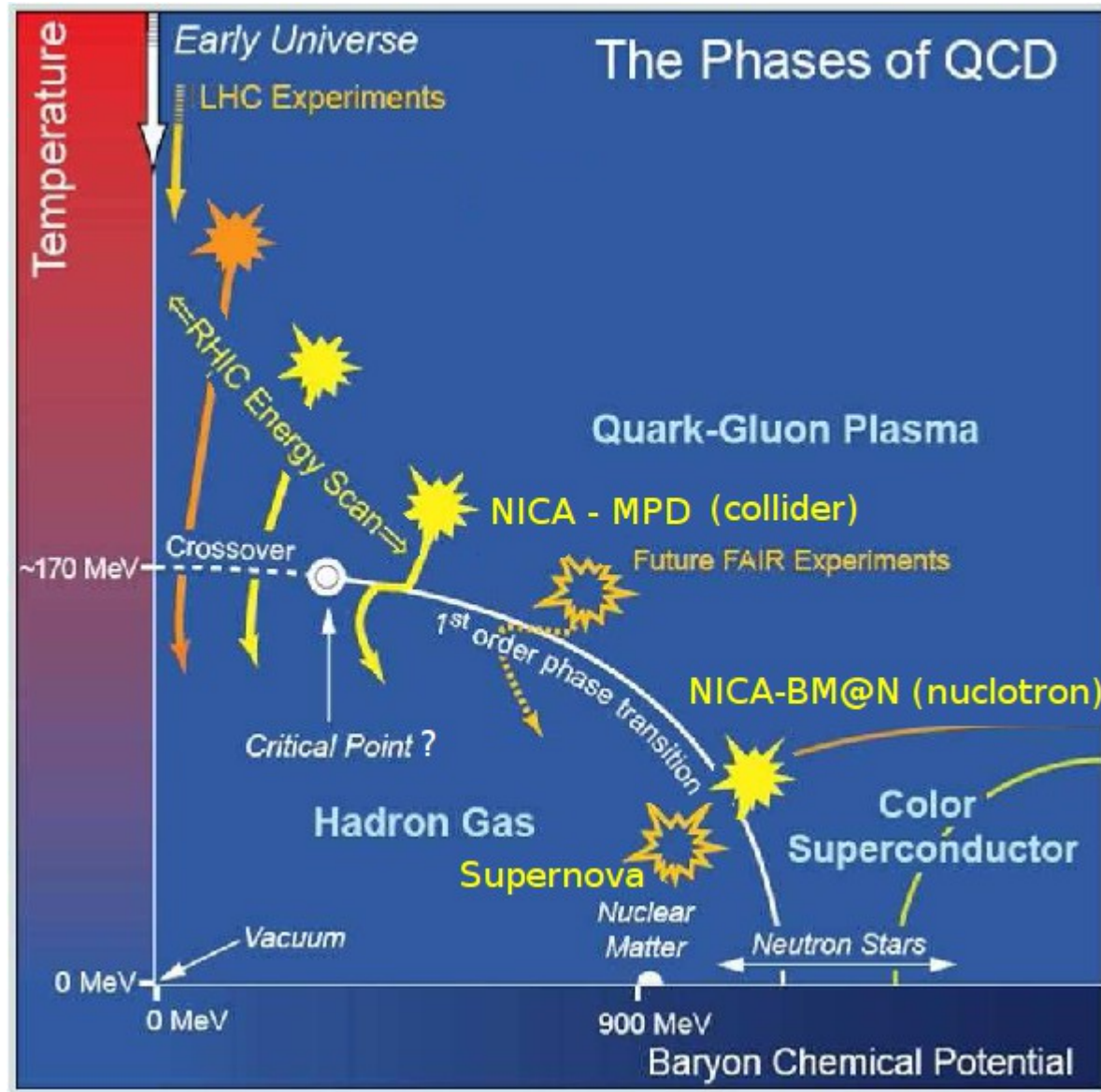
University of Wroclaw, Poland & JINR Dubna & MEPhI Moscow, Russia

- 1. Introduction: Theory of Selfconsistent Quark-Hadron EoS**
- 2. THESCoN: Event Simulation for NICA & FAIR**
A project with FIAS, MEPhI and JINR
- 3. First results: Baryon stopping signal for a 1st order PT**
Particilization and all that ...
- 4. Further developments:**
Flow, Detector response, new class of EoS ...

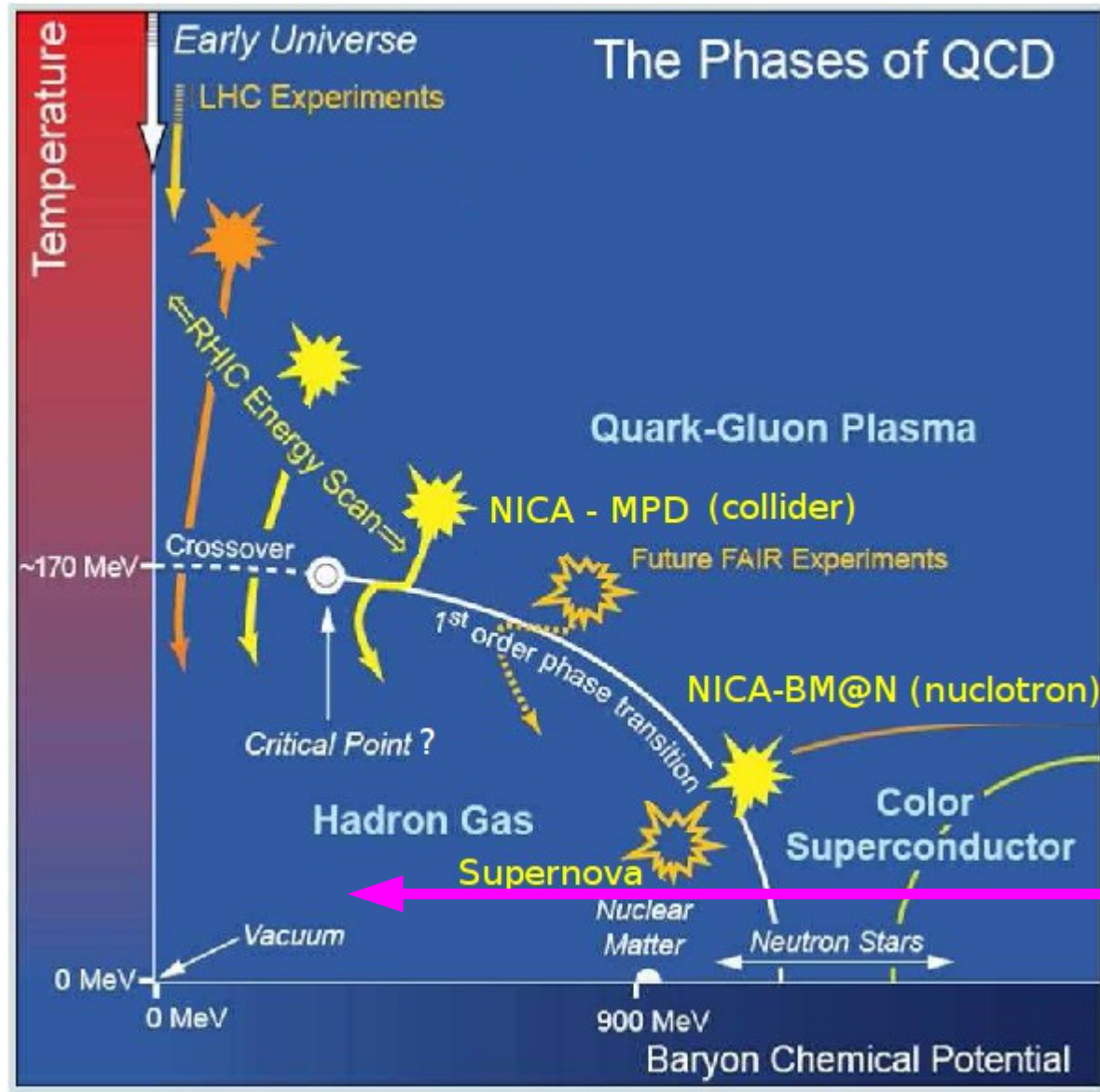
Association of Young Scientists and Specialists, JINR Dubna, 15.03.2016



The Goal: Theory of the QCD Phase Diagram



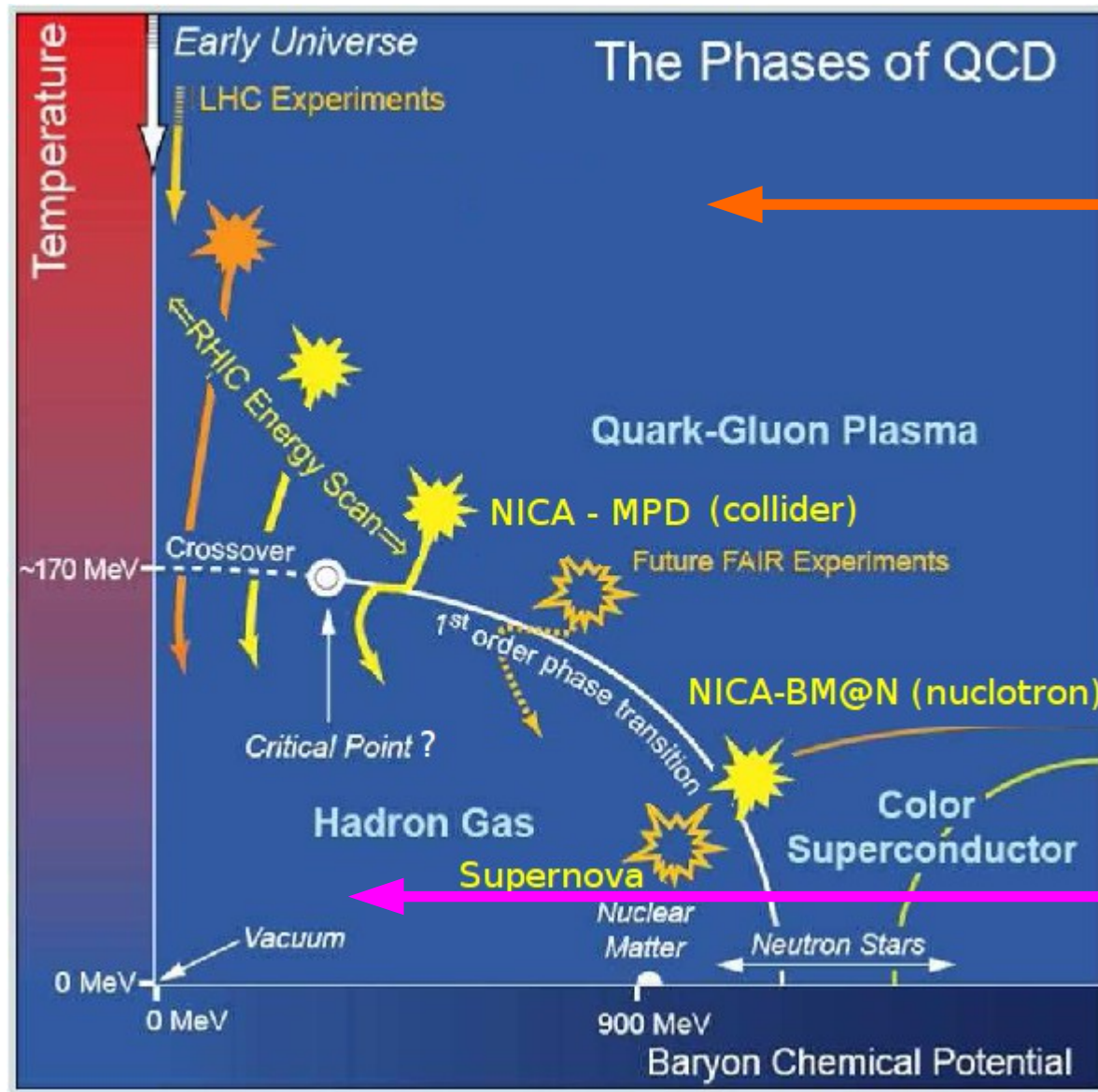
The Goal: Theory of the QCD Phase Diagram



Statistical Model of
Hadron Resonance Gas

Well established for
Description of chemical
freezeout

The Goal: Theory of the QCD Phase Diagram



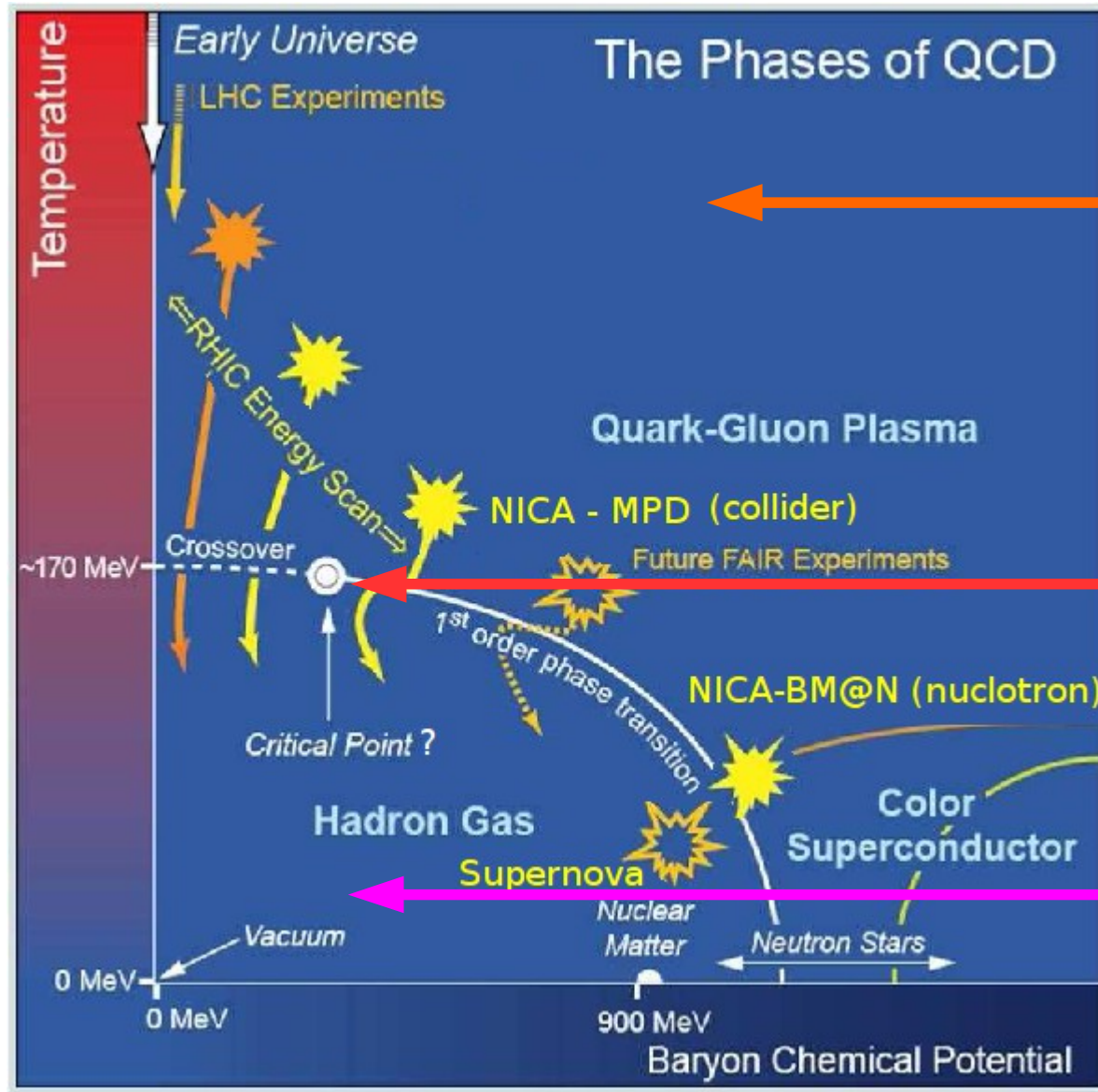
Perturbative QCD

Approximately selfconsistent
HTL resummation
($T > 2.5 T_c$, $\mu > 1500$ MeV)

Statistical Model of
Hadron Resonance Gas

Well established for
Description of chemical
freezeout

The Goal: Theory of the QCD Phase Diagram



Perturbative QCD

Approximately selfconsistent
HTL resummation
($T > 2.5 T_c$, $\mu > 1500$ MeV)

QCD Phase transition(s)

Mott dissociation of hadrons,
Deconfinement, χ SR

Statistical Model of
Hadron Resonance Gas

Well established for
Description of chemical
freezeout

Approximately selfconsistent HTL resumm. QCD

J.-P. Blaizot, E. Iancu, A. Rebhan, Phys. Rev. D 63 (2001) 065003

Skeleton expansion for thermodynamic potential and entropy

$$\beta \Omega[D] = -\log Z = \frac{1}{2} \text{Tr} \log D^{-1} - \frac{1}{2} \text{Tr} \Pi D + \Phi[D]$$

↑
Inv. Temp: $1/T$ trace in conf. Space self-energy related to D

$$-\Phi[D] = 1/12 \text{---} + 1/8 \text{---} + 1/48 \text{---} + \dots$$

Dyson equation: $D^{-1} = D_0^{-1} + \Pi$ Free propagator D_0 is known

Essential property of $\Omega[D]$ is Stationarity under variation of D: $\delta \Omega[D] / \delta D = 0$

This implies $\delta \Phi[D] / \delta D = 1/2 \Pi$

Physical propagator and selfenergy are defined self-consistently !

Self-consistent approximations are defined by the choice of Φ

→ **Φ – derivable theories**

G. Baym, Phys. Rev. 127 (1962) 1391

Approximately selfconsistent HTL resumm. QCD

Matsubara summation:

$$\Omega/V = \int \frac{d^4k}{(2\pi)^4} n(\omega) [\text{Im} \log(-\omega^2 + k^2 + \Pi) - \text{Im} \Pi D] + T\Phi[D]/V$$

Analytic properties:

$$D(\omega, k) = \int_{-\infty}^{\infty} \frac{dk_0}{2\pi} \frac{\rho(k_0, k)}{k_0 - \omega}, \quad \text{Im } D(\omega, k) \equiv \text{Im } D(\omega + i\epsilon, k) = \frac{\rho(\omega, k)}{2}.$$

Thermodynamics from entropy density: $\mathcal{S} = -\partial(\Omega/V)/\partial T$.

$$\mathcal{S} = - \int \frac{d^4k}{(2\pi)^4} \frac{\partial n(\omega)}{\partial T} \text{Im} \log D^{-1}(\omega, k) + \int \frac{d^4k}{(2\pi)^4} \frac{\partial n(\omega)}{\partial T} \text{Im} \Pi(\omega, k) \text{Re } D(\omega, k) + \mathcal{S}'$$

$$\mathcal{S}' \equiv -\left. \frac{\partial(T\Phi/V)}{\partial T} \right|_D + \int \frac{d^4k}{(2\pi)^4} \frac{\partial n(\omega)}{\partial T} \text{Re } \Pi \text{Im } D \xrightarrow{\text{for two-loop skeletons}} 0$$

Loosely speaking: \mathcal{S}' accounts for residual interactions of “independent quasiparticles”

$$d/d\omega [\text{Im} \log D^{-1} + \text{Im} \Pi \text{Re } D] = 2 \text{Im} [D \text{Im}(d/d\omega D^*) \text{Im} \Pi] = 2 \sin^2 \delta d\delta/d\omega, \text{ for } D = |D|e^{i\delta}$$

Approximately selfconsistent HTL resumm. QCD

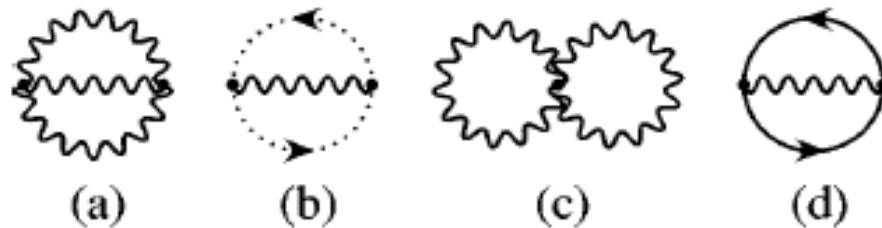
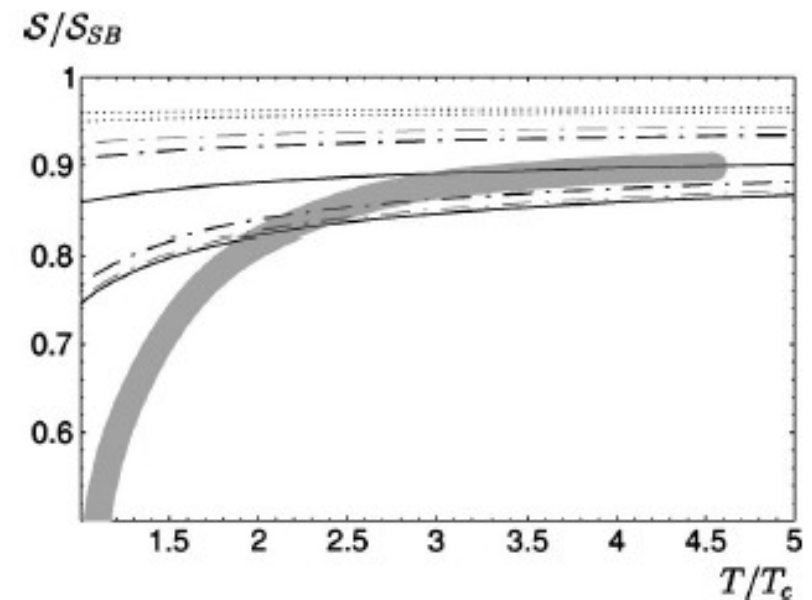


FIG. 3. Diagrams for Φ at 2-loop order in QCD. Wiggly, plain, and dotted lines refer respectively to gluons, quarks, and ghosts.

In ghost-free gauge, HTL resummed QCD thermodyn.



$$S_2 = -\frac{g^2 N_g T}{48} \left\{ \frac{4N + 5N_f}{3} T^2 + \frac{3N_f}{\pi^2} \mu^2 \right\},$$

$$\mathcal{N}_2 = -\frac{g^2 \mu N_g N_f}{16\pi^2} \left(T^2 + \frac{\mu^2}{\pi^2} \right),$$

$$P_2 = -\frac{g^2 N_g}{32} \left\{ \frac{4N + 5N_f}{18} T^4 + \frac{N_f}{\pi^2} \mu^2 T^2 + \frac{N_f}{2\pi^4} \mu^4 \right\}$$

1. Cluster expansion in the 2PI formalism

- Φ — derivable approach to the grand canonical thermodynamic potential
[Baym, Phys. Rev. 127 (1962) 139]

$$J = -\text{Tr} \{ \ln(-G_1) \} - \text{Tr} \{ \Sigma_1 G_1 \} + \text{Tr} \{ \ln(-G_2) \} + \text{Tr} \{ \Sigma_2 G_2 \} + \Phi[G_1, G_2]$$

with full propagators:

$$G_1^{-1}(1, z) = z - E_1(p_1) - \Sigma_1(1, z); G_2^{-1}(12, 1'2', z) = z - E_1(p_1) - E_2(p_2) - \Sigma_2(12, 1'2', z)$$

and selfenergies

$$\Sigma_1(1, 1') = \frac{\delta \Phi}{\delta G_1(1, 1')} ; \Sigma_2(12, 1'2', z) = \frac{\delta \Phi}{\delta G_2^{-1}(12, 1'2', z)}.$$

Because of stationarity equivalent to

$$n = -\frac{1}{\Omega} \frac{\partial J}{\partial \mu} = \frac{1}{\Omega} \sum_1 \int_{-\infty}^{\infty} \frac{d\omega}{\pi} f_1(\omega) S_1(1, \omega),$$

(baryon number conservation)

- Generalization to A-nucleon clusters in nuclear matter

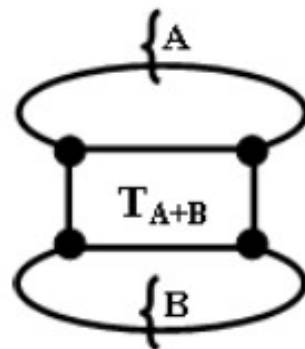
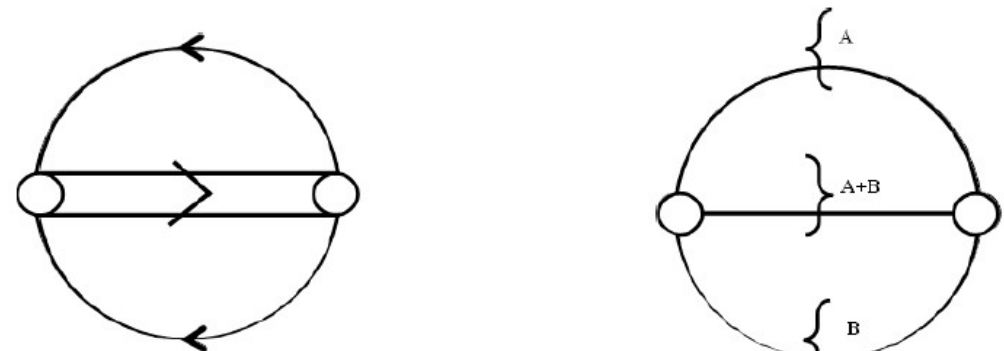
$$\Omega = \sum_A (-1)^A [\text{Tr} \ln (-G_A^{-1}) + \text{Tr} (\Sigma_A G_A)] + \Phi,$$

$$G_A^{-1} = G_A^{(0)-1} - \Sigma_A, \quad \Sigma_A(1 \dots A, 1' \dots A', z_A) = \frac{\delta \Phi}{\delta G_A(1 \dots A, 1' \dots A', z_A)}.$$

1. Cluster expansion in the 2PI formalism

A) Choice of the Φ -functional:

- 2-particle irreducible diagrams
- closed 2-loop diagram involving 3 cluster propagators (A , B , $A+B$) and 2 vertices
- equivalent to 1 T-matrix + 2 propagators



$$\text{Diagram showing the equivalence of a 2-loop diagram to a T-matrix plus two propagators: } \text{Diagram A} = \text{Diagram B}.$$

B) Ansatz for thermodynamic potential:

$$\Omega = \sum_A (-1)^A [\text{Tr} \ln (-G_A^{-1}) + \text{Tr} (\Sigma_A G_A)] + \sum_{A,B} \Phi[G_A, G_B, G_{A+B}] ,$$

$$G_A^{-1} = G_A^{(0)-1} - \Sigma_A , \quad \Sigma_A(1 \dots A, 1' \dots A', z_A) = \frac{\delta \Phi}{\delta G_A(1 \dots A, 1' \dots A', z_A)} .$$

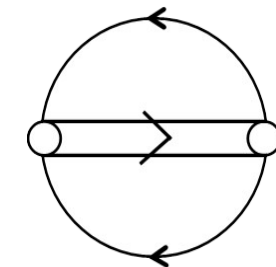
C) Check: conservation laws, e.g.:

(correspondence to GF formalism)

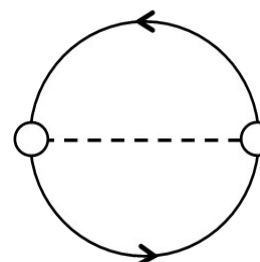
$$n = -\frac{1}{V} \frac{\partial \Omega}{\partial \mu} = \frac{1}{V} \sum_1 \int_{-\infty}^{\infty} \frac{d\omega}{\pi} f_1(\omega) A_1(1, \omega)$$

1. Cluster virial expansion in the 2PI formalism, Examples:

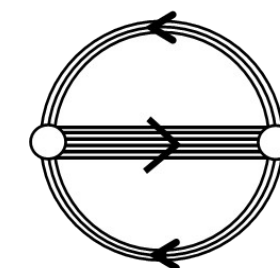
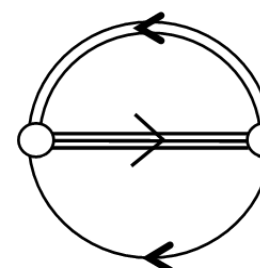
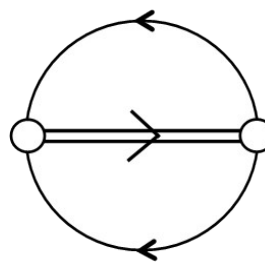
A) Deuterons in nuclear matter (check):



B) Mesons in quark matter:

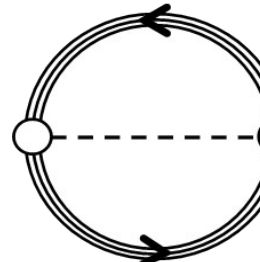
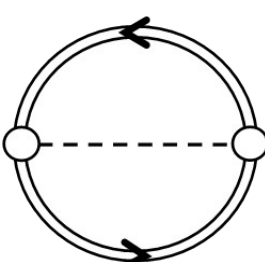


C) Nucleons in quark matter:



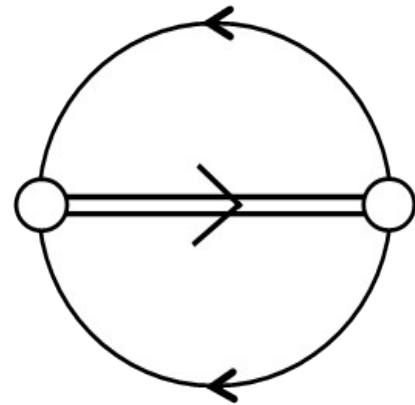
D) Nucleons and mesons (hadron resonance gas) in quark matter:

B) + C) +

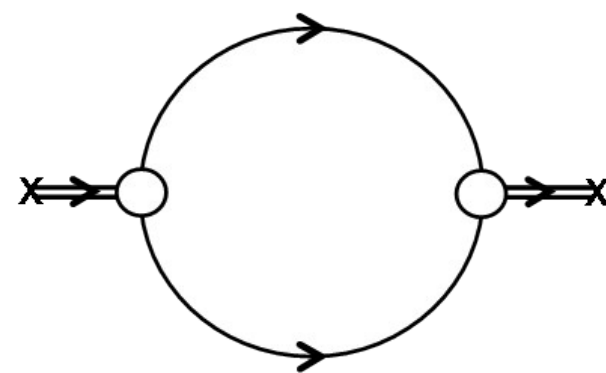


2. Example A: Deuterons in nuclear matter

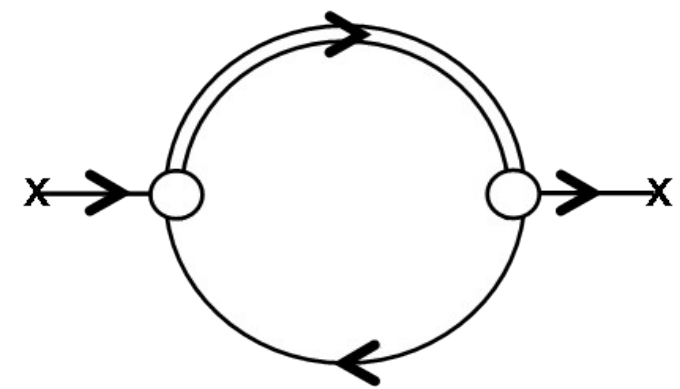
Φ -functional



deuteron selfenergy “ Π ”



nucleon selfenergy



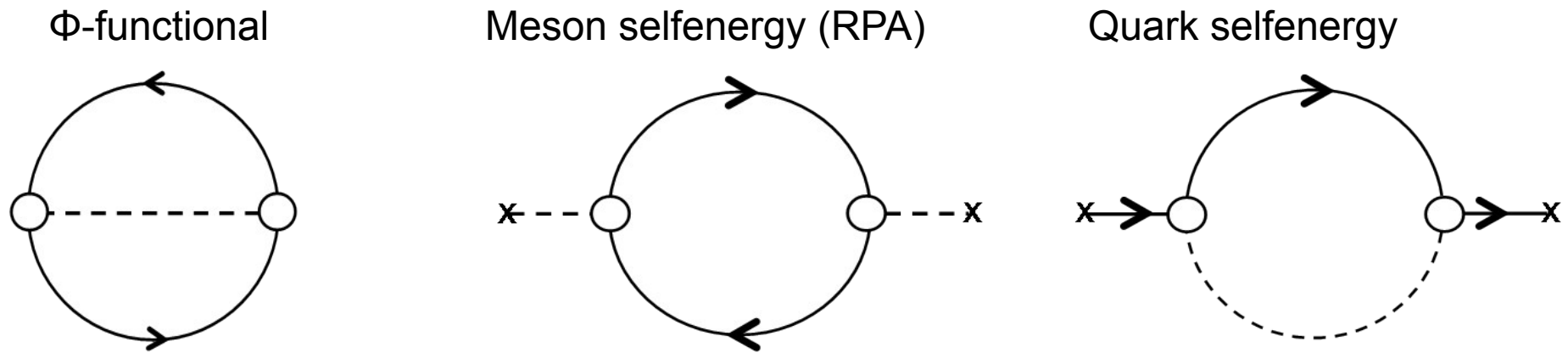
$$T^{-1} = V^{-1} - \Pi$$

Bethe-Salpeter equation for deuteron T-matrix, ladder approximation

$$\Sigma(1, z) = \sum_2 \int \frac{d\omega}{2\pi} A(2, \omega) \left\{ f(\omega) V(12, 12) - \int \frac{dE}{\pi} \Im T(12, 12; E + i\eta) \frac{f(\omega) + g(E)}{E - z - \omega} \right\}$$

$$n(\mu, T) = n_{\text{free}}(\mu, T) + 2n_{\text{corr}}(\mu, T) , \quad n_{\text{sc}} = \int \frac{dE}{2\pi} g(E) 2 \sin^2 \delta(E) \frac{d\delta(E)}{dE} .$$

3. Example B: Mesons in quark matter



$$T_M^{-1}(q, \omega + i\eta) = G_S^{-1} - \Pi_M(q, \omega + i\eta) = |T_M(q, \omega)|^{-1} e^{-i\delta_M(q, \omega)}, \quad \delta_M(q, \omega) = \arctan(\Im T_M / \Re T_M)$$

$$\Omega = \Omega_{\text{MF}} + \Omega_M, \quad \sigma_{\text{MF}} = 2N_f N_c G_S \int \frac{d^3 p}{(2\pi)^3} \frac{m}{E_p} [1 - f_-(E_p) - f_+(E_p)],$$

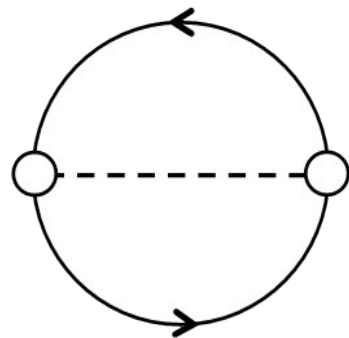
$$\Omega_{\text{MF}} = \frac{\sigma_{\text{MF}}^2}{4G_S} - 2N_c N_f \int \frac{d^3 p}{(2\pi)^3} \left[E_p + T \ln \left(1 + e^{-(E_p - \Sigma_+ - \mu)/T} \right) + T \ln \left(1 + e^{-(E_p + \Sigma_- + \mu)/T} \right) \right],$$

$$\Omega_M = d_M \int \frac{d^3 k}{(2\pi)^3} \int \frac{d\omega}{2\pi} \left\{ \omega + 2T \ln \left[1 - e^{-\omega/T} \right] 2 \sin^2 \delta_M(k, \omega) \frac{\delta_M(k, \omega)}{d\omega} \right\},$$

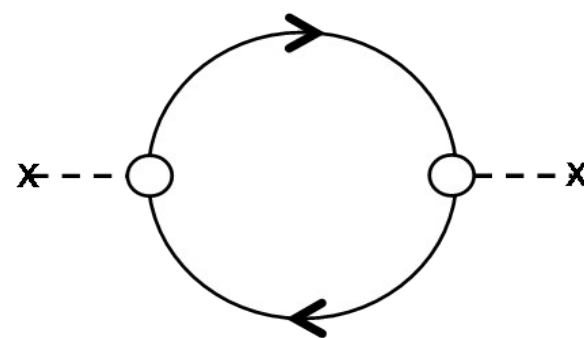
$$\Sigma_M(0, p_0) = d_M \int \frac{d^4 q}{(2\pi)^4} \pi \rho_M(q, q_0) \left\{ \frac{(\gamma_0 + m/E_q)[1 + g(q_0) - f_-(E_q)]}{q_0 - p_0 + E_q - \mu - i\eta} + \frac{(\gamma_0 - m/E_q)[g(q_0) + f_+(E_q)]}{q_0 - p_0 - E_q - \mu - i\eta} \right\},$$

3. Example B: Mesons in quark matter

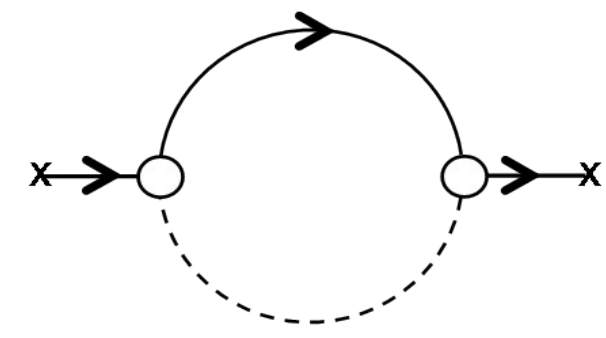
Φ -functional



Meson selfenergy (RPA)



Quark selfenergy



$$T_M^{-1}(q, \omega + i\eta) = G_S^{-1} - \Pi_M(q, \omega + i\eta) = |T_M(q, \omega)|^{-1} e^{-i\delta_M(q, \omega)}, \quad \delta_M(q, \omega) = \arctan(\Im T_M / \Re T_M)$$

$$\Omega = \Omega_{\text{MF}} + \Omega_M, \quad \sigma_{\text{MF}} = 2N_f N_c G_S \int \frac{d^3 p}{(2\pi)^3} \frac{m}{E_p} [1 - f_-(E_p) - f_+(E_p)],$$

$$\Omega_{\text{MF}} = \frac{\sigma_{\text{MF}}^2}{4G_S} - 2N_c N_f \int \frac{d^3 p}{(2\pi)^3} \left[E_p + T \ln \left(1 + e^{-(E_p - \Sigma_+ - \mu)/T} \right) + T \ln \left(1 + e^{-(E_p + \Sigma_- + \mu)/T} \right) \right],$$

$$\Omega_M = d_M \int \frac{d^3 k}{(2\pi)^3} \int \frac{d\omega}{2\pi} \left\{ \omega + 2T \ln \left[1 - e^{-\omega/T} \right] \boxed{2 \sin^2 \delta_M(k, \omega)} \frac{\delta_M(k, \omega)}{d\omega} \right\} \boxed{\text{not yet!}}$$

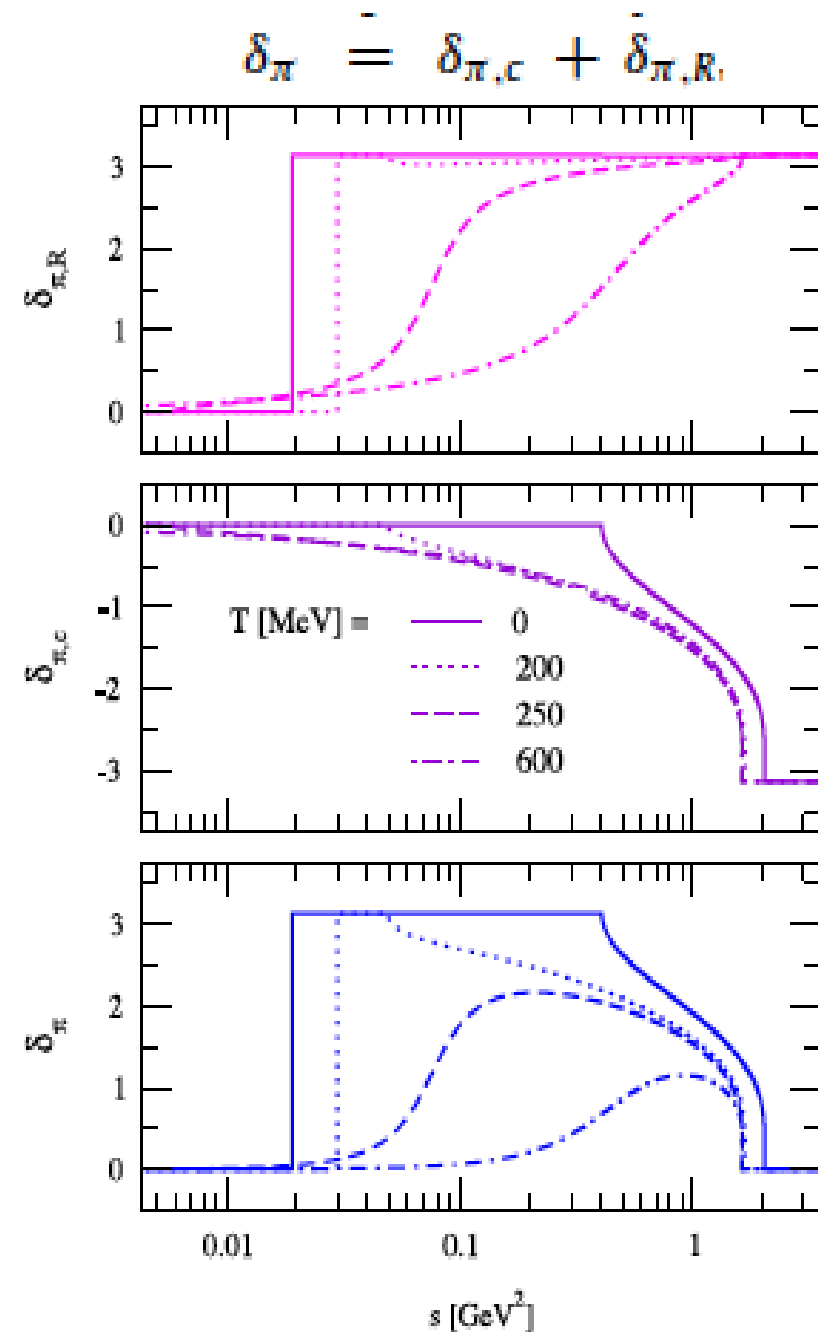
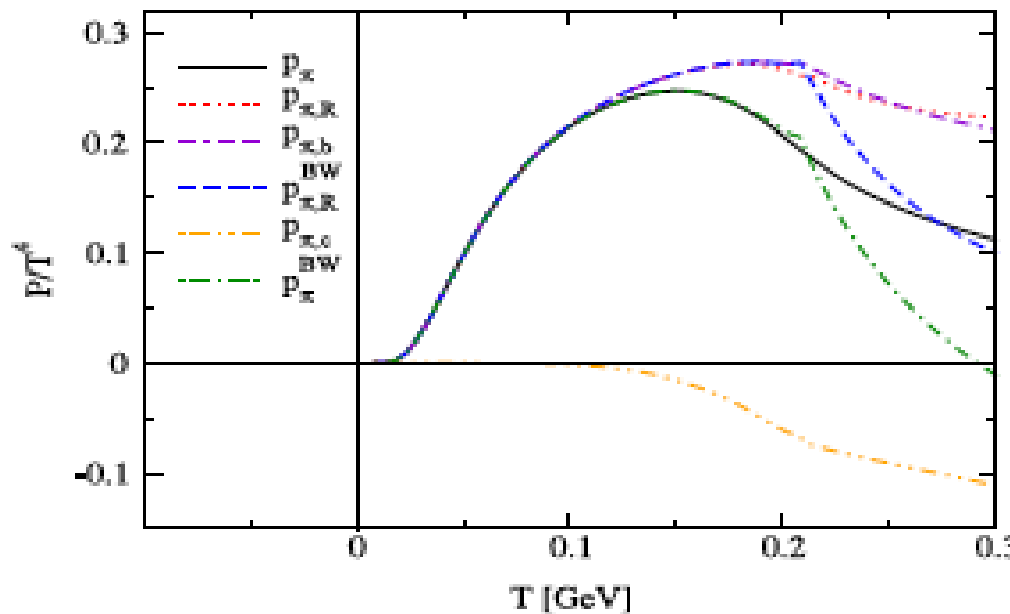
$$\Sigma_M(0, p_0) = d_M \int \frac{d^4 q}{(2\pi)^4} \pi \rho_M(q, q_0) \left\{ \frac{(\gamma_0 + m/E_q)[1 + g(q_0) - f_-(E_q)]}{q_0 - p_0 + E_q - \mu - i\eta} + \frac{(\gamma_0 - m/E_q)[g(q_0) + f_+(E_q)]}{q_0 - p_0 - E_q - \mu - i\eta} \right\},$$

3. Example B: Mesons in quark matter

$$\Omega_X(T, \mu) = -d_X \int \frac{d^3q}{(2\pi)^3} \int_{-\infty}^{\infty} \frac{d\omega}{2\pi} n_X^-(\omega) \delta_X(\omega, \mathbf{q}),$$

$$\int_0^{\infty} d\omega \frac{1}{\pi} \frac{d\delta_X(\omega; T)}{d\omega} = 0 = \underbrace{\int_0^{\omega_{\text{thr}}(T)} d\omega \frac{1}{\pi} \frac{d\delta_X(\omega; T)}{d\omega}}_{n_{B,X}(T)} + \underbrace{\frac{1}{\pi} \int_{\omega_{\text{thr}}(T)}^{\infty} d\omega \frac{d\delta_X(\omega; T)}{d\omega}}_{\frac{1}{\pi} [\delta_X(\infty; T) - \delta_X(\omega_{\text{thr}}; T)]},$$

$$p_\pi(T) = -d_\pi T \int \frac{d^3q}{(2\pi)^3} \int_0^{\infty} \frac{d\omega}{\pi} \ln(1 - e^{-\omega/T}) \frac{d\delta_\pi(\omega, \mathbf{q})}{d\omega}$$

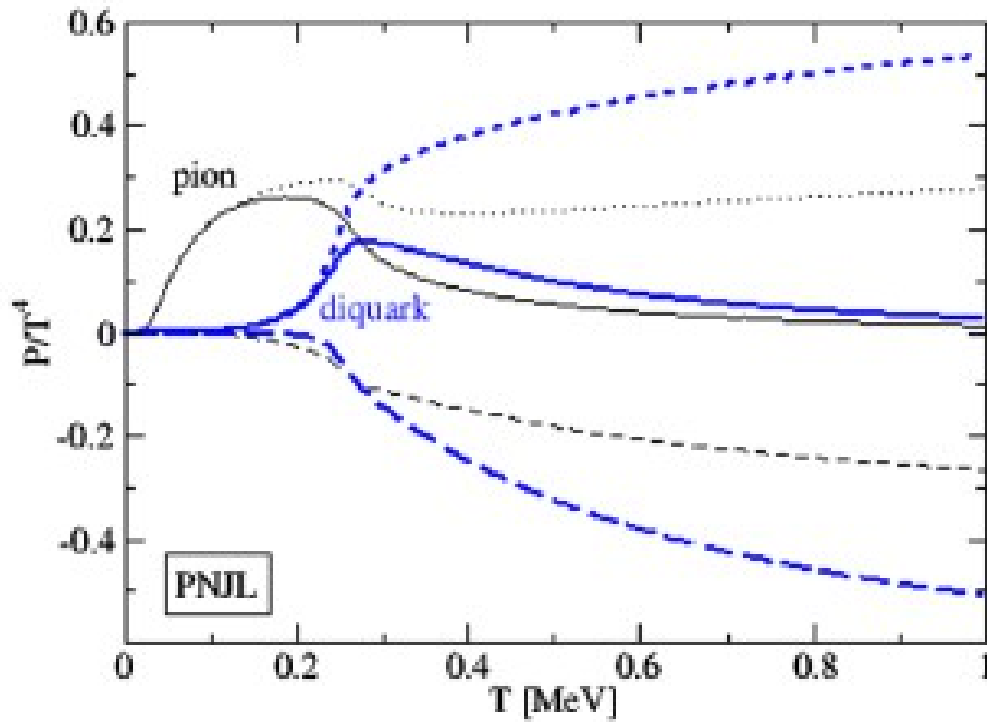


3. Example B*: Mesons+diquarks in quark matter

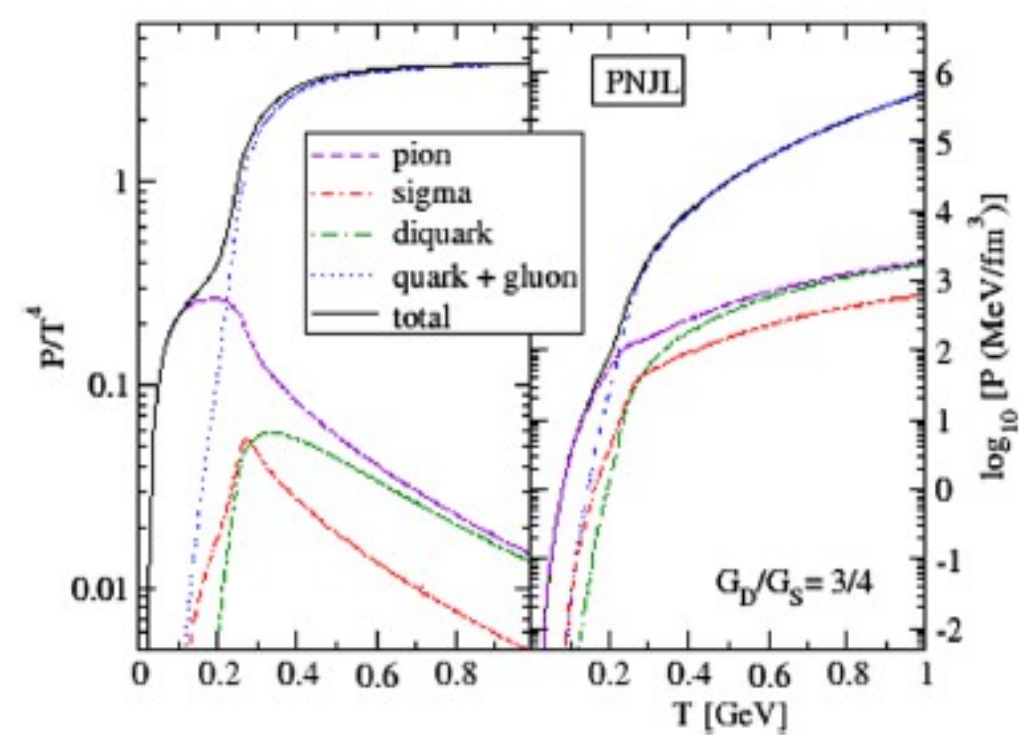
$$\Omega_Q = -\frac{2N_c N_f}{3} \int \frac{dp}{2\pi^2} \frac{p^4}{E_p} [f_\Phi^+(E_p) + f_\Phi^-(E_p)], \quad f_\Phi^+(E_p) = \frac{(\bar{\Phi} + 2\Phi Y)Y + Y^3}{1 + 3(\bar{\Phi} + \Phi Y)Y + Y^3}, \quad Y = e^{-(E_p - \mu)/T}$$

$$\Omega_D = -3 \int \frac{d^3 p}{(2\pi)^3} \int \frac{d\omega}{2\pi} [g_\Phi^+(\omega) + g_\Phi^-(\omega)] \delta_D(\omega), \quad g_\Phi^+(\omega) = \frac{(\Phi - 2\bar{\Phi}X)X + X^3}{1 - 3(\Phi - \bar{\Phi}X)X - X^3} \quad X = e^{-(\omega - 2\mu)/T}$$

Suppression of colored states by Polyakov-loop Φ

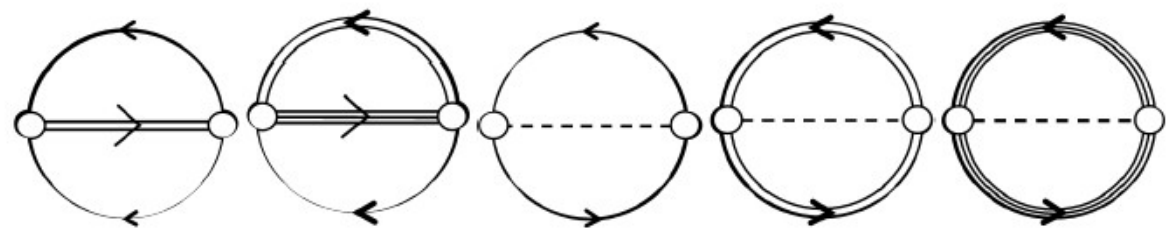


Confinement: $\Phi=0$

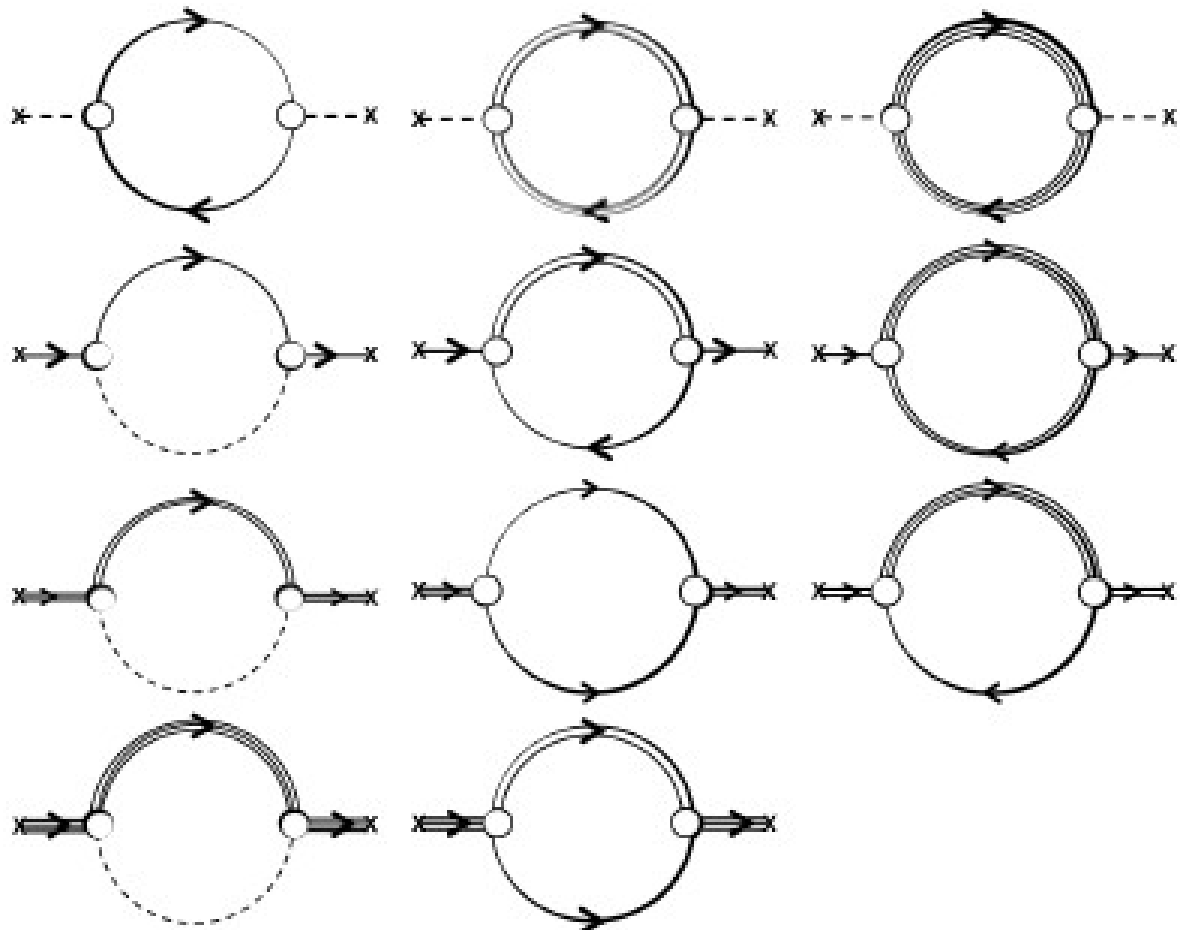


3. Example C: Hadron resonance gas – toy model

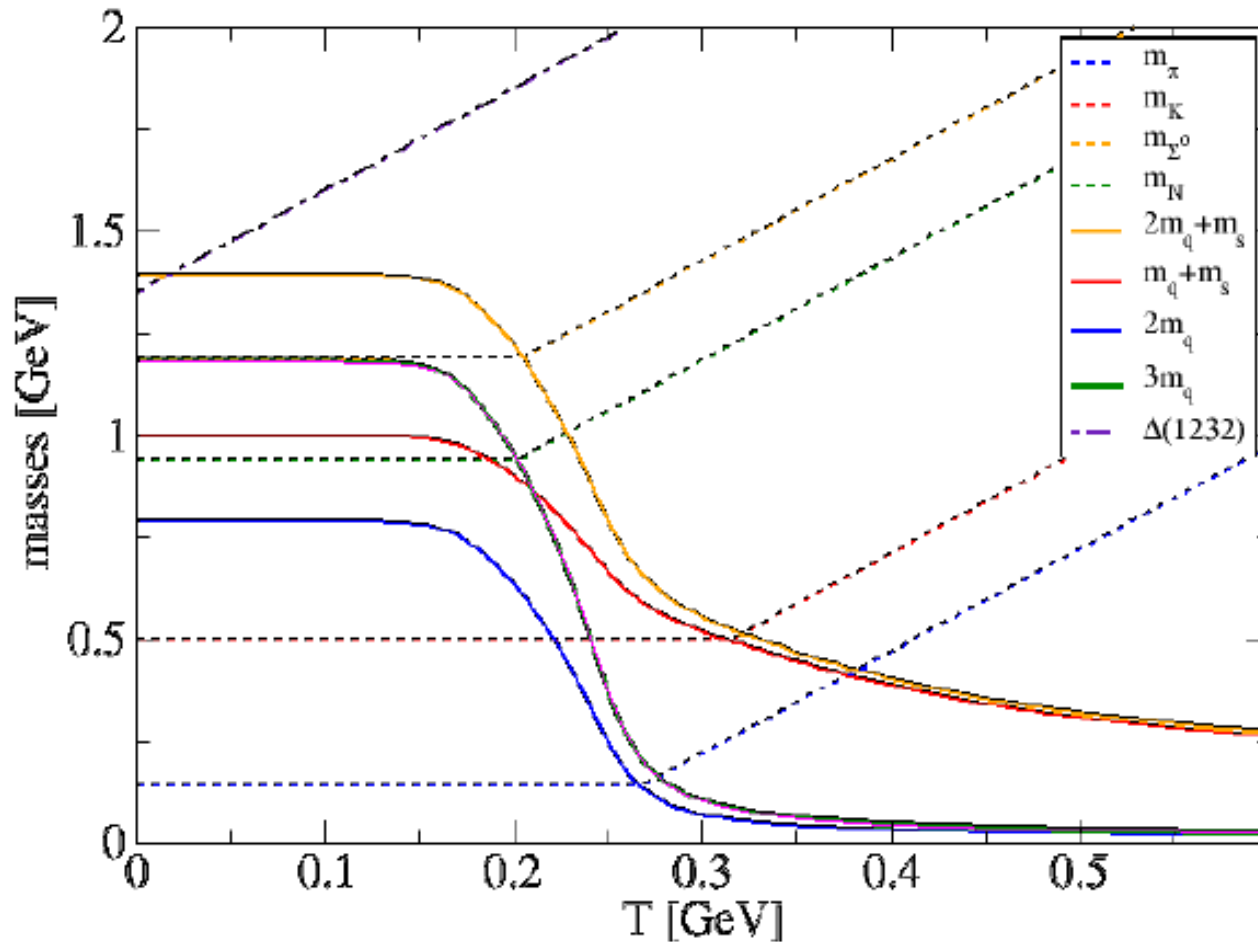
Φ -functional:



Selfenergies:



3. Example C: Hadron resonance gas – toy model

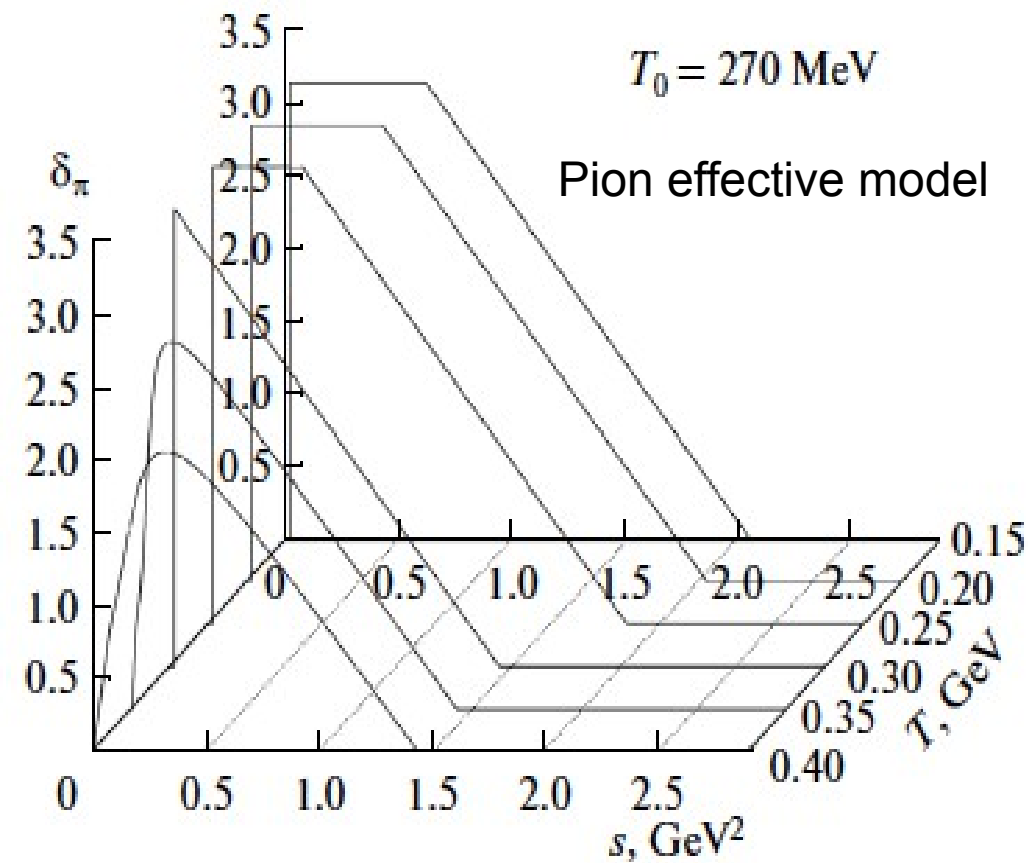
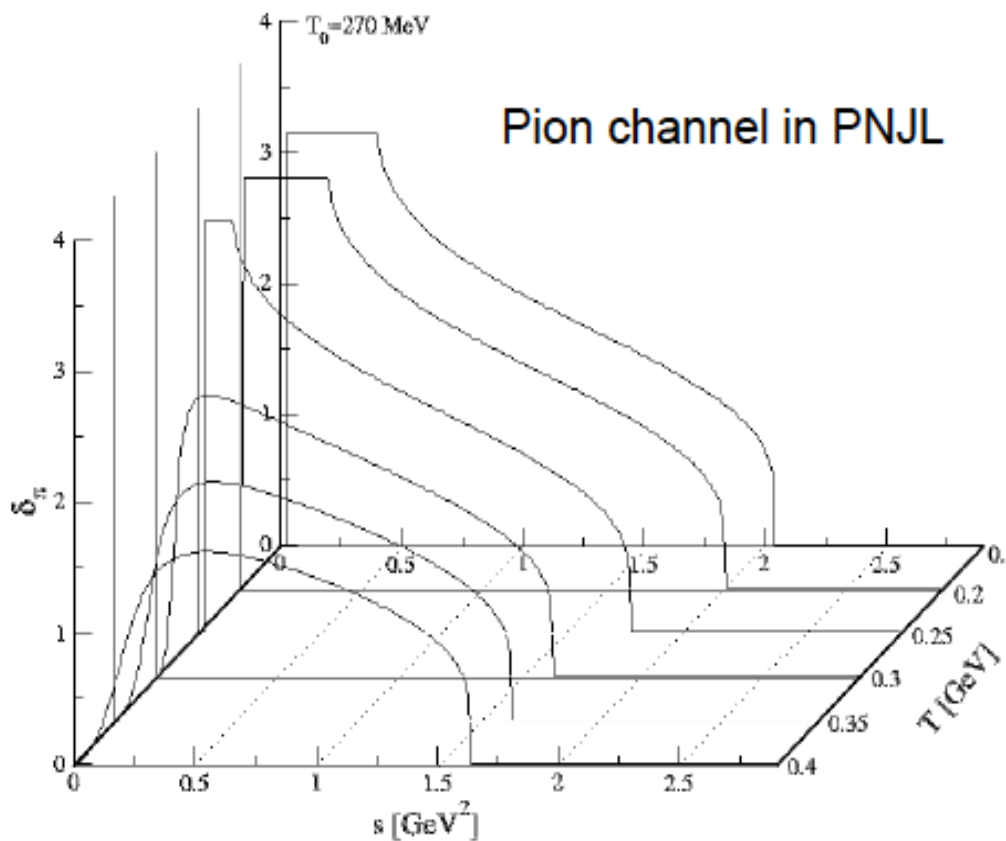


$$M_i(T) = M_i(0) + \Gamma_i(T) ,$$

$$\Gamma_i(T) = a (T - T_{\text{Mott},i}) \Theta(T - T_{\text{Mott},i})$$

$$\begin{aligned} M_i(T_{\text{Mott},i}) &= m_{\text{thr},i}(T_{\text{Mott},i}) , \\ m_{\text{thr,M}}(T) &= (2 - N_s)m(T) + N_s m_s(T) \\ m_{\text{thr,B}}(T) &= (3 - N_s)m(T) + N_s m_s(T) \end{aligned}$$

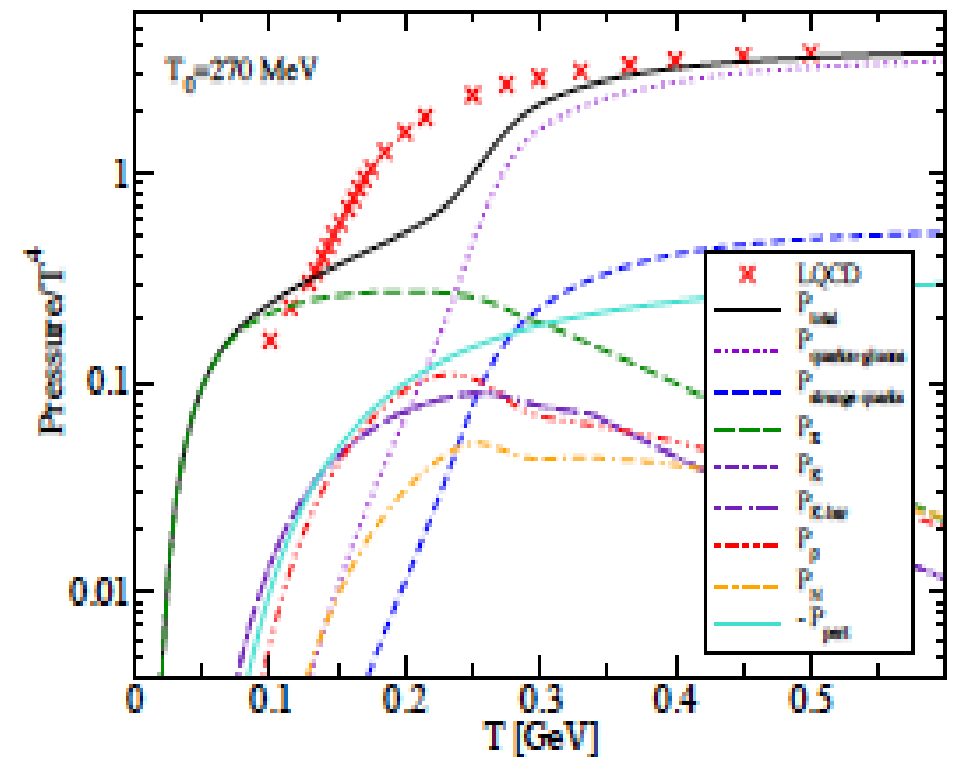
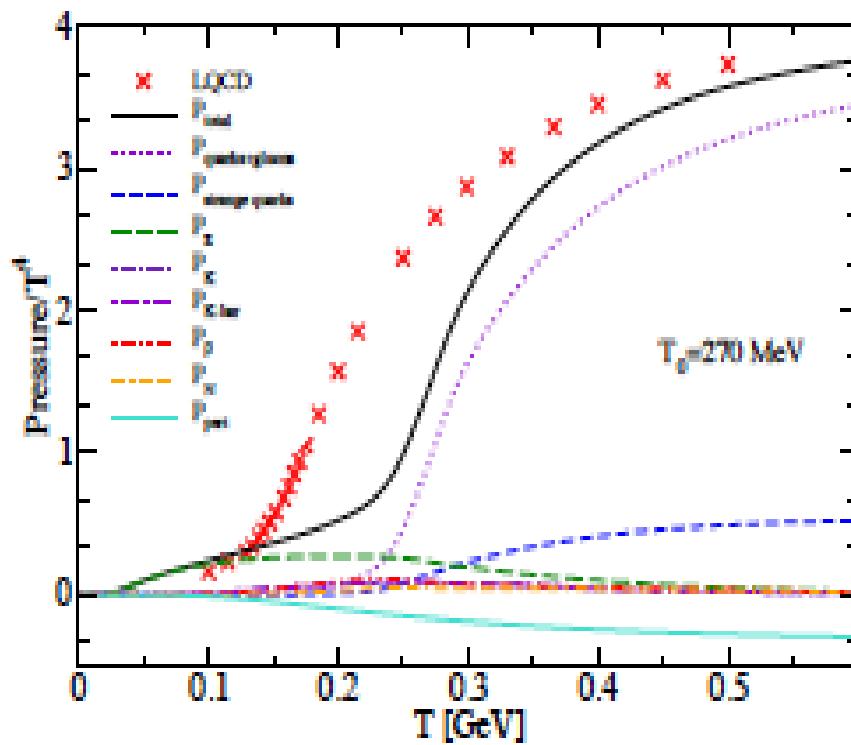
3. Example C: Hadron resonance gas – toy model



Effective model for in-medium hadron phase shifts

$$\delta_i(s; T) = \left[\frac{\pi}{2} + \arctan \left(\frac{s - M_i^2(T)}{M_i(T)\Gamma_i(T)} \right) \right] \left\{ \Theta[m_{\text{thr},i}^2 - s] + \Theta[s - m_{\text{thr},i}^2] \Theta[m_{\text{thr},i}^2 + N_i^2 \Lambda^2 - s] \left[\frac{[m_{\text{thr},i}^2 + N_i^2 \Lambda^2 - s]}{N_i^2 \Lambda^2} \right] \right\}$$

3. Example C: Hadron resonance gas – toy model

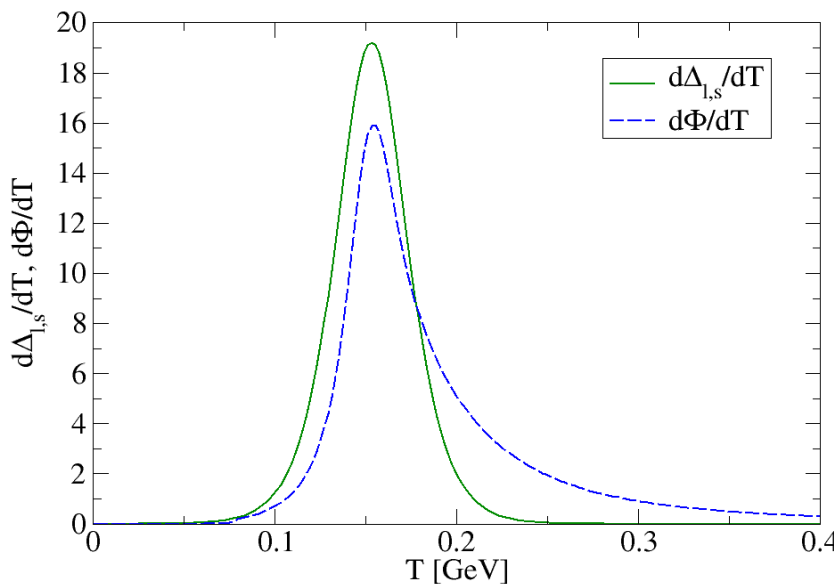
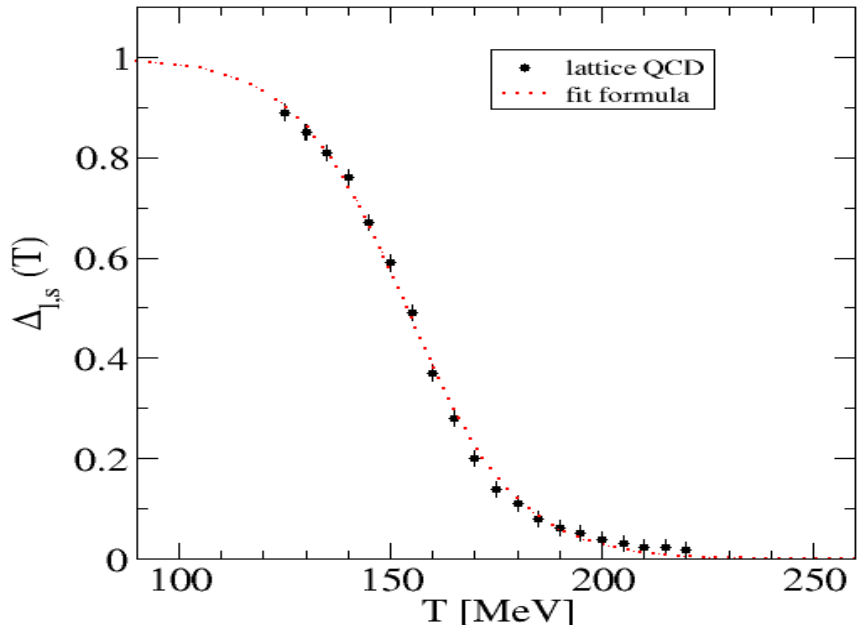


$$P_i(T) = d_i \int_0^\infty \frac{dp p^2}{2\pi^2} \int_0^\infty \frac{dM}{\pi} \frac{M}{\sqrt{p^2 + M^2}} f_i(\sqrt{p^2 + M^2}) \delta_i(M^2; T)$$

$$P_i(T) = \mp d_i \int_0^\infty \frac{dp p^2}{2\pi^2} \int_0^\infty dM T \ln(1 \mp e^{-\sqrt{p^2+M^2}/T}) \frac{1}{\pi} \frac{d\delta_i(M^2; T)}{dM}$$

$$P(T) = \sum_{i=M,B} P_i(T) + P_{\text{PNJL}}(T) + P_{\text{pert}}(T)$$

3. Example C: Mott HRG – improved toy model



$$P_{\text{PNJL}}(T) = P_{\text{FG}}(T) + \mathcal{U}[\Phi; T] ,$$

$$P_{\text{FG}}(T) = 4 \sum_{n=u,d,s} \int \frac{d^3 p}{(2\pi)^3} T \ln [1 + 3\Phi(Y + Y^2) + Y^3]$$

$$Y(E_p) = \exp(-E_p/T)$$

$$\mathcal{U}[\Phi; T] = -\frac{a(T)}{2}\Phi^2 + b(T) \ln(1 - 6\Phi^2 + 8\Phi^3 - 3\Phi^4)$$

T-dependent quark masses from fit to LQCD

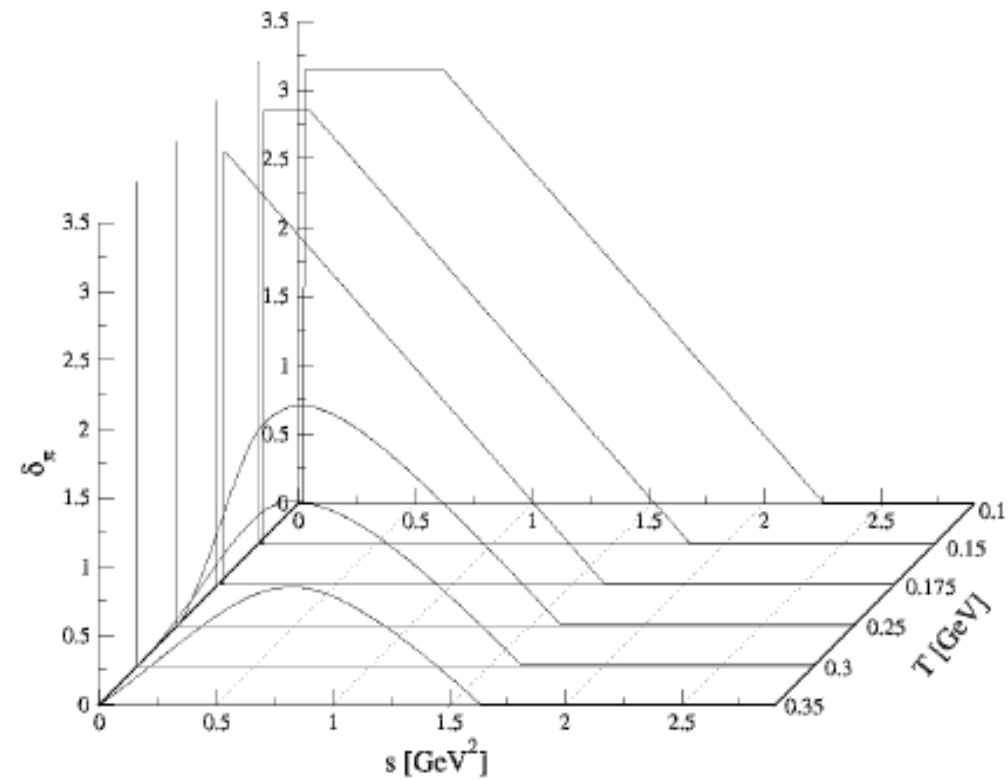
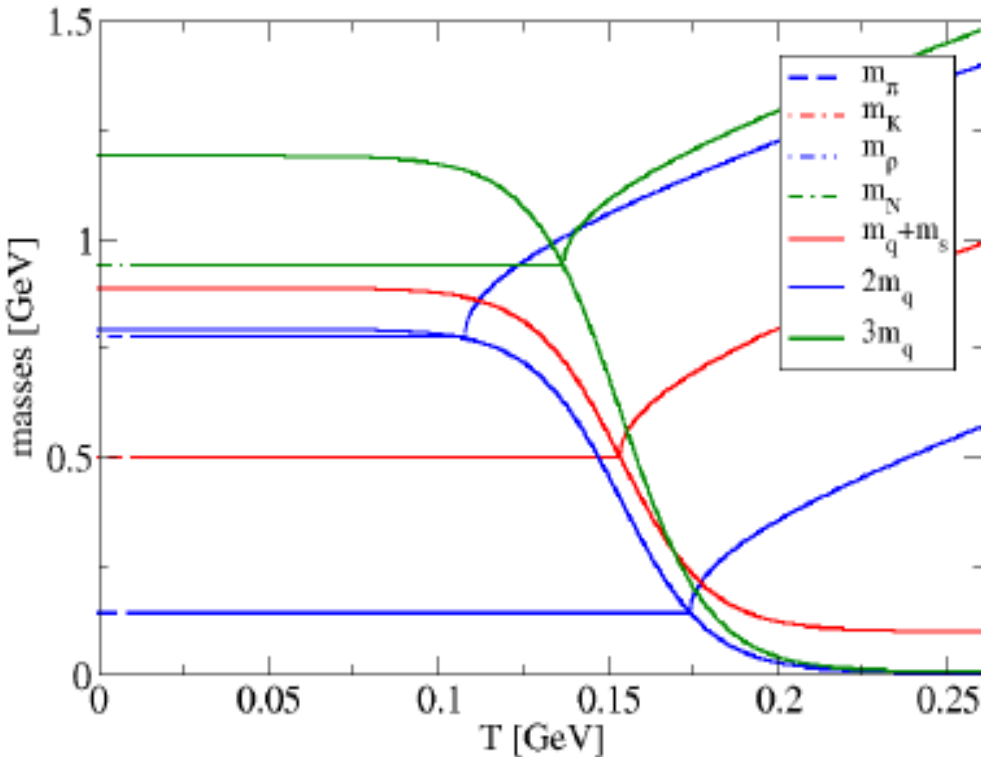
$$m(T) = [m(0) - m_0]\Delta_{l,s}(T) + m_0 ,$$

$$m_s(T) = m(T) + m_s - m_0 ,$$

$$\Delta_{l,s}(T) = \frac{1}{2} \left[1 - \tanh \left(\frac{T - T_c}{\delta_T} \right) \right]$$

$$T_c = 154 \text{ MeV} \quad \delta_T = 26 \text{ MeV}$$

3. Example C: Mott HRG – improved toy model



Hadrons + Mott effect

$$P_i(T) = \mp d_i \int_0^\infty \frac{dp}{2\pi^2} \frac{p^2}{2\pi^2} \int_0^\infty dM T \ln \left(1 \mp e^{-\sqrt{p^2+M^2}/T} \right) \frac{2}{\pi} \sin^2 \delta_i(M^2; T) \frac{d\delta_i(M^2; T)}{dM}$$

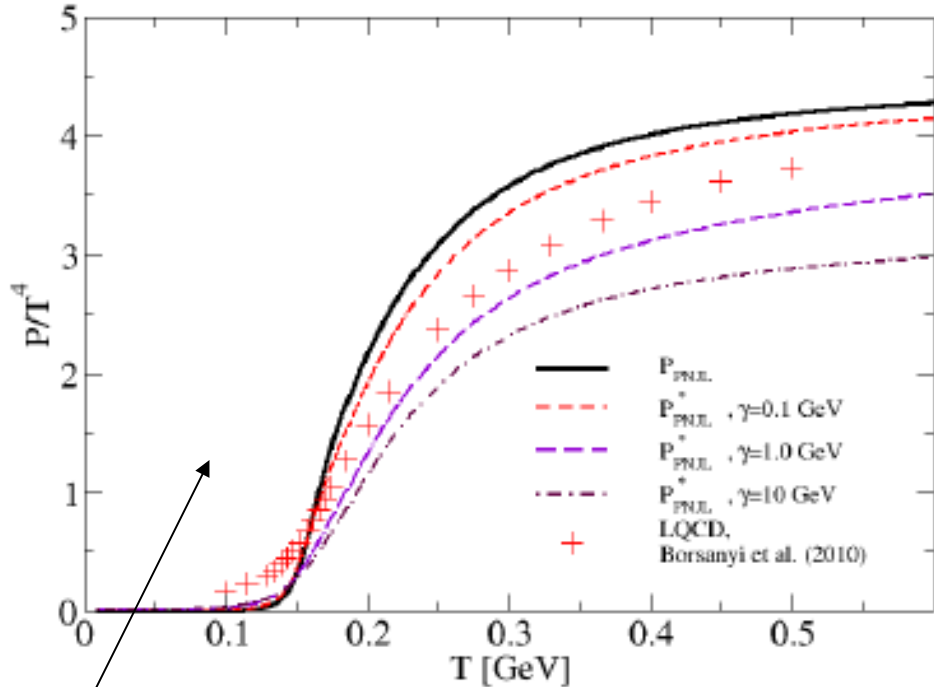
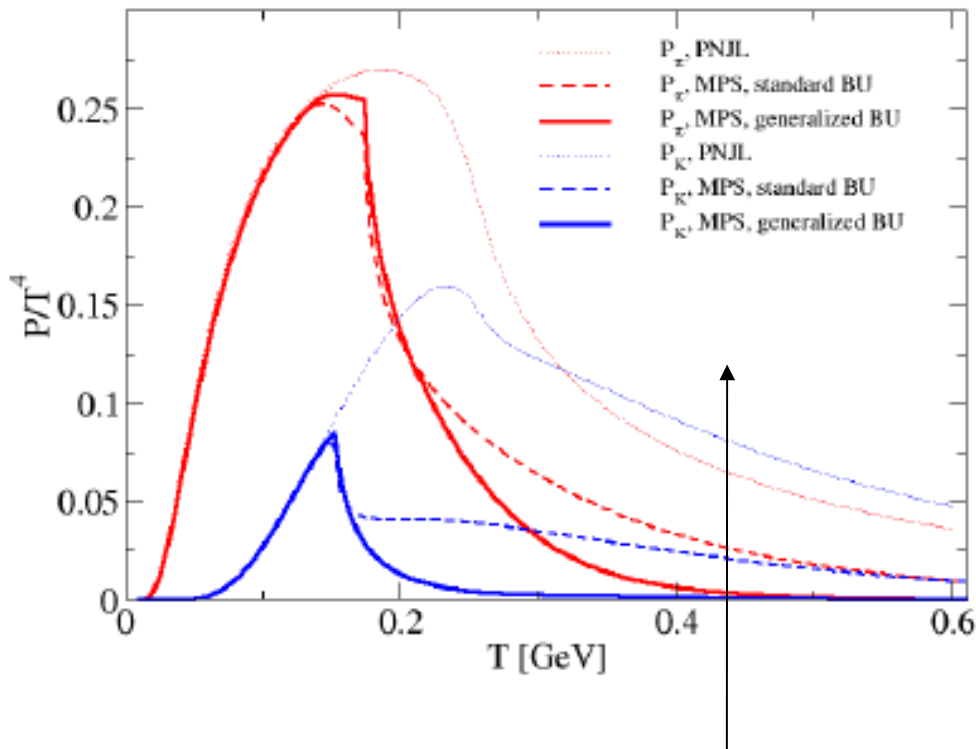
Quarks + rescattering effects

$$f_\Phi(\omega) = \frac{\Phi(1+2Y)Y + Y^3}{1 + 3\Phi(1+Y)Y + Y^3},$$

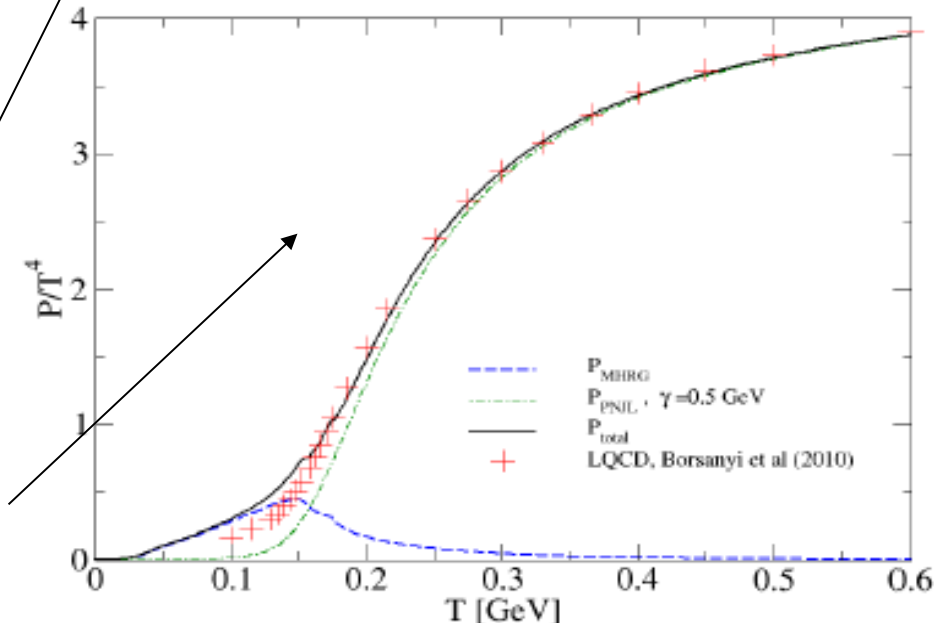
$$P_{\text{FG}}^*(T) = 4N_c \sum_{q=u,d,s} \int \frac{dp}{2\pi^2} \frac{p^2}{2\pi^2} \int \frac{d\omega}{\pi} f_\Phi(\omega) \delta_q(\omega; \gamma),$$

$$\delta_q(\omega; \gamma) = \frac{\pi}{2} + \arctan \left[\frac{\omega - \sqrt{p^2 + m_q^2}}{\gamma} \right]$$

3. Example C: Mott HRG – improved toy model

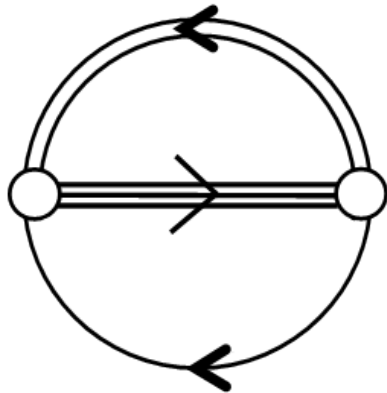


- Mott dissociation of hadrons (here π , K) at the Chiral restoration temperature $T_c = 153$ MeV
- Asymptotic behaviour of scaled quark-gluon Pressure can be adjusted with rescattering Parameter gamma
- Very good correspondence between lattice QCD Thermodynamics and improved MHRG model; Hadronic and partonic contributions quantified

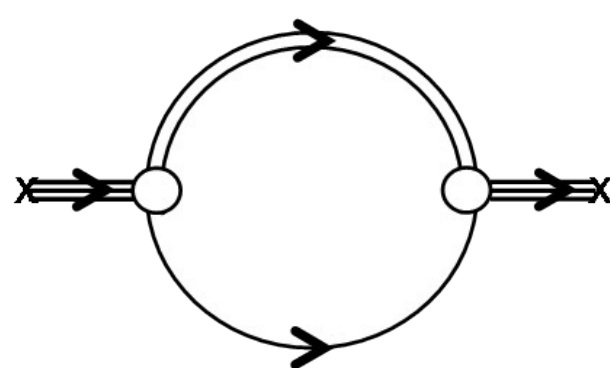


3. Example D: Nucleons in quark matter

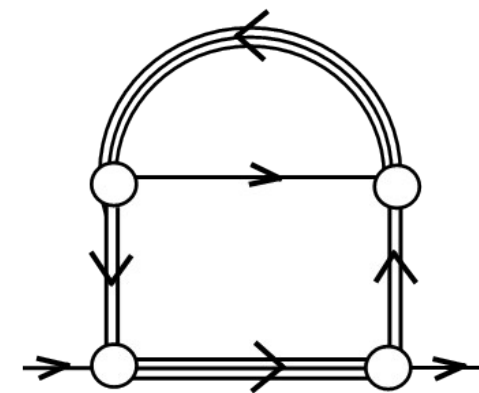
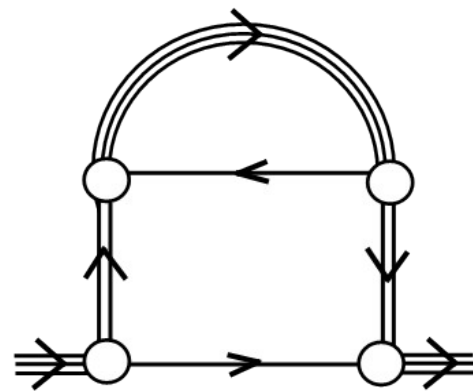
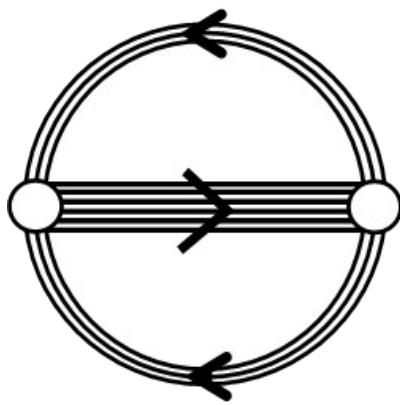
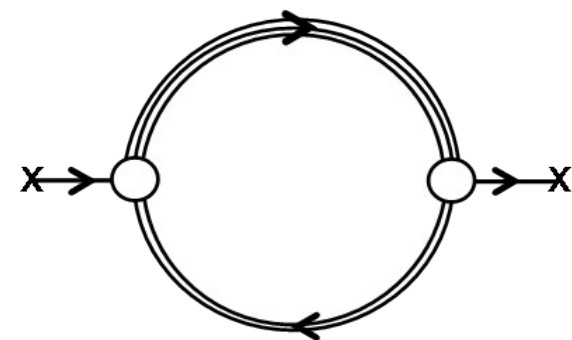
Φ -functional



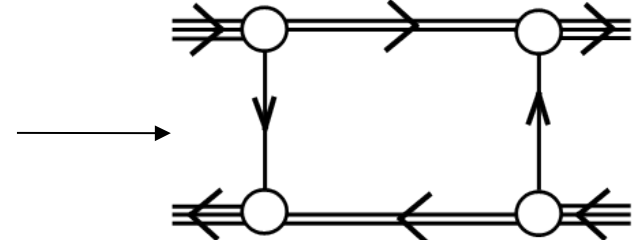
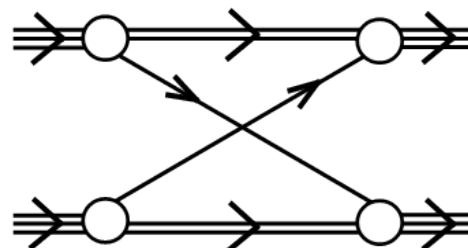
nucleon selfenergy



quark selfenergy

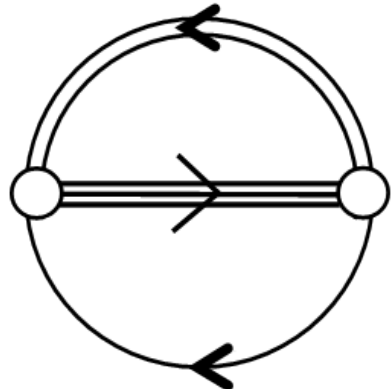


quark exchange interaction
between nucleons:

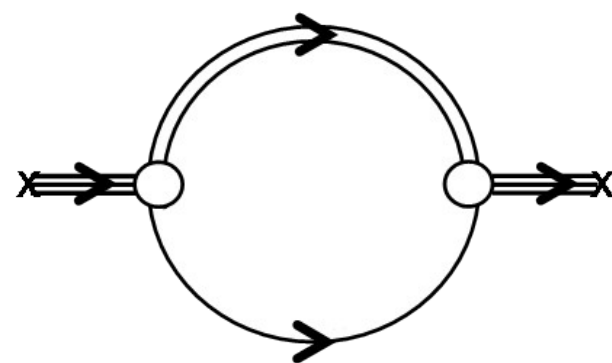


5. Example D: Nucleons in quark matter

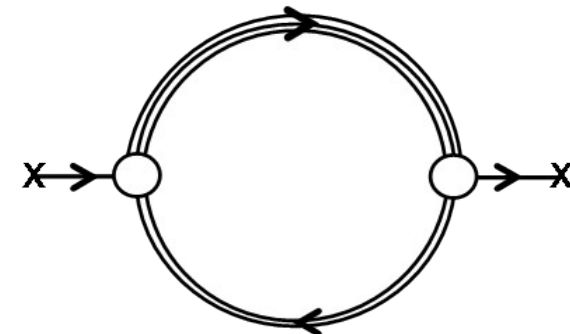
Φ -functional



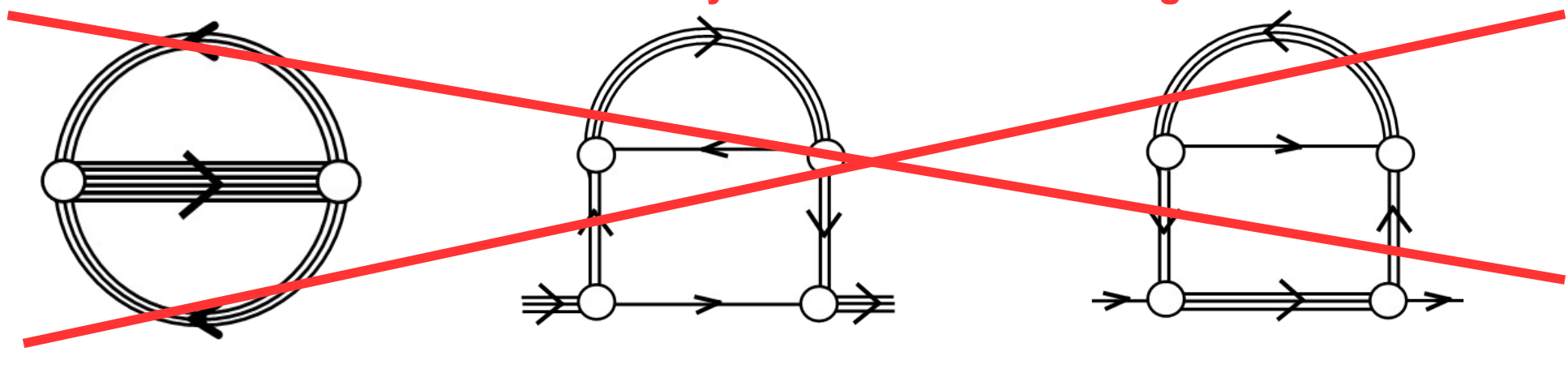
nucleon selfenergy



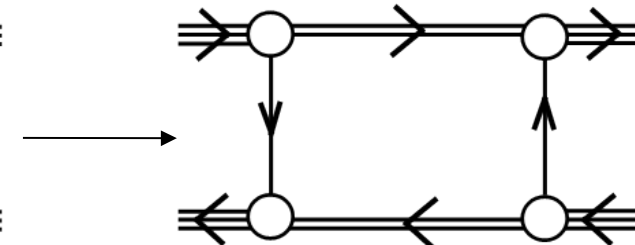
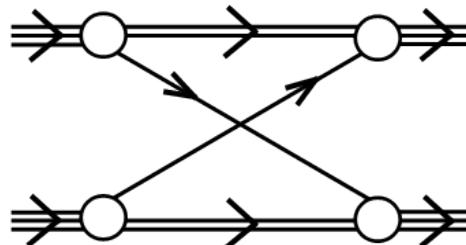
quark selfenergy



Not new! Already contained in above diagrams!

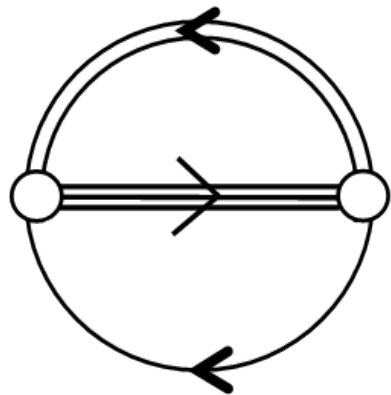


quark exchange interaction
between nucleons:

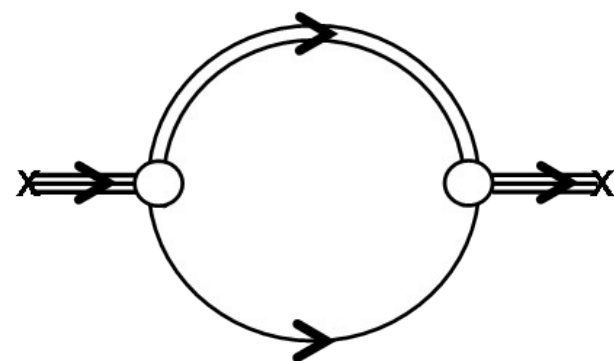


5. Example D: Nucleons in quark matter

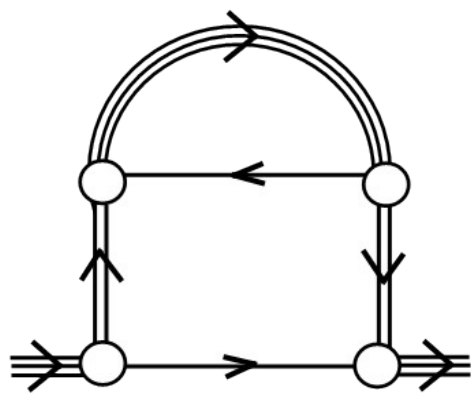
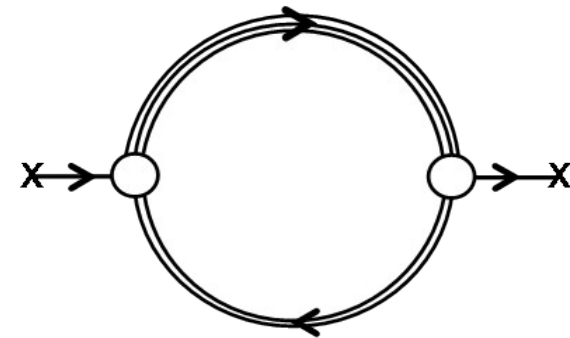
Φ -functional



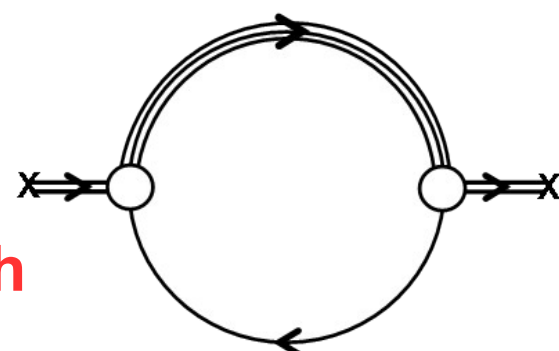
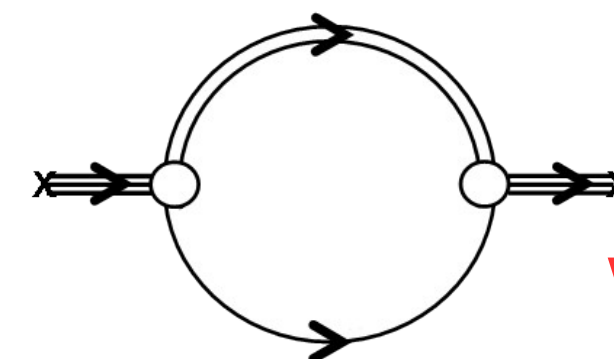
nucleon selfenergy



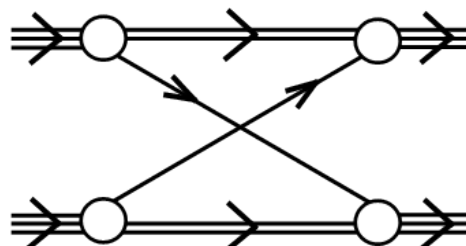
quark selfenergy



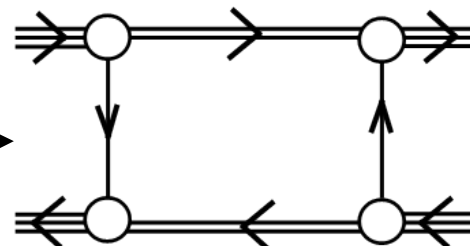
=



quark exchange interaction
between nucleons:



→



Intermezzo: Structure of the baryon?



12-Apostle
Church,
Kars

Intermezzo: Structure of the baryon?



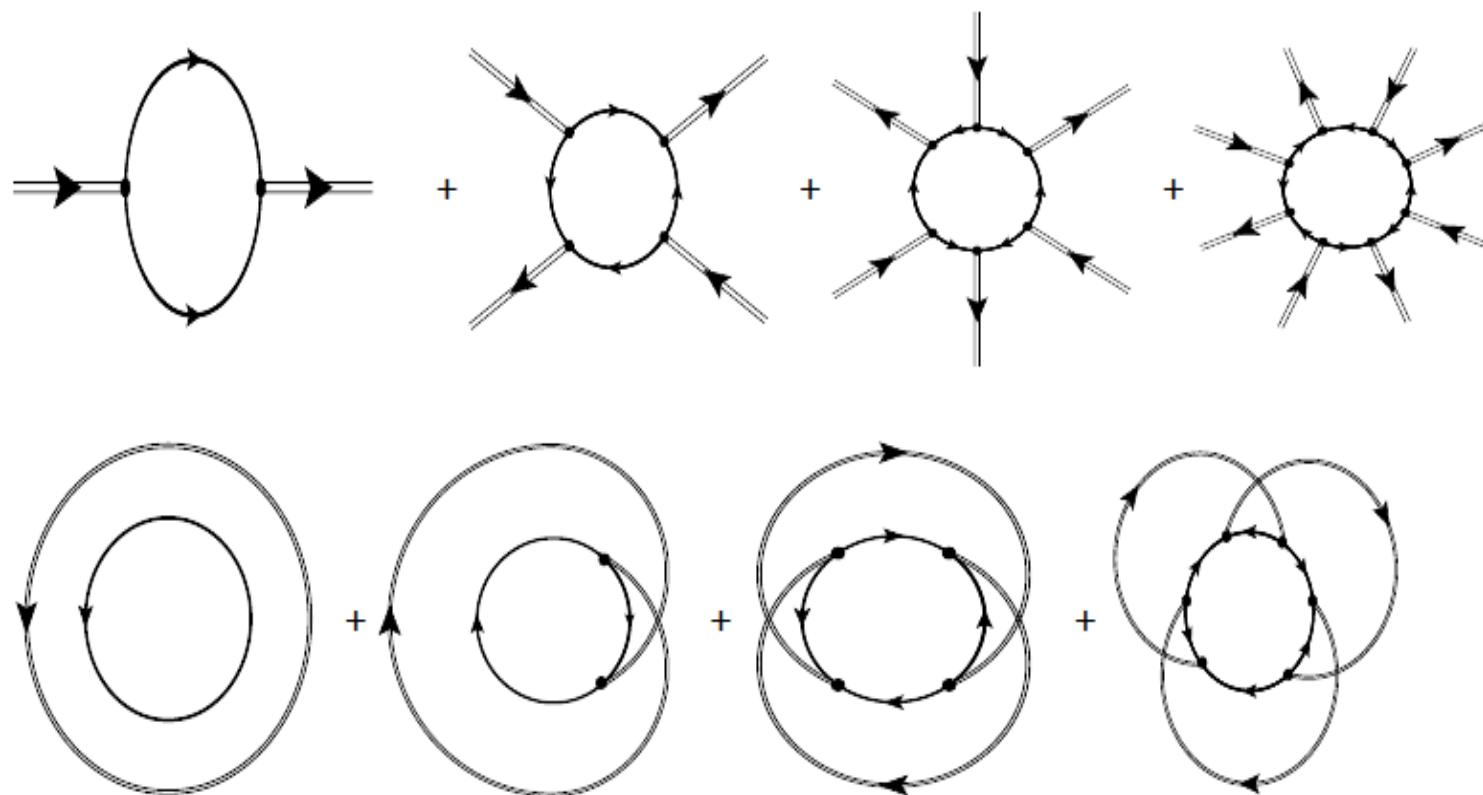
12-Apostle
Church,
Kars

Intermezzo: Structure of the baryon?

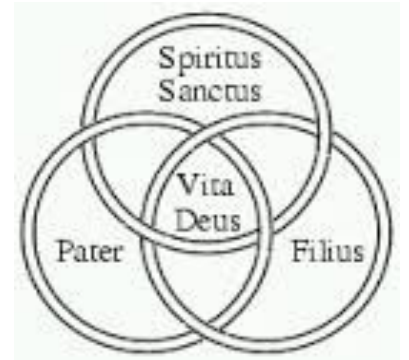
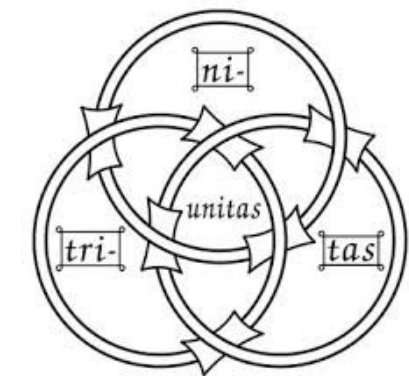
$$Z_{\text{fluct}} = \int D\Delta^\dagger D\Delta D\phi \exp\left\{-\frac{|\Delta|^2}{4G_D} - \frac{\phi^2}{4G} - Tr \ln S^{-1}[\Delta, \Delta^\dagger, \phi]\right\}$$

Cahill, Roberts, Prashifka: Aust. J. Phys. 42 (1989) 129, 161

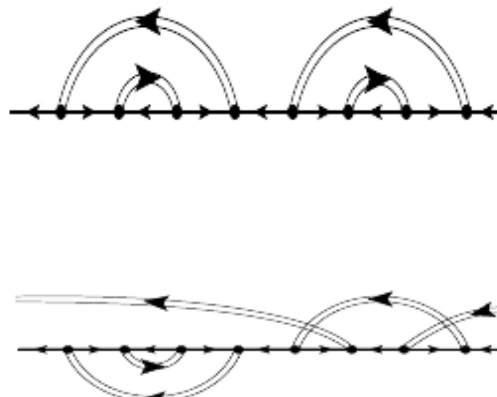
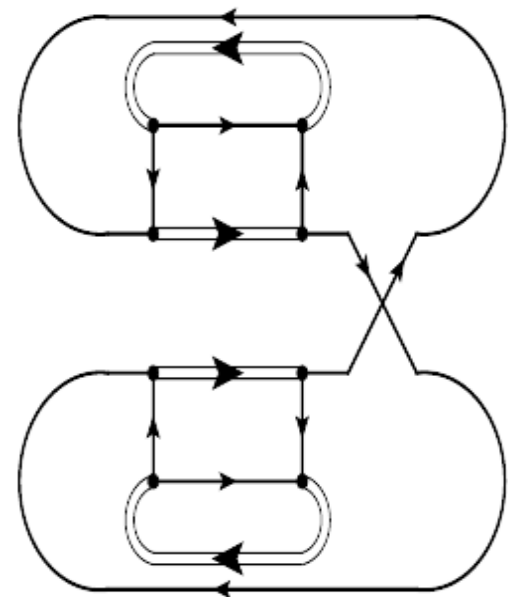
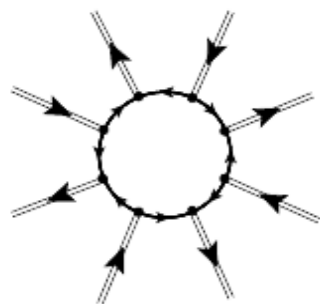
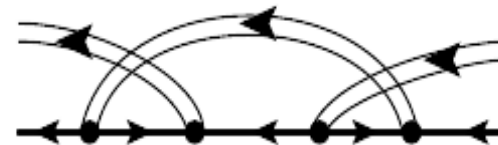
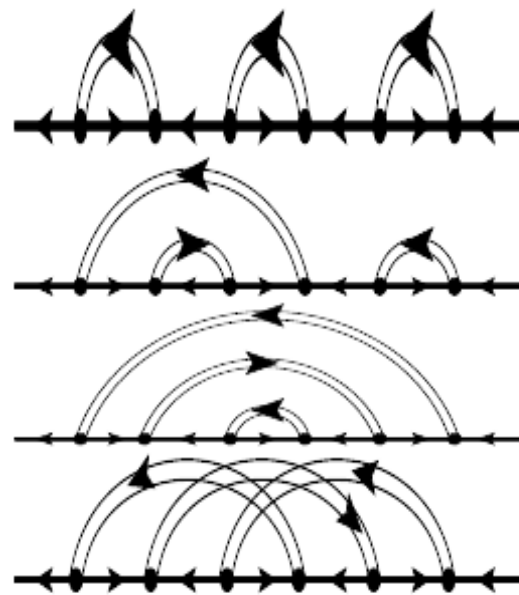
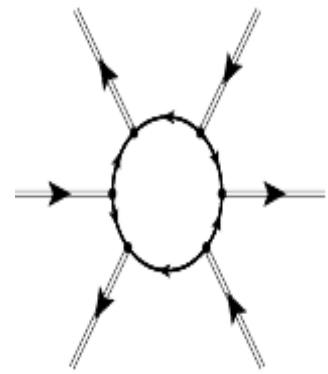
Cahill, ibid, 171; Reinhardt: PLB 244 (1990) 316; Buck, Alkofer, Reinhardt: PLB 286 (1992) 29



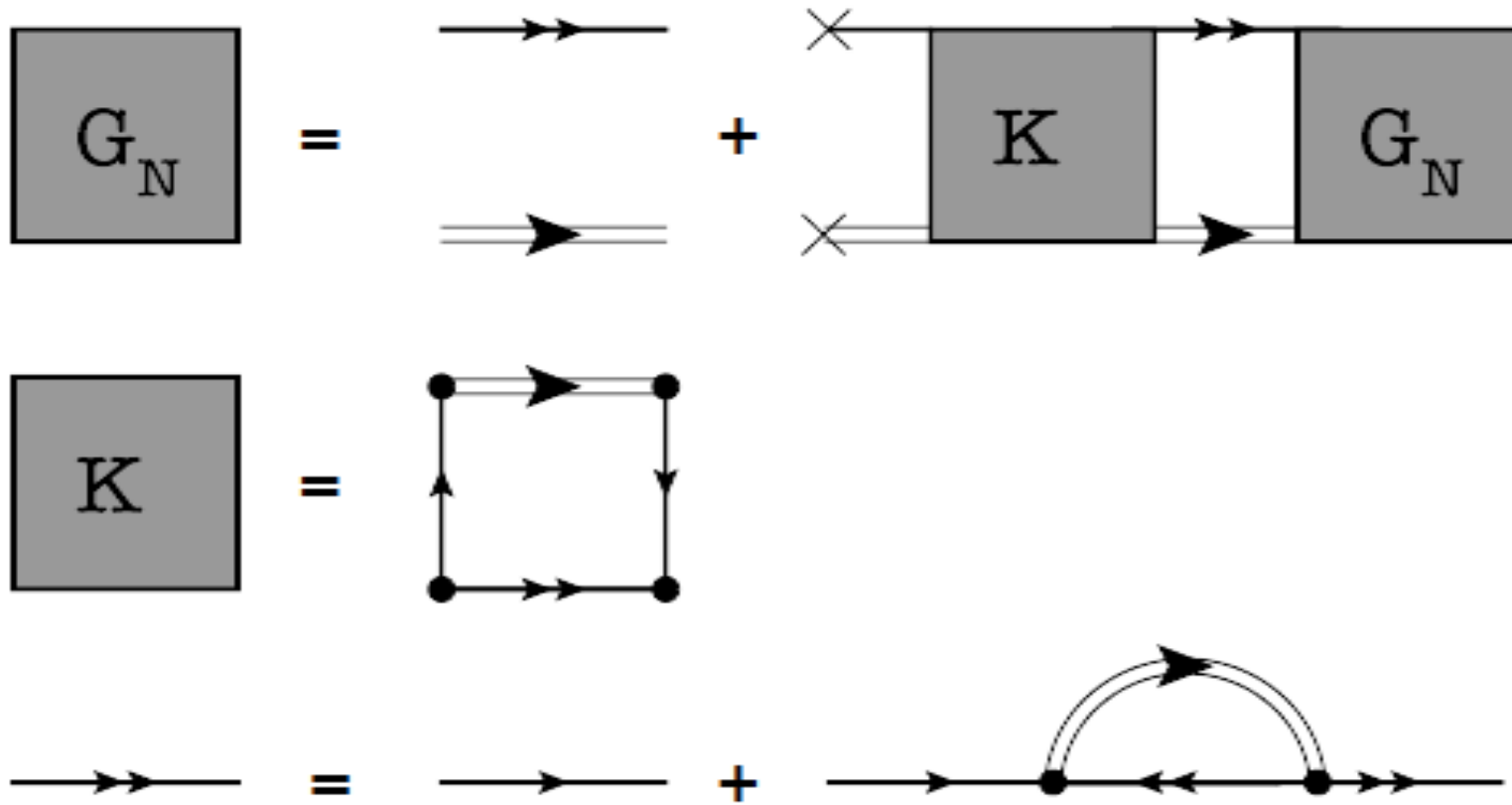
Borromean ? !!



Intermezzo: Structure of the baryon?



Intermezzo: Structure of the baryon?



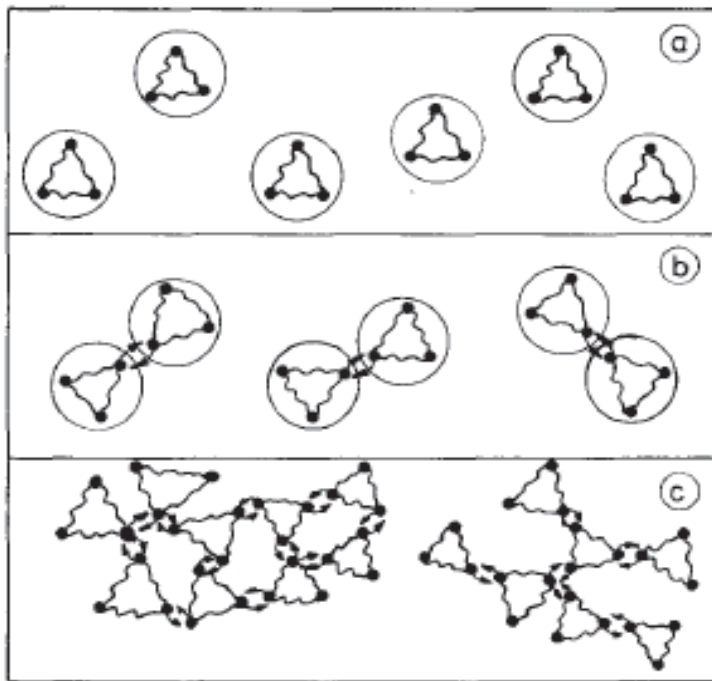
Generalized Bethe-Salpeter equation for the baryon

Dyson-Schwinger equation for the quarks ... important:

Bethe-Salpeter (RPA) equation for the diquark propagator must be **consistent** !

==> see the Phi- derivable approach !

4. Example C: Pauli blocking among baryons

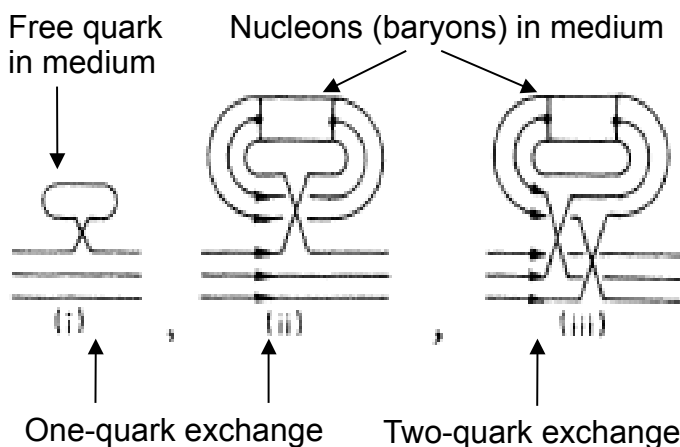


a) Low density: Fermi gas of nucleons (baryons)

b) ~ saturation: Quark exchange interaction and Pauli blocking among nucleons (baryons)

c) high density: Quark cluster matter (string-flip model ...)

Roepke & Schulz, Z. Phys. C 35, 379 (1987); Roepke, DB, Schulz, PRD 34, 3499 (1986)



Nucleon (baryon) self-energy --> Energy shift

$$\begin{aligned} \Delta E_{\nu P}^{\text{Pauli}} = & \sum_{123} |\psi_{\nu P}(123)|^2 [E(1)+E(2)+E(3)-E_{\nu P}^0] [f_{a_1}(1)+f_{a_2}(2)+f_{a_3}(3)] \\ & + \sum_{123} \sum_{456} \sum_{\nu P'} \psi_{\nu P}^*(123) \psi_{\nu P'}(456) f_3(E_{\nu P'}^0) \{ \delta_{36} \psi_{\nu P}(123) \psi_{\nu P'}^*(456) - \psi_{\nu P}(453) \psi_{\nu P'}^*(126) \} \\ & \times [E(1)+E(2)+E(3)+E(4)+E(5)+E(6)-E_{\nu P}^0-E_{\nu P'}^0] \\ = & \Delta E_{\nu P}^{\text{Pauli, free}} + \Delta E_{\nu P}^{\text{Pauli, bound}}. \end{aligned}$$



PHYSICAL REVIEW D

VOLUME 34, NUMBER 11

1 DECEMBER 1986

Pauli quenching effects in a simple string model of quark/nuclear matter

G. Röpke and D. Blaschke

Department of Physics, Wilhelm-Pieck-Universität, 2500 Rostock, German Democratic Republic

H. Schulz

*Central Institute for Nuclear Research, Rossendorf, 8051 Dresden, German Democratic Republic
and The Niels Bohr Institute, 2100 Copenhagen, Denmark*

(Received 16 December 1985)

4. Example C: Pauli blocking in NM - details

$$\Sigma_\nu(p, p_{Fn}, p_{Fp}) = \sum_{\nu'=\{n,p\}} \sum_{\alpha=1,2} C_{\nu\nu'}^{(\alpha)} W_\alpha(p_{F\nu'}, p)$$

$$W_\alpha(p_{F\nu'}, p) = \frac{\Omega}{2\pi^2} \int_0^{p_{F\nu'}} p'^2 \bar{V}^{(\alpha)}(p, p') dp';$$

$$\bar{V}^{(\alpha)}(p, p') = \frac{1}{2} \int_{-1}^1 V^{(\alpha)}(\vec{p}, \vec{p}') dz;$$

$$V^{(\alpha)}(\vec{p}, \vec{p}') = \frac{V_0 b}{\Omega m} \left(\frac{15}{2} - \lambda_\alpha^2 (\vec{p} - \vec{p}')^2 \right) \exp(-\lambda_\alpha^2 (\vec{p} - \vec{p}')^2).$$

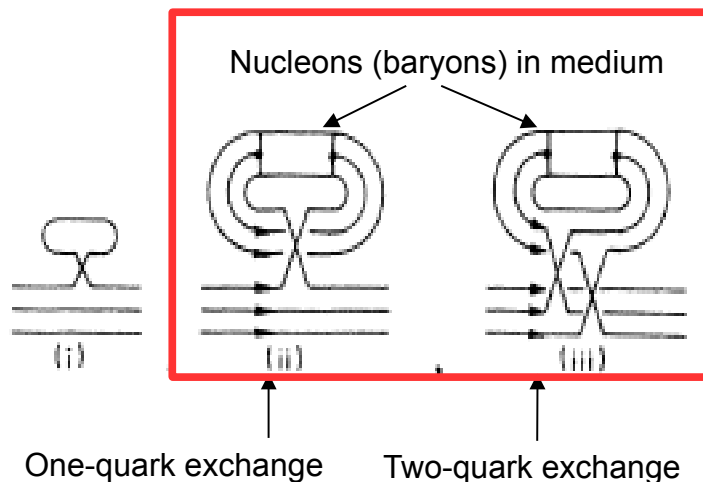
	$C_n^{(1)\nu}$	$C_n^{(2)\nu}$
neutron	$-\frac{96}{243}$	$\frac{10}{27}$
proton	$-\frac{28}{81}$	$\frac{8}{27}$

$$b^{-2} = \sqrt{3}m\omega$$

$$\omega = 178.425 \text{ MeV}$$

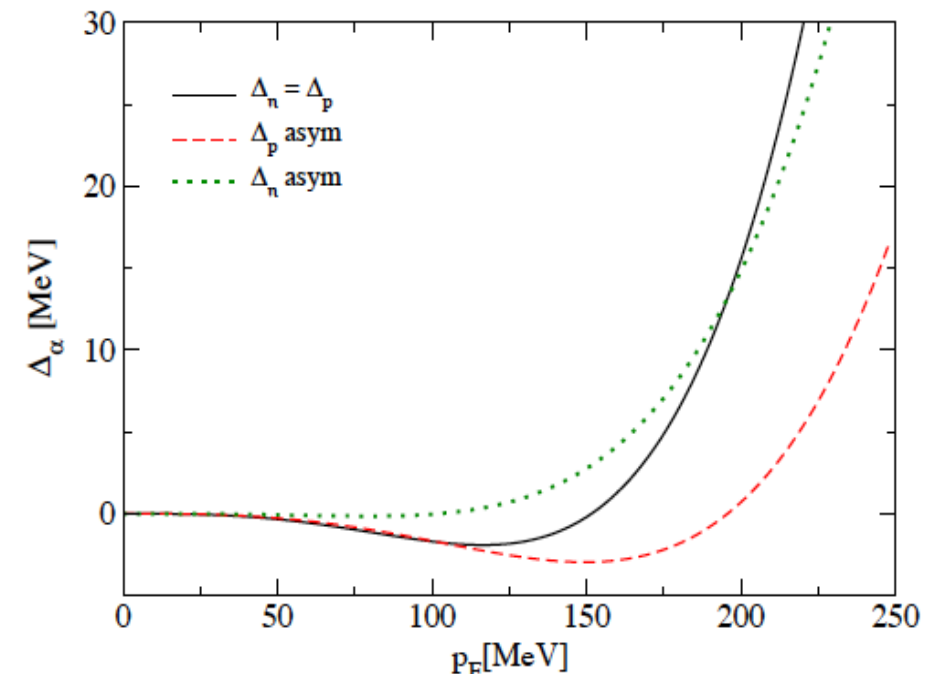
$$m = 350 \text{ MeV} \quad b = 0.6 \text{ fm}$$

$$V_0 = \frac{9\sqrt{3}\pi^{3/2}}{2} \text{ and } \lambda_\alpha = \frac{b}{\sqrt{3}\alpha}.$$



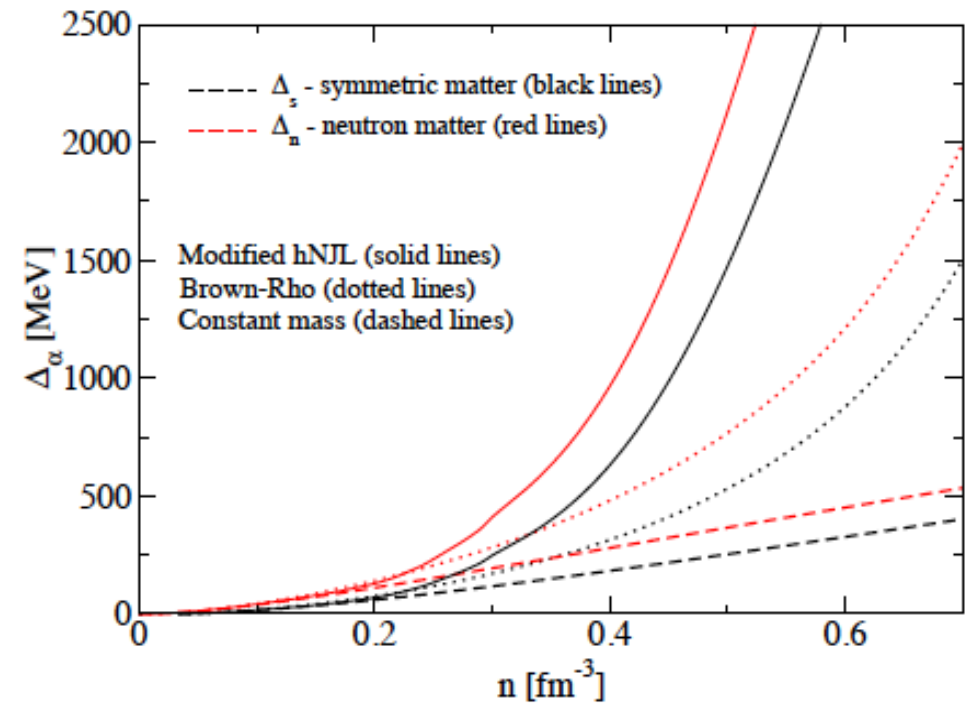
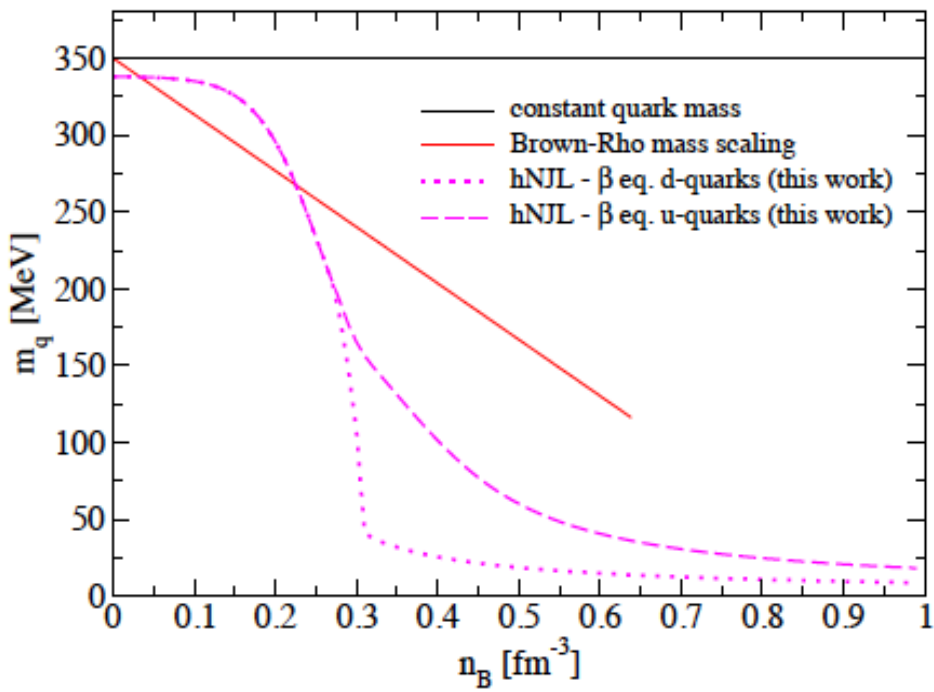
$$W_\alpha(p_{F\nu'}, p) = \frac{V_0 b}{32\pi^2 \lambda_\alpha^4 m} \{ 12\lambda_\alpha \sqrt{\pi} [\operatorname{erf}(\lambda_\alpha(p_{F\nu'} - p)) + \operatorname{erf}(\lambda_\alpha(p_{F\nu'} + p))] \\ + \frac{1}{p} [(11 - 2\lambda_\alpha^2 p_{F\nu'}(p_{F\nu'} + p)) e^{-\lambda_\alpha^2(p_{F\nu'} + p)^2} \\ + (11 - 2\lambda_\alpha^2 p_{F\nu'}(p_{F\nu'} - p)) e^{-\lambda_\alpha^2(p_{F\nu'} - p)^2}] \}$$

$$\Delta_{\nu_A, P}^{Pauli} = \frac{1}{24\sqrt{3}\pi} \frac{b}{m} \sum_{\nu'} [15a_{\nu,\nu'} P_F(\nu')^3 + \frac{17}{12}b_{\nu,\nu'} b^2 (P_F^2 + P_F(\nu')^2) P_F(\nu')^3]$$



4. Example C: Pauli blocking in NM – details

New aspect: chiral restoration --> dropping quark mass



**Increased baryon swelling at supersaturation densities:
--> dramatic enhancement of the Pauli repulsion !!**

4. Example C: Pauli blocking in NM – results

New EoS: Joining RMF (Linear Walecka) for pointlike baryons with chiral Pauli blocking

$$p = \frac{1}{4\pi^2} \sum_{\nu} \left[-E_{\nu}^* m_{\nu}^{*2} p_{F\nu} + \frac{2}{3} E_{\nu}^* p_{F\nu}^3 + m_{\nu}^{*4} \log \left(\frac{E_{\nu}^* + p_{F\nu}}{m_{\nu}^*} \right) \right]$$

$$+ \frac{1}{2} \left(\frac{g_{\omega}}{m_{\omega}} \right)^2 n^2 - \frac{1}{2} \left(\frac{g_{\sigma}}{m_{\sigma}} \right)^2 n_s^2 + p_{ex};$$

$$\epsilon = \frac{1}{4\pi^2} \sum_{\nu} \left[2 E_{\nu}^{*3} p_{F\nu} - E_{\nu}^* m_{\nu}^{*2} p_{F\nu} - m_{\nu}^{*4} \log \left(\frac{E_I^* + p_{F\nu}}{m_{\nu}^*} \right) \right]$$

$$+ \frac{1}{2} \left(\frac{g_{\omega}}{m_{\omega}} \right)^2 n^2 + \frac{1}{2} \left(\frac{g_{\sigma}}{m_{\sigma}} \right)^2 n_s^2 + \epsilon_{ex},$$

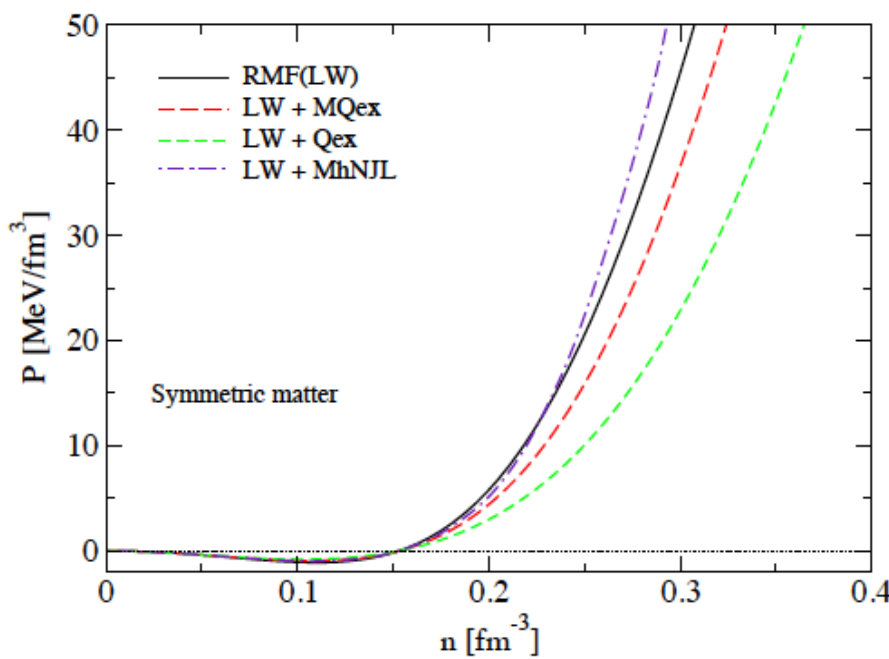
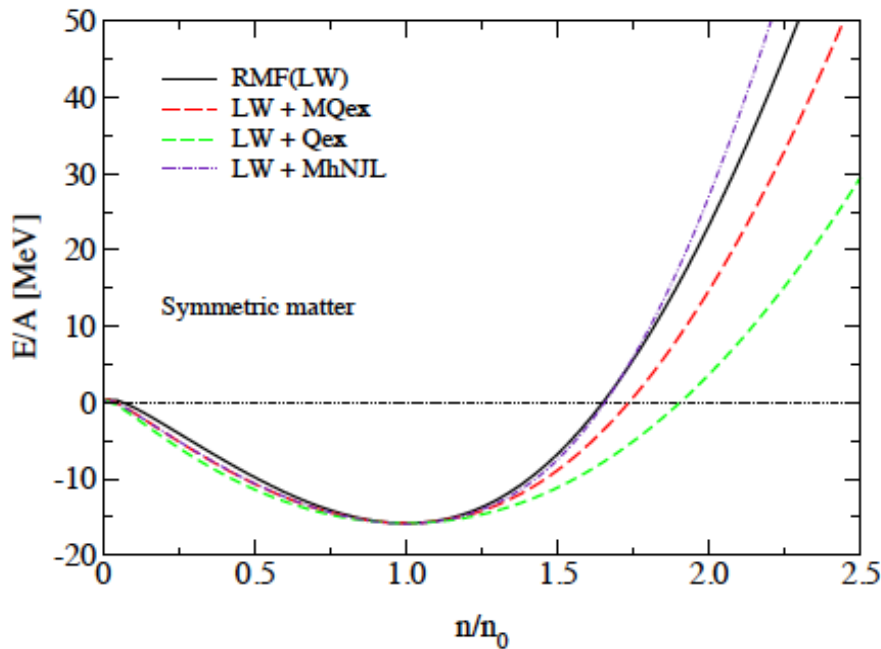
$$\mu_{ex,\nu} = \Delta_{\nu}(n, x) = \Sigma_{\nu}(p_{F,\nu}; p_{Fn}, p_{Fp}),$$

$$\epsilon_{ex} = \sum_{\nu} \int_0^n dn' \{x \Delta_p(n', x) + (1-x) \Delta_n(n', x)\},$$

$$p_{ex} = \sum_{\nu} \mu_{ex,\nu} n_{\nu} - \epsilon_{ex},$$

$$\begin{aligned} n_{s,\nu} &= \frac{m_{\nu}^*}{\pi^2} \left[E_{\nu}^* p_{F\nu} - m_{\nu}^{*2} \log \left(\frac{E_{\nu}^* + p_{F\nu}}{m_{\nu}^*} \right) \right], \\ E_{\nu}^* &= \sqrt{m_{\nu}^{*2} + p_{F\nu}^2} \\ n_{\nu} &= \frac{p_{F\nu}^3}{3\pi^2}, \\ m_{\nu}^* &= m_{\nu} - \left(\frac{g_{\sigma}}{m_{\sigma}} \right)^2 n_{s,\nu}, \\ \mu_{\nu} &= E_{\nu}^* + \left(\frac{g_{\omega}}{m_{\omega}} \right)^2 n_{\nu} + \mu_{ex,\nu}. \end{aligned}$$

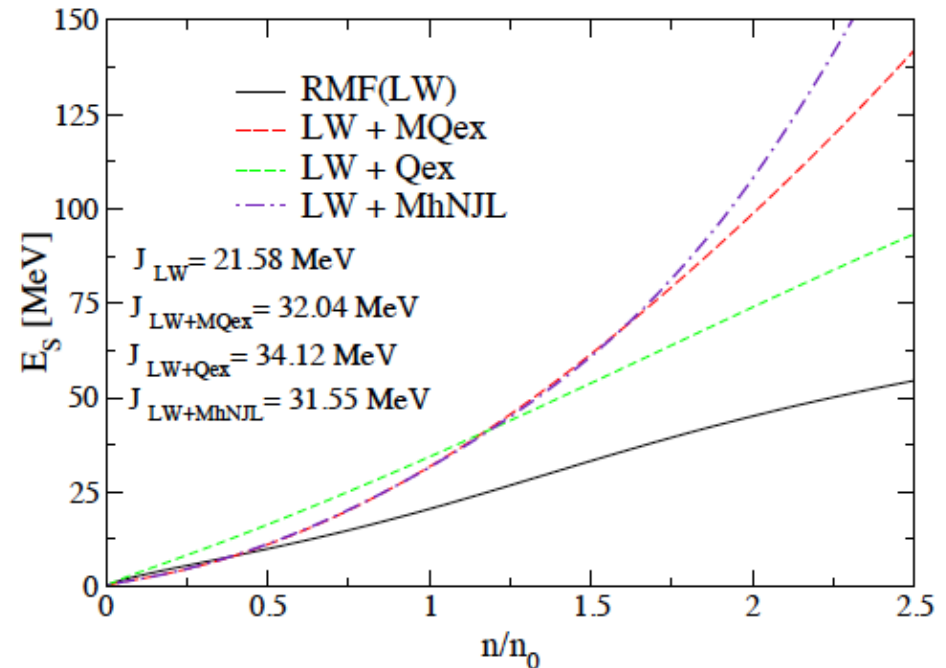
4. Example C: Pauli blocking in NM – results



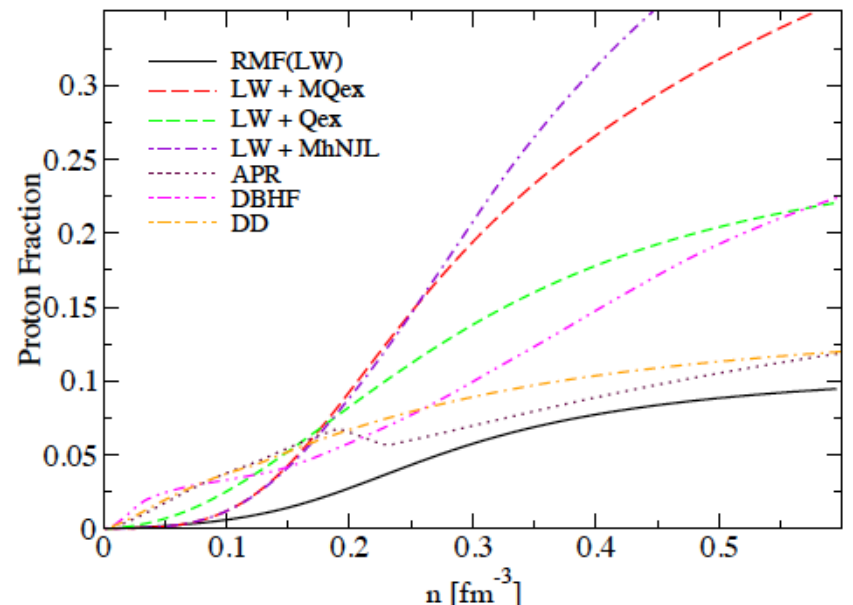
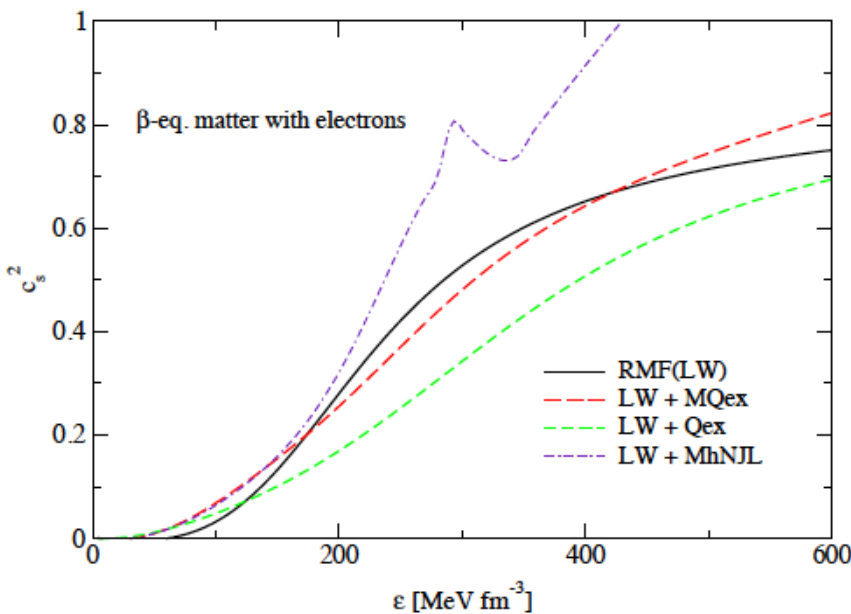
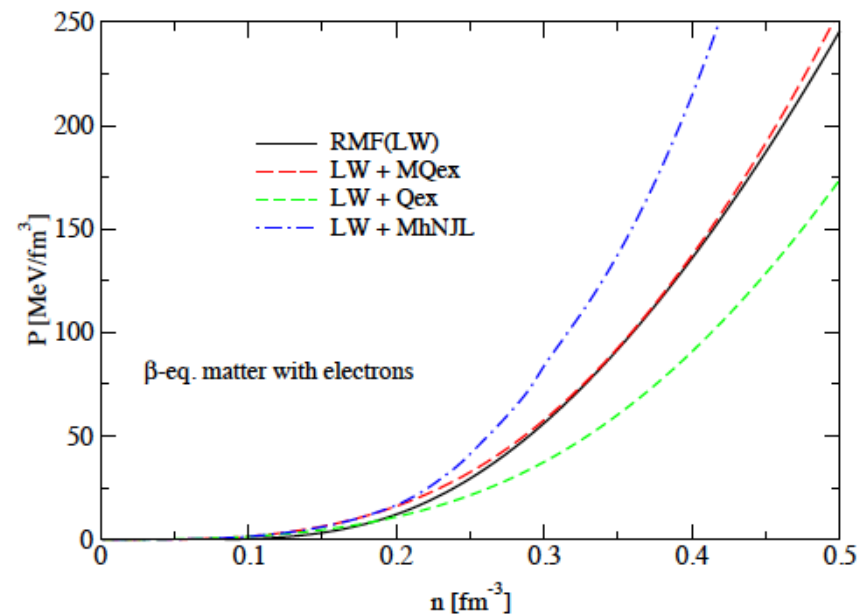
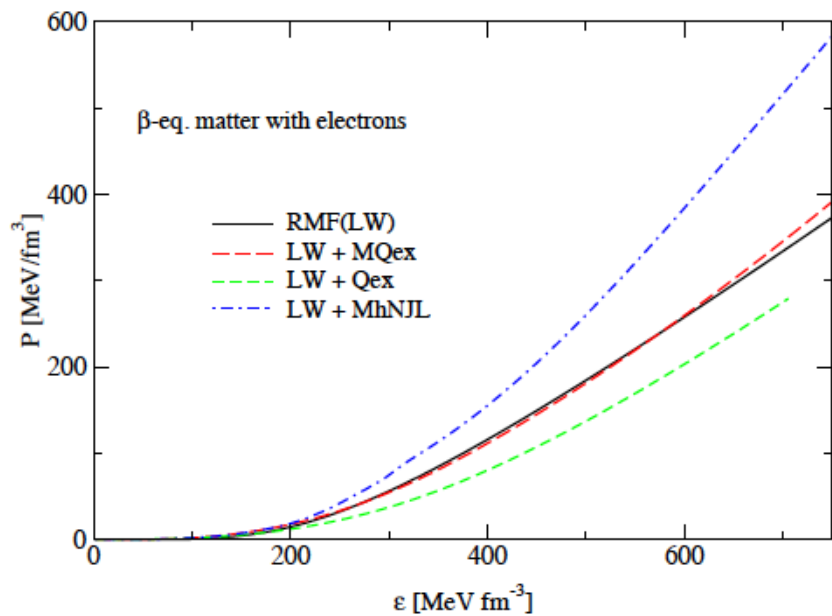
Parametrization: from saturation properties

	$(g_\omega/m_\omega)^2 [\text{fm}^2]$	$(g_\sigma/m_\sigma)^2 [\text{fm}^2]$
RMF (LW)	11.6582	15.2883
LW+Qex	6.11035	9.91197
LW+MQex	6.59170	13.29118
LW+MhNJL	9.25683	13.9474

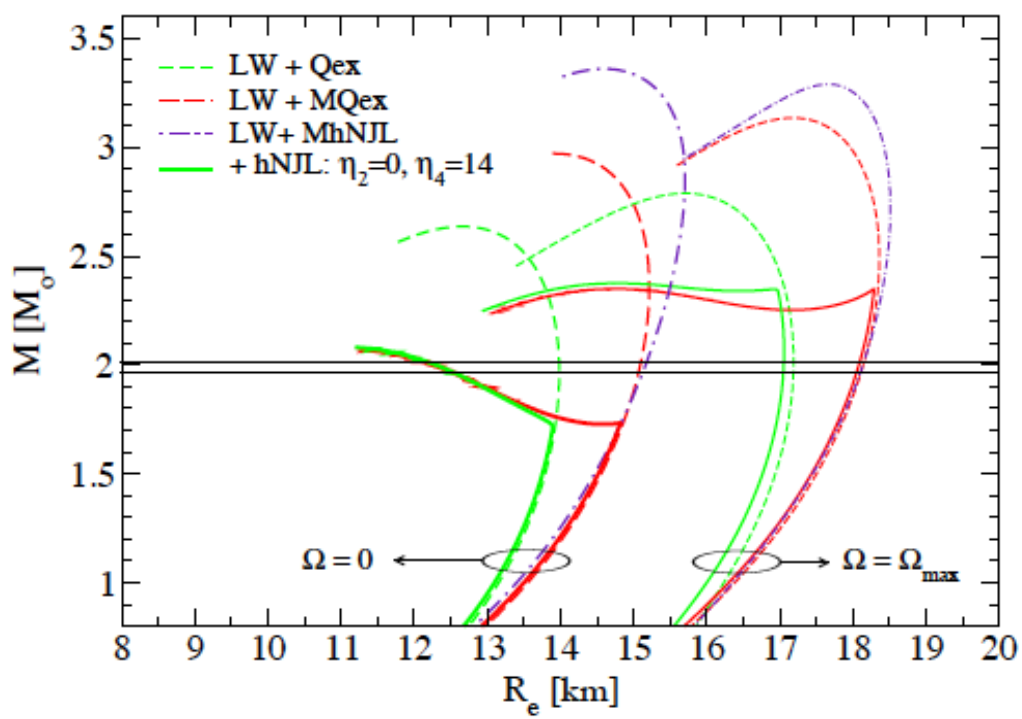
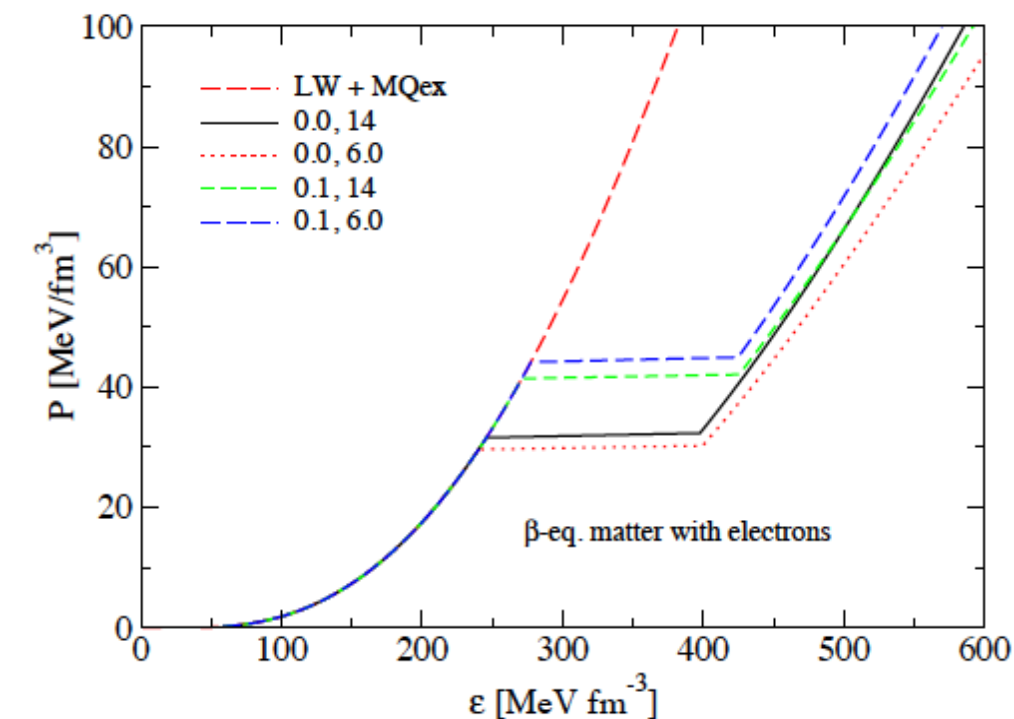
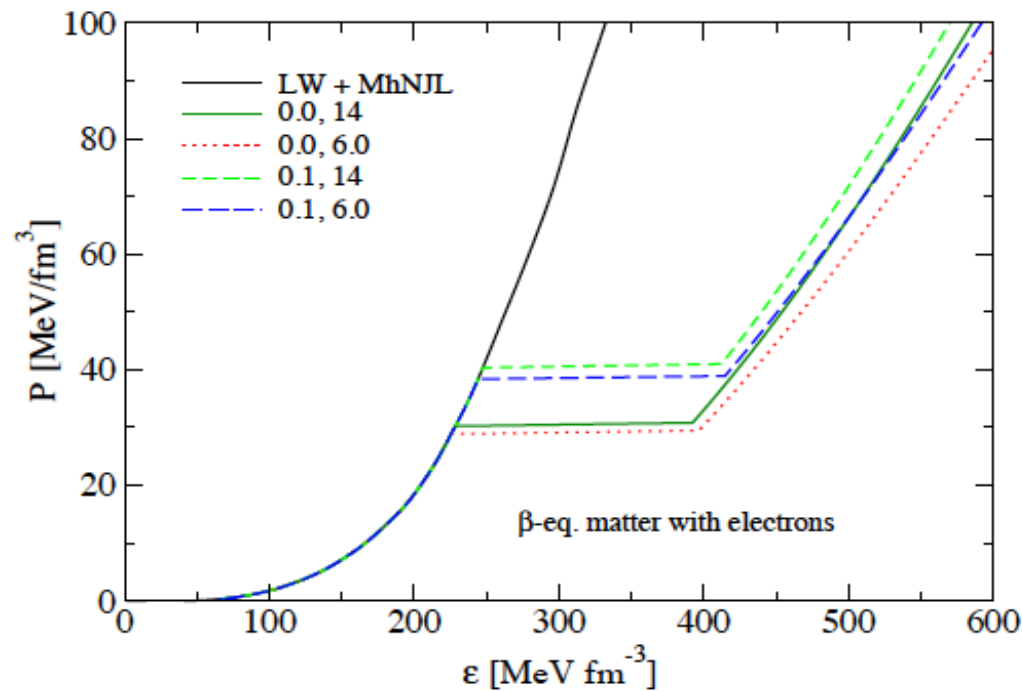
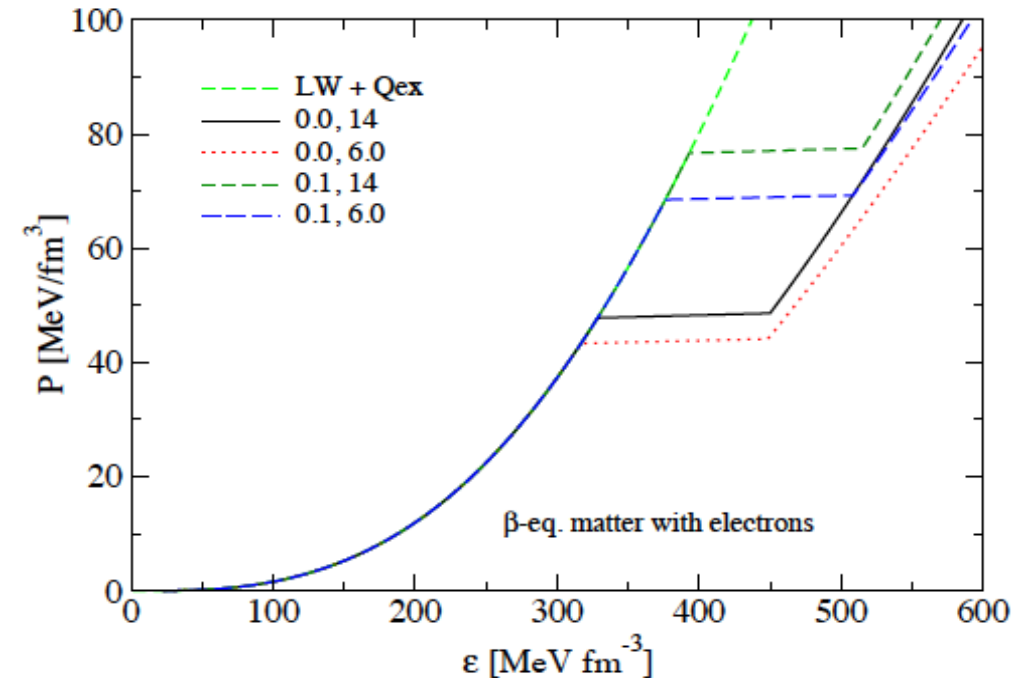
Prediction: symmetry energy



4. Example C: Pauli blocking in NM – results



4. Example C: Pauli blocking in NM – results



4. Example C: Pauli blocking in NM – Summary

Pauli blocking selfenergy (cluster meanfield) calculable in potential models for baryon structure

Partial replacement of other short-range repulsion mechanisms (vector meson exchange)

Modern aspects:

- onset of chiral symmetry restoration enhances nucleon swelling and Pauli blocking at high n
- quark exchange among baryons -> six-quark wavefunction -> “bag melting” -> deconfinement

Chiral stiffening of nuclear matter --> reduces onset density for deconfinement

Hybrid EoS:

Convenient generalization of RMF models,

Take care: eventually aspects of quark exchange already in density dependent vertices!

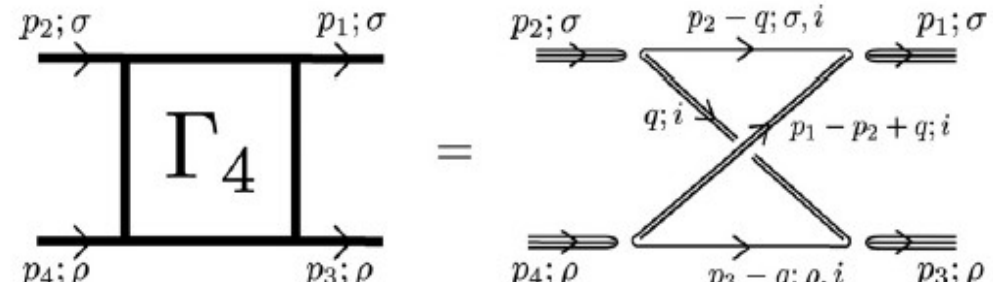
Other baryons:

- hyperons
- deltas

Again calculable, partially done in nonrelativistic quark exchange models, chiral effects not yet!

Relativistic generalization:

Box diagrams of quark-diquark model ...



4a. Pauli blocking effect → Excluded volume

Well known from modeling dissociation of clusters in the supernova EoS:

- excluded volume: Lattimer-Swesty (1991), Shen-Toki-Oyematsu-Sumiyoshi (1996), ...
- Pauli blocking: Roepke-Grigo-Sumiyoshi-Shen (2003), Typel et al. PRC 81 (2010)
- excl. Vol. vs. Pauli blocking: Hempel, Schaffner-Bielich, Typel, Roepke PRC 84 (2011)

Here: nucleons as quark clusters with finite size --> excluded volume effect !

$$\text{Available volume fraction: } \Phi = V_{\text{av}}/V = 1 - v \sum_{i=n,p} n_i, \quad v = \frac{1}{2} \frac{4\pi}{3} (2r_{\text{nuc}})^3 = 4V_{\text{nuc}}$$

$$\text{Equations of state for T=0 nuclear matter: } p_{\text{tot}}(\mu_n, \mu_p) = \frac{1}{\Phi} \sum_{i=n,p} p_i + p_{\text{mes}},$$

$$E_{\text{tot}}(\mu_n, \mu_p) = -p_{\text{tot}} + \sum_{i=n,p} \mu_i n_i,$$

$$p_i = \frac{1}{4} (E_i n_i - m_i^* n_i^{(s)}),$$

$$\text{Effective mass: } m_i^* = m_i - S_i.$$

$$n_i = \frac{\Phi}{3\pi^3} k_i^3,$$

$$n_i^{(s)} = \frac{\Phi m_i^*}{2\pi^2} \left[E_i k_i - (m_i^*)^2 \ln \frac{k_i + E_i}{m_i^*} \right],$$

$$\text{Scalar meanfield: } S_i \sim n_i^{(s)}$$

$$E_i = \sqrt{k_i^2 + (m_i^*)^2} = \mu_i - V_i - \frac{v}{\Phi} \sum_{j=p,n} p_j,$$

$$\text{Vector meanfield: } V_i \sim n_i$$

4b. Stiff quark matter at high densities

S. Benic, Eur. Phys. J. A 50, 111 (2014)

$$\mathcal{L} = \bar{q}(i\partial - m)q + \mu_q \bar{q}\gamma^0 q + \mathcal{L}_4 + \mathcal{L}_8 , \quad \mathcal{L}_4 = \frac{g_{20}}{\Lambda^2}[(\bar{q}q)^2 + (\bar{q}i\gamma_5\tau q)^2] - \frac{g_{02}}{\Lambda^2}(\bar{q}\gamma_\mu q)^2 ,$$

$$\mathcal{L}_8 = \frac{g_{40}}{\Lambda^8}[(\bar{q}q)^2 + (\bar{q}i\gamma_5\tau q)^2]^2 - \frac{g_{04}}{\Lambda^8}(\bar{q}\gamma_\mu q)^4 - \frac{g_{22}}{\Lambda^8}(\bar{q}\gamma_\mu q)^2[(\bar{q}q)^2 + (\bar{q}i\gamma_5\tau q)^2]$$

Meanfield approximation: $\mathcal{L}_{\text{MF}} = \bar{q}(i\partial - M)q + \tilde{\mu}_q \bar{q}\gamma^0 q - U ,$

$$M = m + 2\frac{g_{20}}{\Lambda^2}\langle\bar{q}q\rangle + 4\frac{g_{40}}{\Lambda^8}\langle\bar{q}q\rangle^3 - 2\frac{g_{22}}{\Lambda^8}\langle\bar{q}q\rangle\langle q^\dagger q\rangle^2 ,$$

$$\tilde{\mu}_q = \mu_q - 2\frac{g_{02}}{\Lambda^2}\langle q^\dagger q\rangle - 4\frac{g_{04}}{\Lambda^8}\langle q^\dagger q\rangle^3 - 2\frac{g_{22}}{\Lambda^8}\langle\bar{q}q\rangle^2\langle q^\dagger q\rangle ,$$

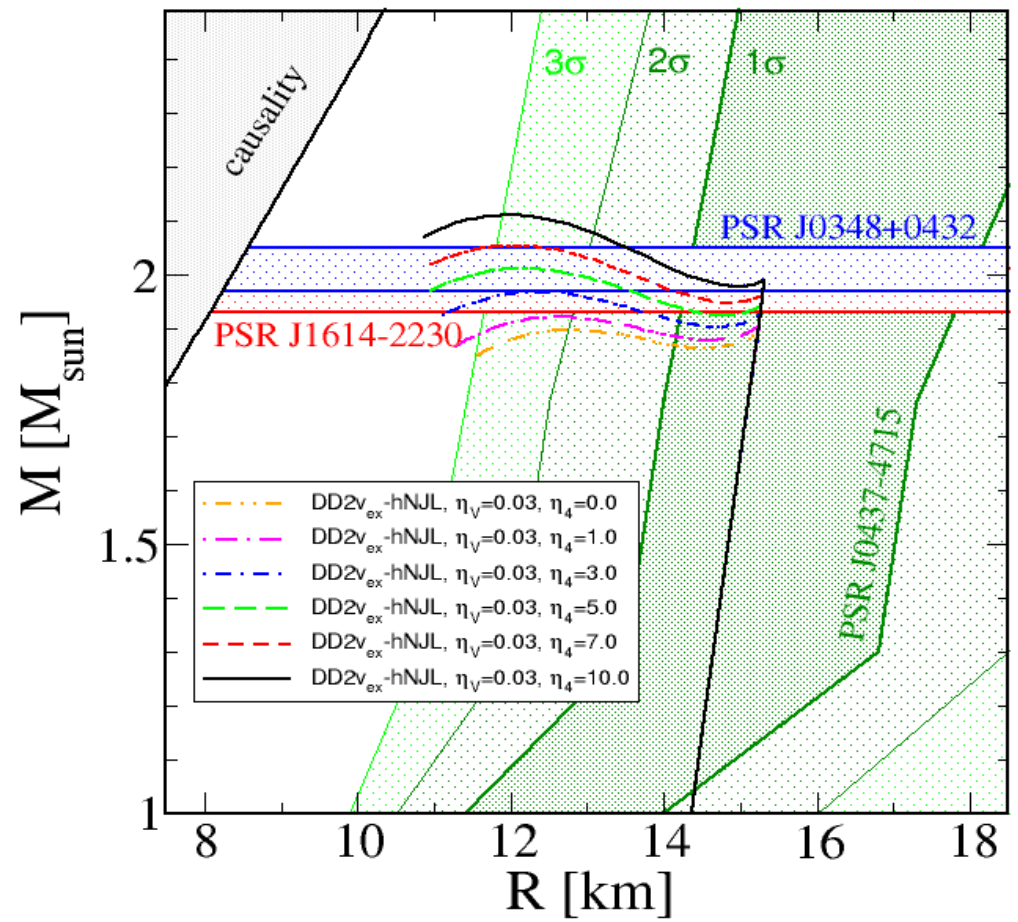
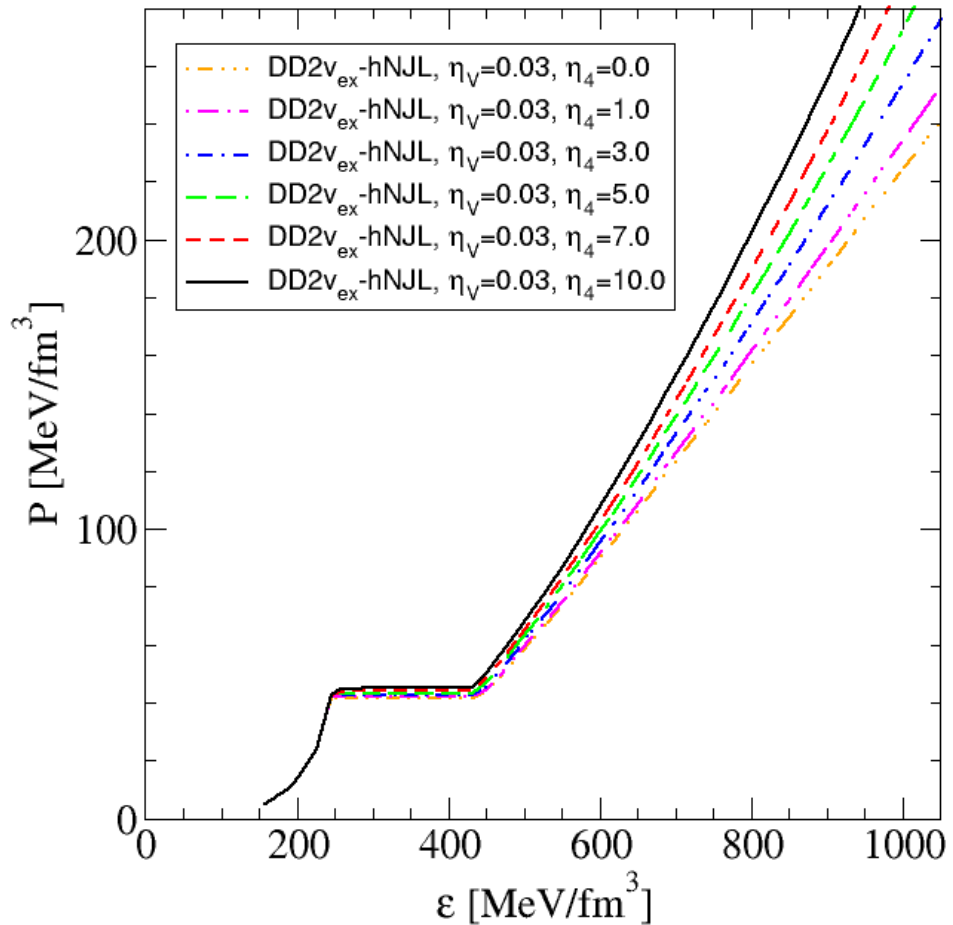
$$U = \frac{g_{20}}{\Lambda^2}\langle\bar{q}q\rangle^2 + 3\frac{g_{40}}{\Lambda^8}\langle\bar{q}q\rangle^4 - 3\frac{g_{22}}{\Lambda^8}\langle\bar{q}q\rangle^2\langle q^\dagger q\rangle^2 - \frac{g_{02}}{\Lambda^2}\langle q^\dagger q\rangle^2 - 3\frac{g_{04}}{\Lambda^8}\langle q^\dagger q\rangle^4 .$$

Thermodynamic Potential:

$$\Omega = U - 2N_f N_c \int \frac{d^3 p}{(2\pi)^3} \left\{ E + T \log[1 + e^{-\beta(E-\tilde{\mu}_q)}] + T \log[1 + e^{-\beta(E+\tilde{\mu}_q)}] \right\} + \Omega_0$$

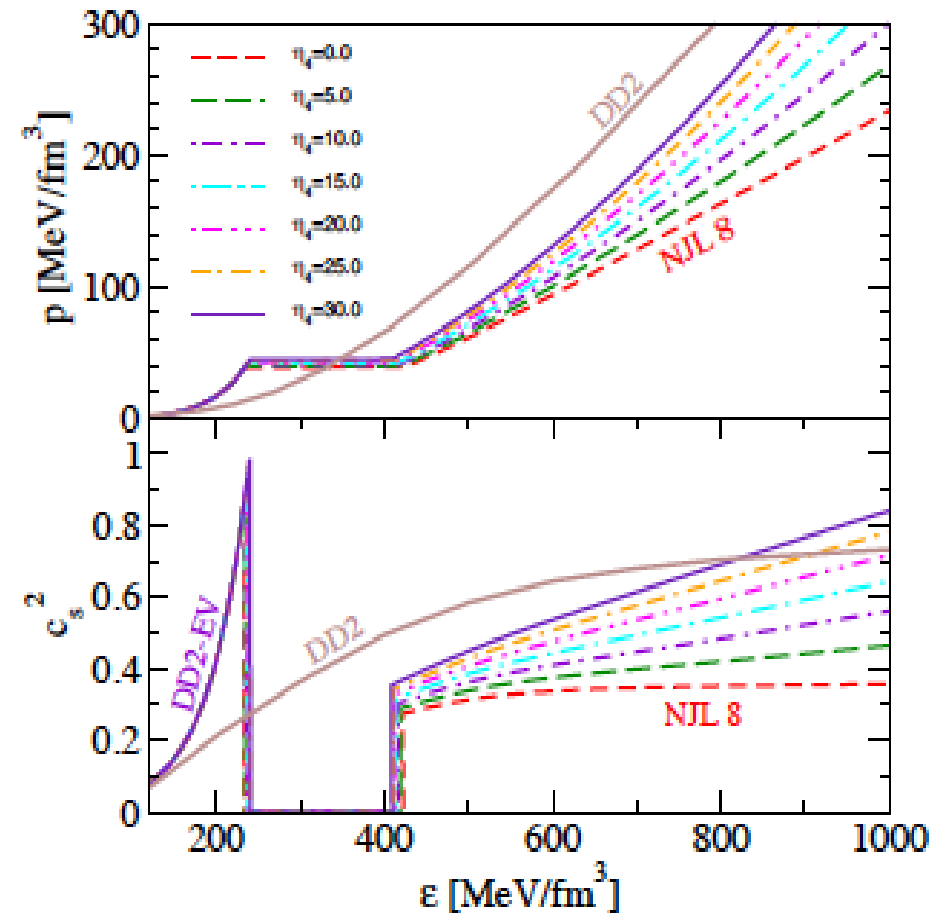
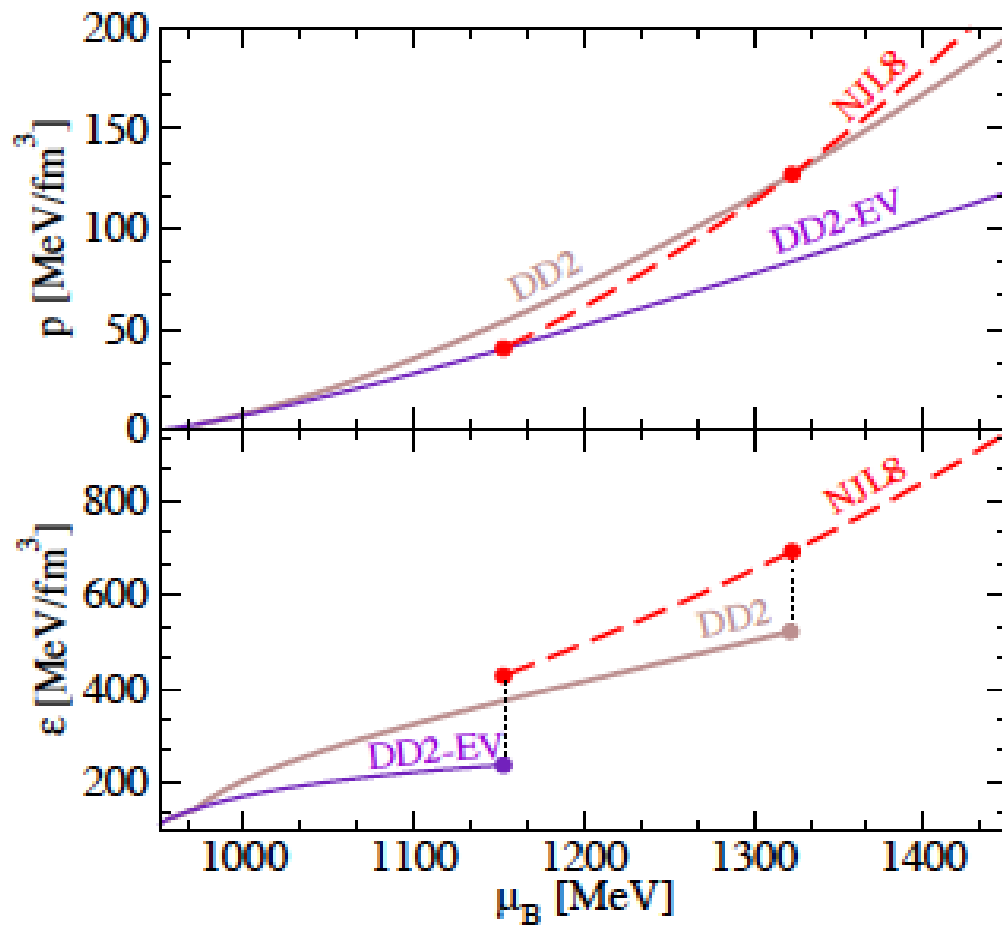
Result: high-mass twins \leftrightarrow 1st order PT

S. Benic, D. Blaschke, D. Alvarez-Castillo, T. Fischer, S. Typel, arxiv:1411.2856



Hybrid EoS supports M-R sequences with high-mass twin compact stars

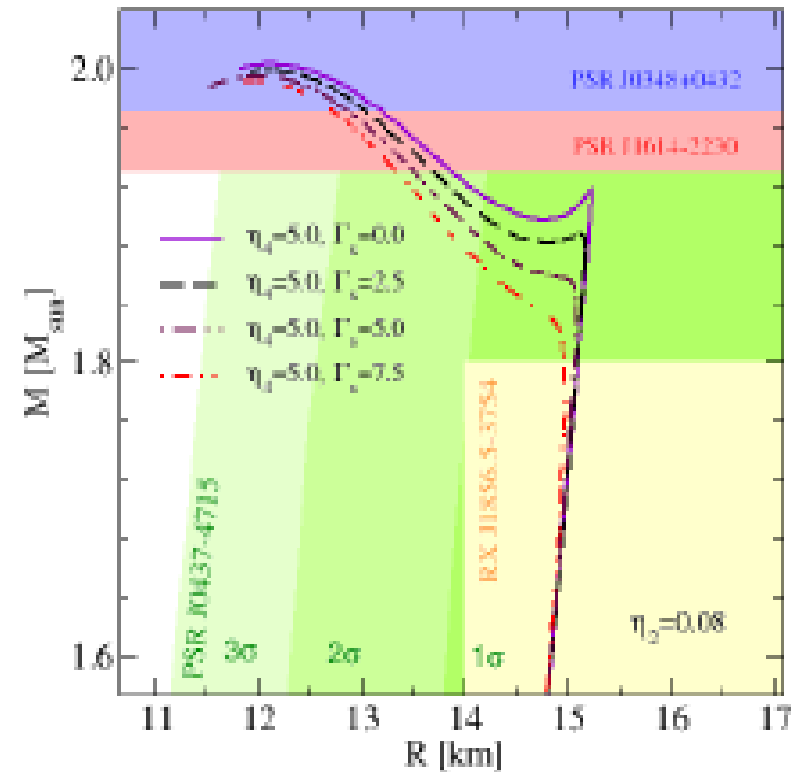
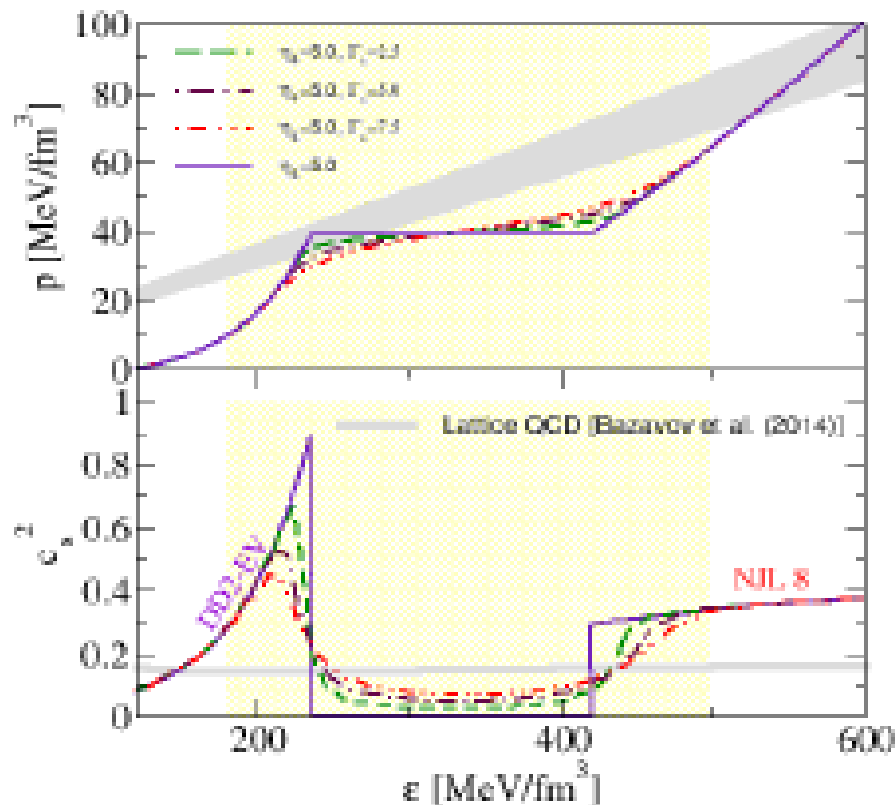
4b. Stiff quark matter at high densities



Here: Stiffening of dense hadronic matter by excluded volume in density-dependent RMF

4b. Stiff quark matter at high densities

Estimate effects of structures in the phase transition region (“pasta”)



High-mass Twins relatively robust against “smoothing” the Maxwell transition construction

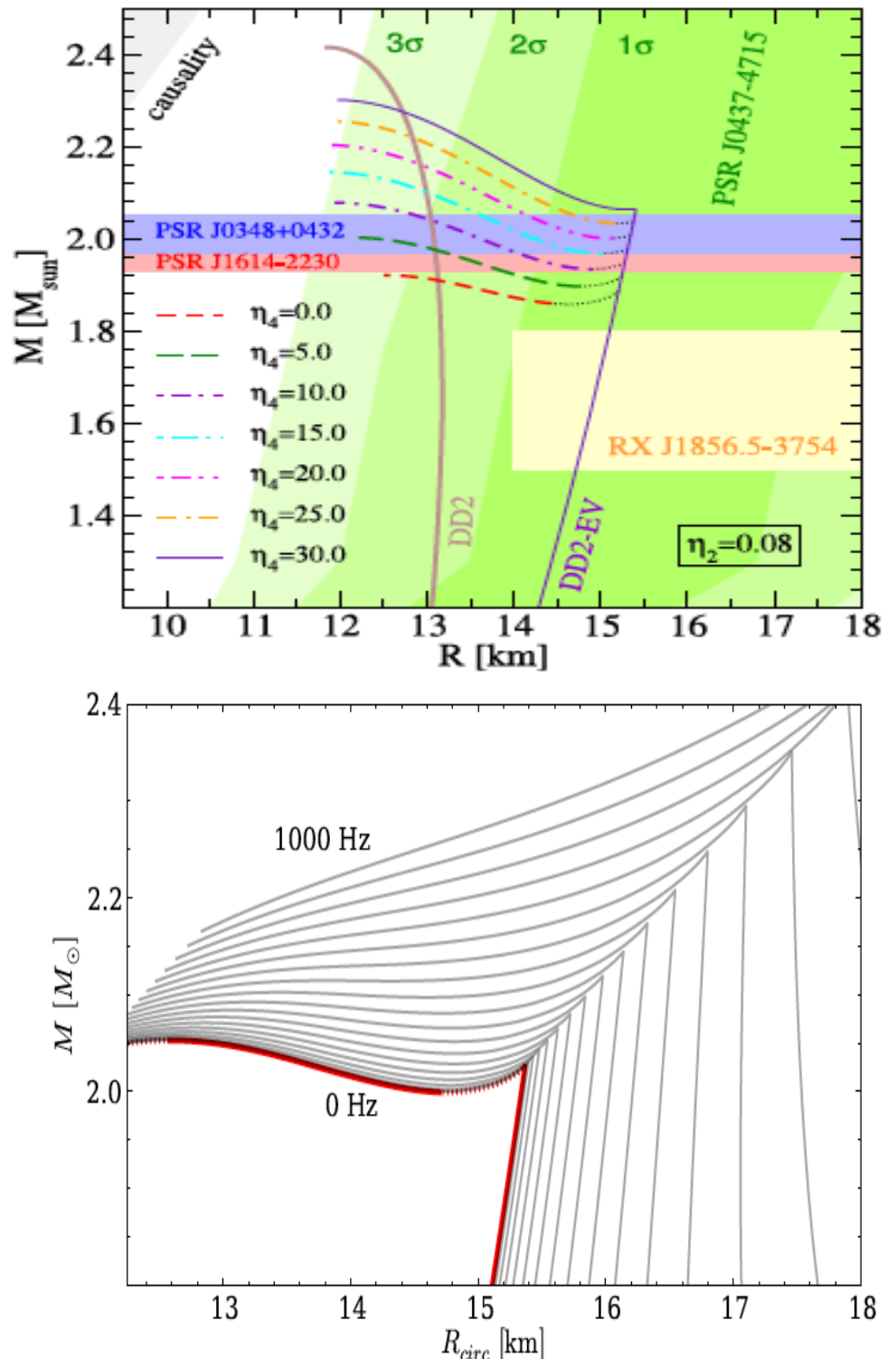
D. Alvarez-Castillo, D.B., arxiv:1412.8463

4c. Rotation

- existence of $2 M_{\text{sun}}$ pulsars and possibility of high-mass twins raises question for their inner structure:
(Q)uark or (N)ucleon core ??
--> degenerate solutions
--> transition from N to Q branch
- PSR J1614-2230 is millisecond pulsar, period $P = 3.41 \text{ ms}$, consider rotation !
- transitions N --> Q must be considered for rotating configurations:
--> how fast can they be?

(angular momentum J and baryon mass should be conserved simultaneously)
- similar scenario as fast radio bursts (Falcke-Rezzolla, 2013) or braking index (Glendenning-Pei-Weber, 1997)

M. Bejger, D.B., work in preparation (2015)



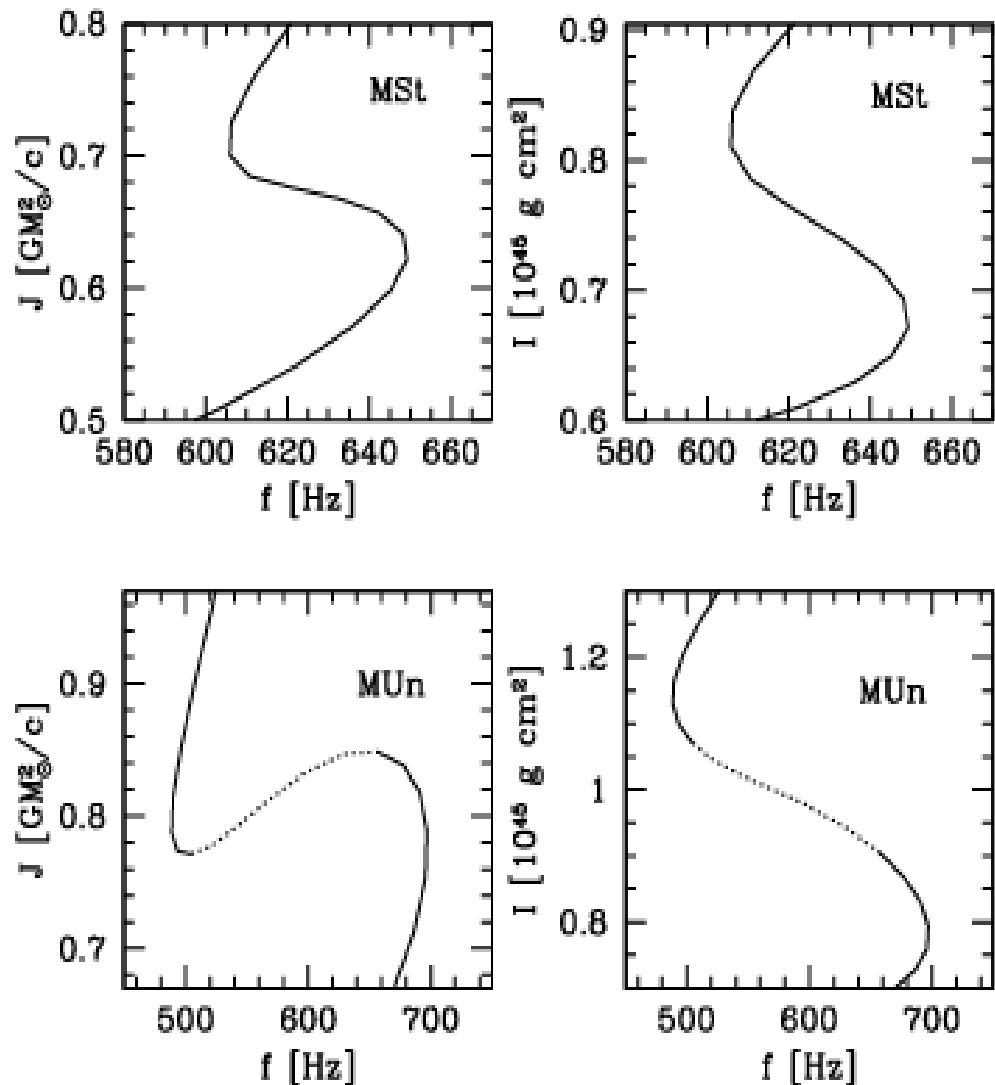
4c. Rotation and stability

- ★ Back-bending is connected to the existence of a minimum of M_b along $f = \text{const.}$ sequence,
- ★ Change in stability corresponds to extremum of M or M_b at fixed J :

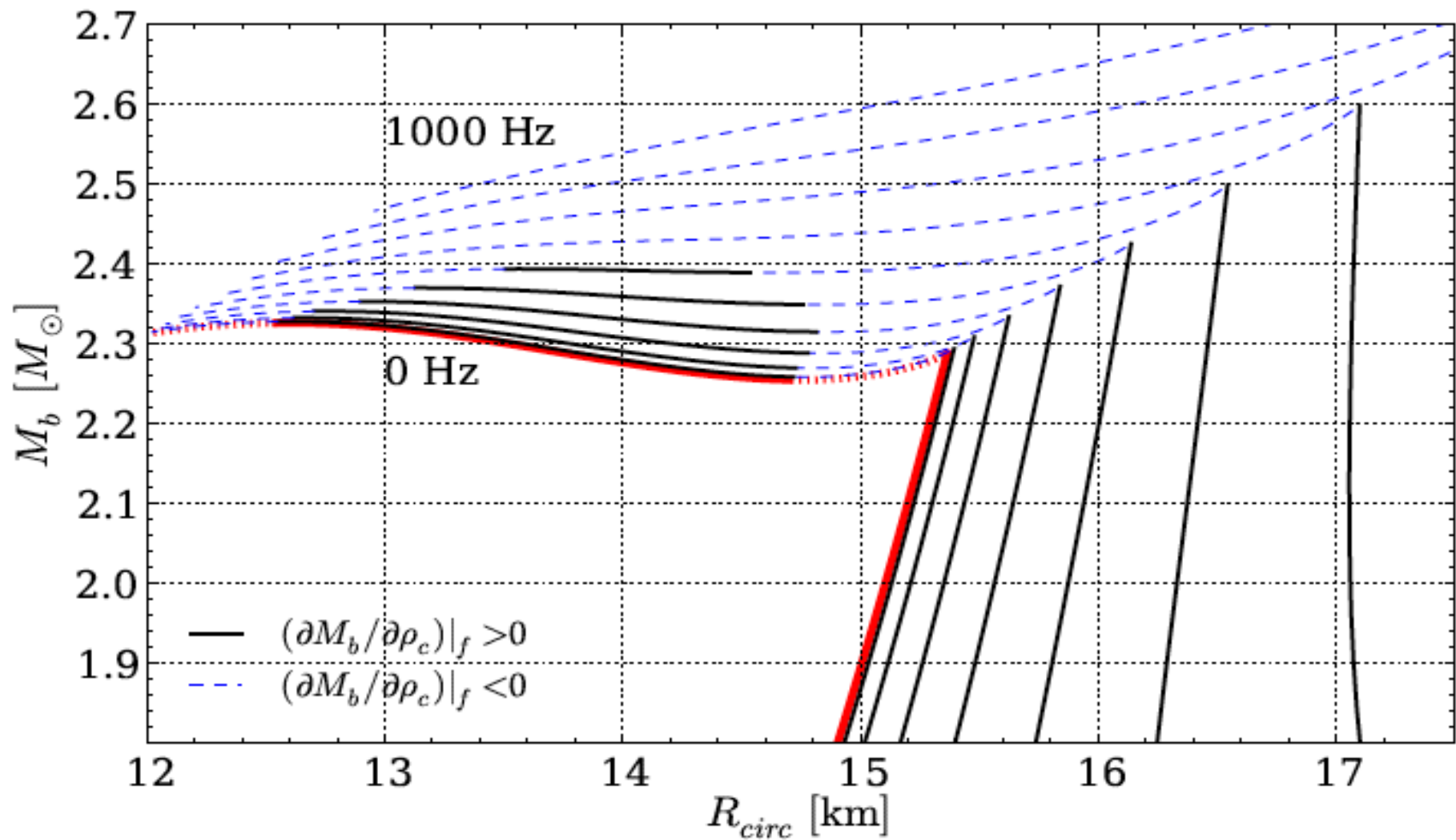
$$\left(\frac{\partial M}{\partial \lambda_c} \right)_J = 0, \quad \left(\frac{\partial M_b}{\partial \lambda_c} \right)_J = 0,$$

or to extremum of J at fixed either M or M_b :

$$\left(\frac{\partial J}{\partial \lambda_c} \right)_M = 0, \quad \left(\frac{\partial J}{\partial \lambda_c} \right)_{M_b} = 0.$$

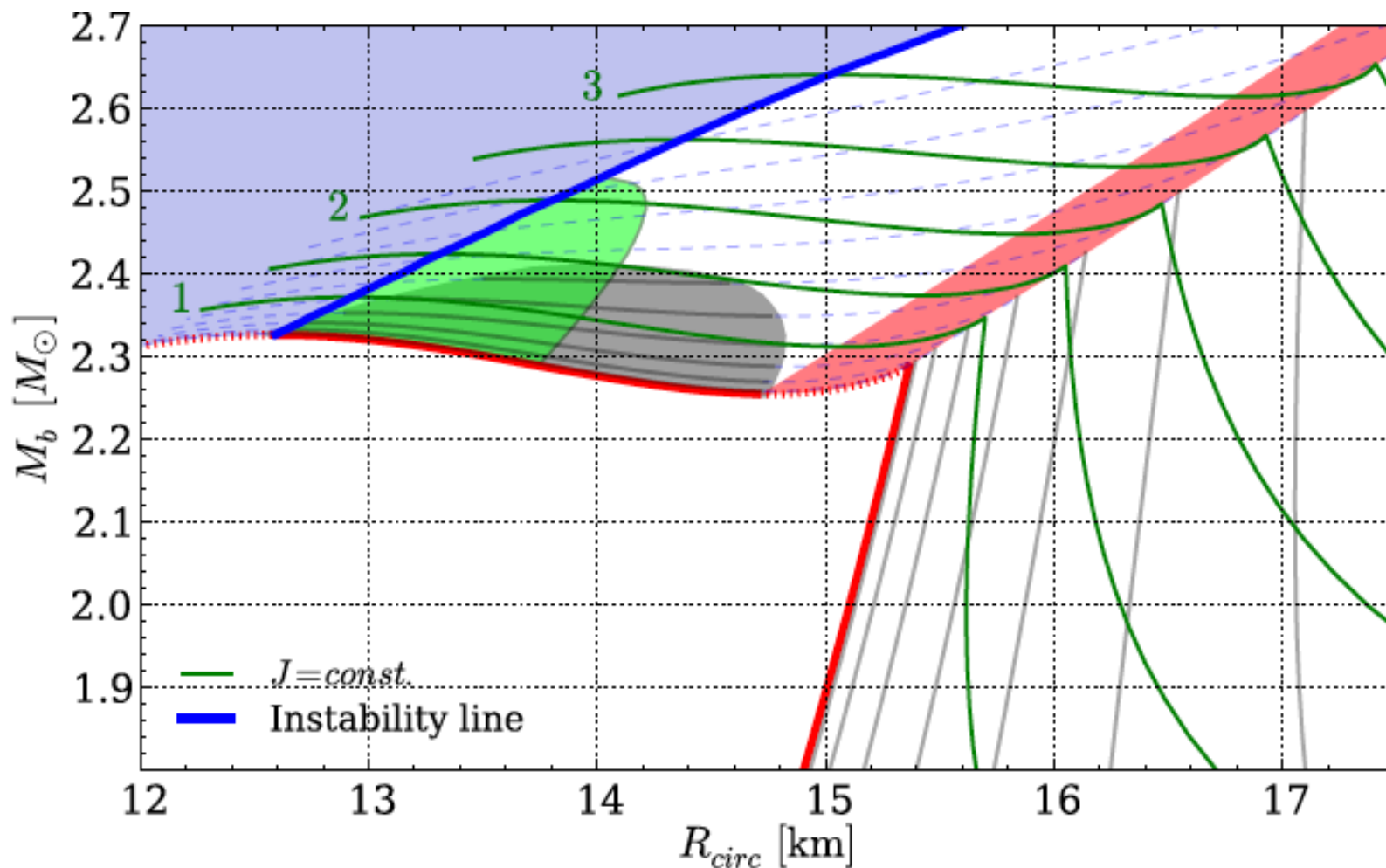


4c. Rotation and stability



Large regions of backbending phenomenon
(NS spins up while losing angular momentum due to the dense matter EoS)

4c. Rotation and stability



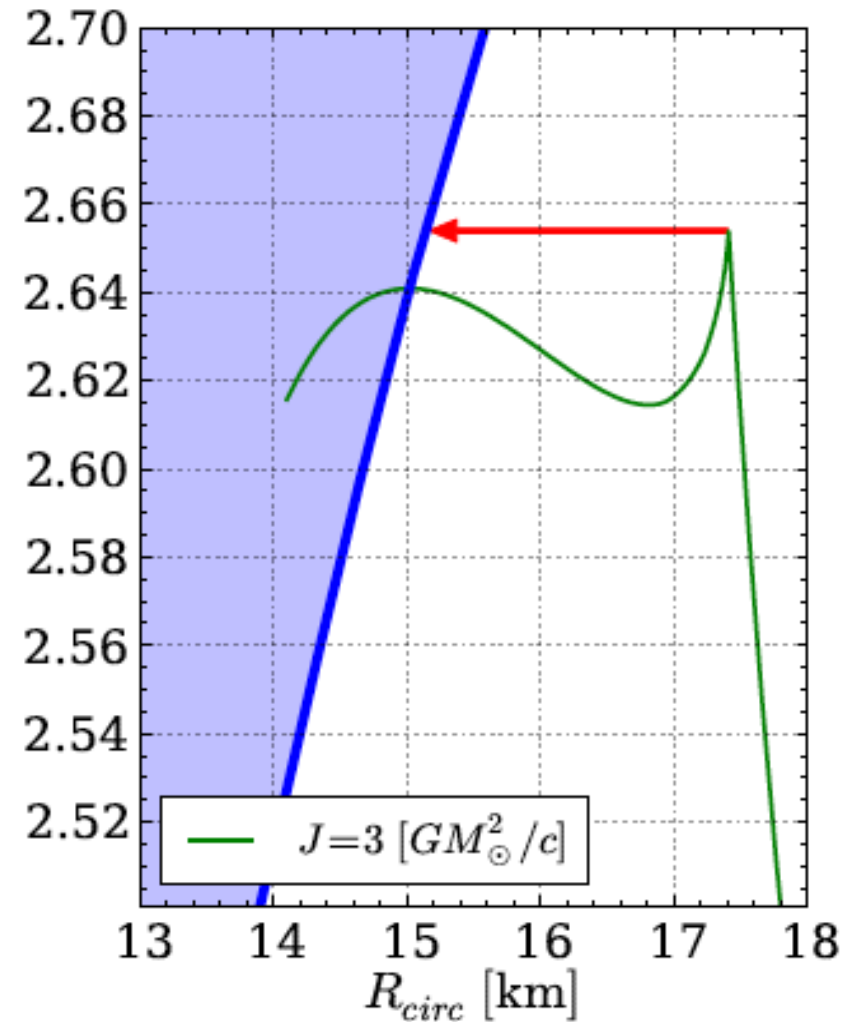
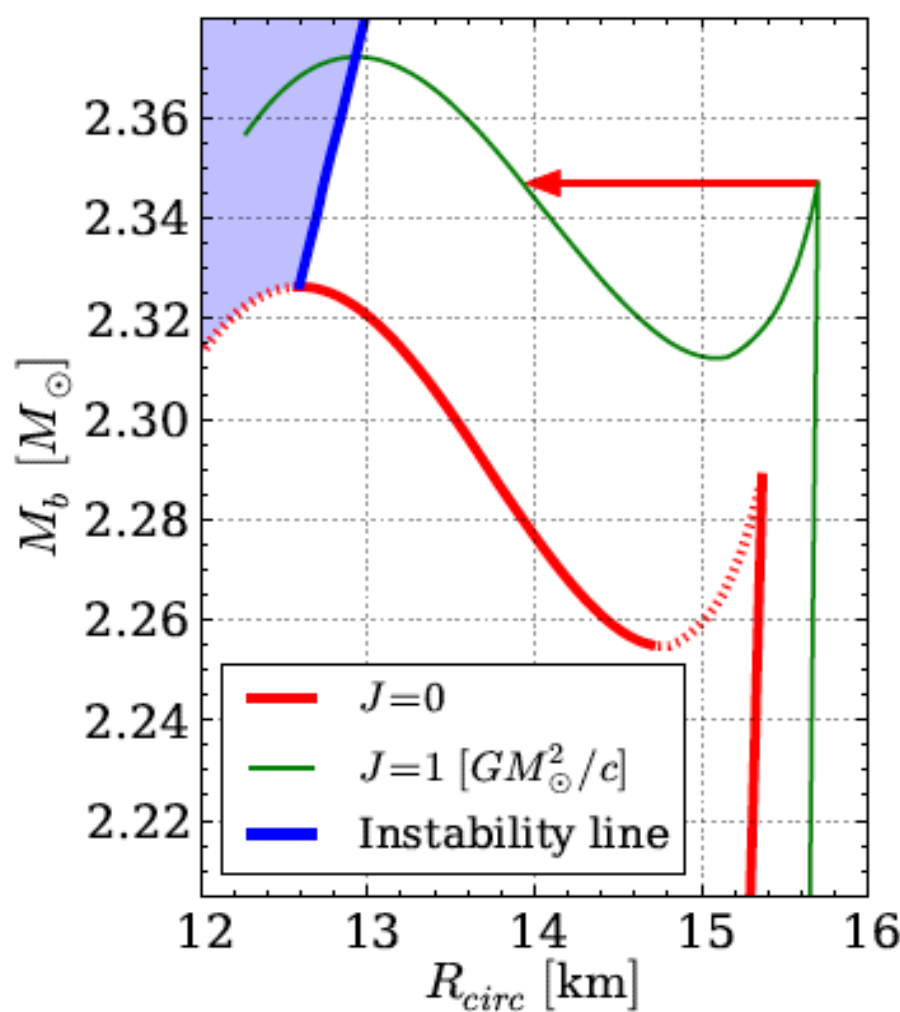
Red region - strong phase-transition instability,

Blue region - unstable w.r.t axisymmetric oscillations,

Grey region - no back-bending,

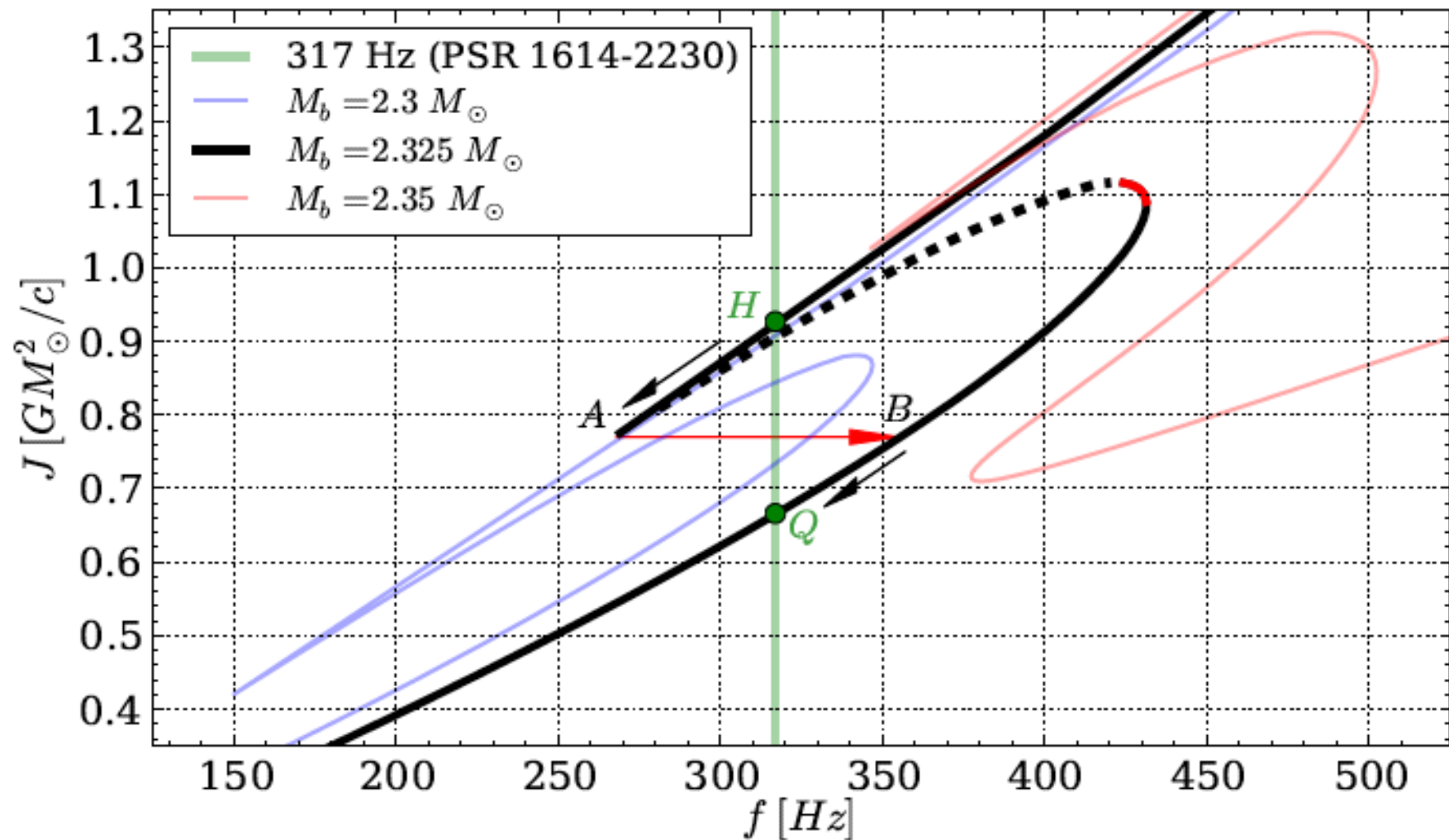
Green region - stable twin branch reached after the mini-collapse from the tip of $J = \text{const.}$ curve, along $M_b = \text{const.}$

4c. Rotation and stability



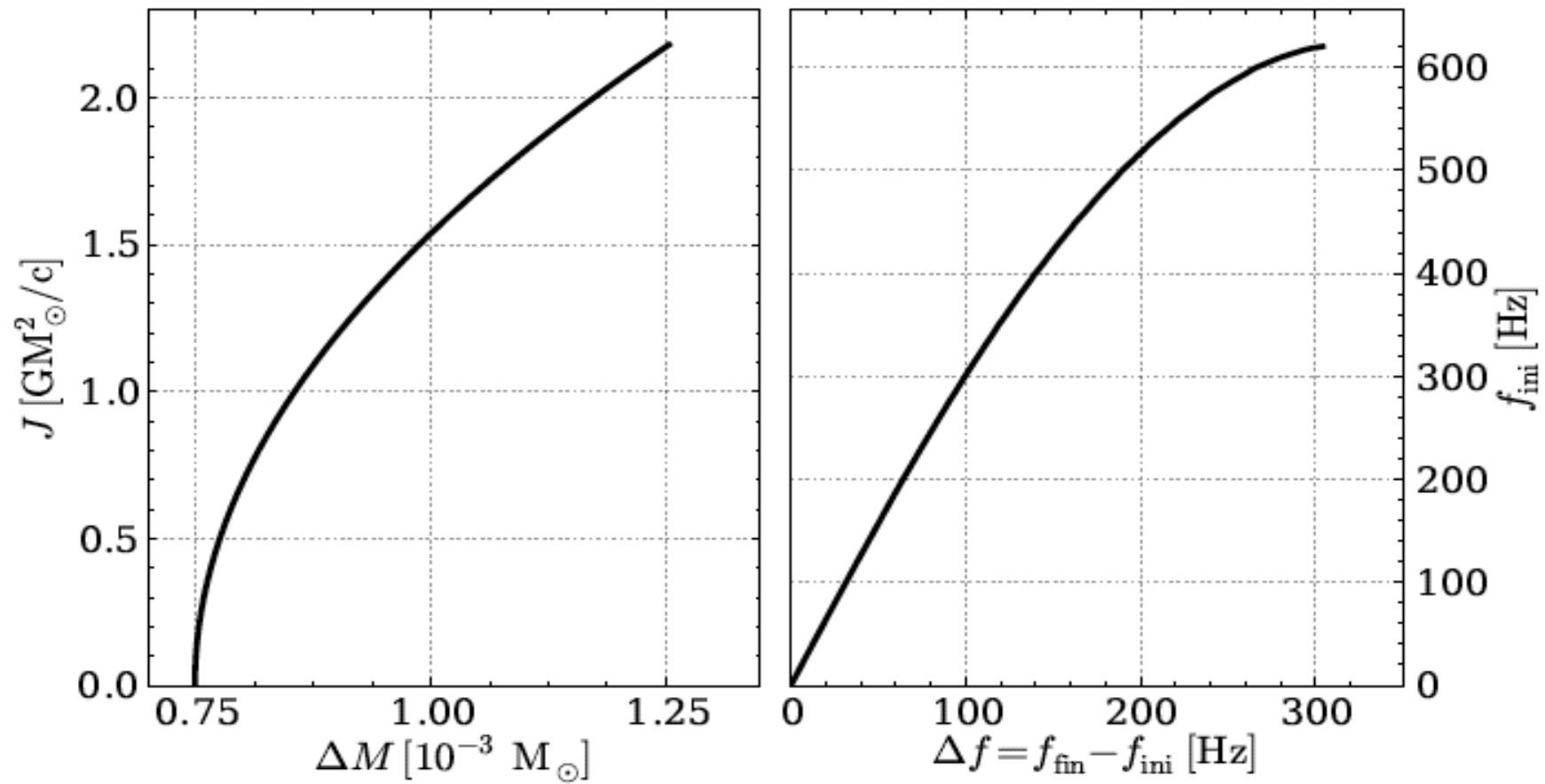
Stars with too much angular momentum e.g., *spun-up by accretion* end up in the instability.

4c. Constraints from mass and frequency



For NSs with measured gravitational mass M and frequency - possibility to put limits on M_b , J , moment of inertia I , core EOS composition etc.

4c. Energy release and spin-up (glitch)



Left panel: energy release (difference in the gravitational mass) vs J of the configuration entering the strong phase-transition instability.

Right panel: spin-up Δf (difference between the final and initial spin frequency) against the spin frequency of the initial configuration.

4c. Rotation - summary

This type of instability EOS provides a "natural" explanation for:

- ★ Lack of back-bending in radiopulsar timing,
- ★ Spin frequency cut-off at some moderate (but > 716 Hz) frequency,
- ★ Falcke & Rezzolla Fast Radio Burst (FRB) engine
 - ★ catastrophic mini-collapse to the second branch (or to a black hole),
 - ★ massive rearrangement of the magnetic field → energy emission.

Astrophysical predictions:

- ★ Way to constraint on M_b , J , I , core EOS etc.,
- ★ Specific shape of NS-BH mass function (no mass gap?)
 - population of massive, low B-field NSs (radio-dead?),
 - population of massive, high B-field NSs (collapse enhances the field?),
- ★ Characteristic burst-like signature in GW emission during the mini-collapse.

4d. New Bayesian Analysis scheme

JOURNAL OF PHYSICS: CONFERENCE SERIES

The open access journal for conferences

15th International Conference on Strangeness in Quark Matter (SQM2015)

Dubna, Russia
6–11 July 2015

Editors: David E. Alvarez-Castillo, David Blaschke, Vladimir Kekelidze,
Victor Matveev and Alexander Sorin

Volume 668 2016

jpcs.iop.org



IOP Publishing

Strategy towards event simulations testing PT signal

Two alternative approaches:

I) Direct approach based on transport codes:

Particle trajectories are followed;

Properties of the medium are encoded in propagators and cross sections

→ UrQMD (Aichelin et al.),

→ PHSD (Bratkovskaya, Cassing, et al.),

→ PHSD + SACA (Bratkovskaya, Aichelin, LeFevre, et al.)

II) Hybrid approach:

Joins hydrodynamic evolution of a (multi-)fluid system described by an **EoS** with
Particle transport via a procedure called "**particlization**" (Karpenko)

Particularly suitable for studying effects of a strong phase transition in model EoS

a) Sandwich: UrQMD + hydro + hadronic cascade (H. Petersen et al.)

→ PT in hydro stage only

b) **3-fluid hydro**dynamics (Ivanov) + particlization (Karpenko)

→ PT in baryon stopping regime already!

(main difference to sandwich; appropriate for energy range of NICA / CBM)

Both approaches provide the inputs for the simulation of the **detector response**
(GEANT-MPD: Rogachevsky, Merts, Batyuk, Wielanek, et al.)

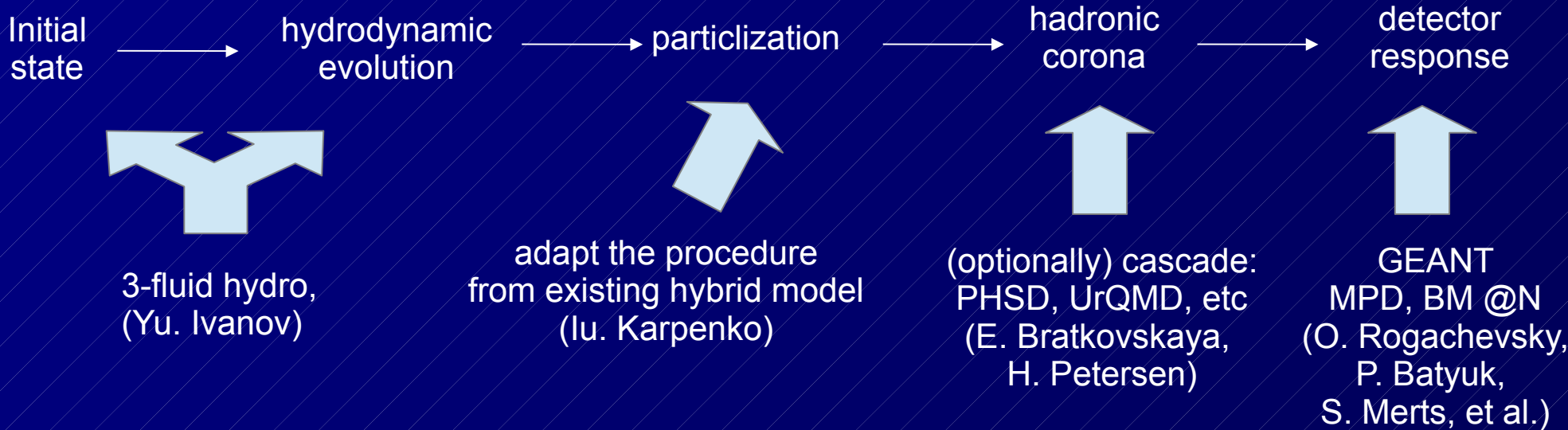
Hydrodynamic modelling for NICA / FAIR

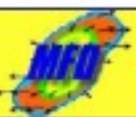
More complicated for lower energies:

- baryon stopping effects,
- finite baryon chemical potential,
- EoS unknown from first principles

We want to simulate the effects of, and ultimately discriminate different EoS/PT types

The model has to be coupled to a detector response code to simulate detector events





3-Fluid Dynamics

Baryon Stopping

JINR,
24.08.10

Model

Rapidity Density

Fit

Reduced curvature

Trajectories

Crossover
Summary

Produced particles
populate mid-rapidity
⇒ fireball fluid



Target-like fluid:

$$\partial_\mu J_t^\mu = 0$$

Leading particles carry bar. charge

$$\partial_\mu T_t^{\mu\nu} = -F_{tp}^\nu + F_{ft}^\nu$$

exchange/emission

Projectile-like fluid:

$$\partial_\mu J_p^\mu = 0,$$

$$\partial_\mu T_p^{\mu\nu} = -F_{pt}^\nu + F_{fp}^\nu$$

Fireball fluid:

$$J_f^\mu = 0,$$

Baryon-free fluid

$$\partial_\mu T_f^{\mu\nu} = F_{pt}^\nu + F_{tp}^\nu - F_{fp}^\nu - F_{ft}^\nu$$

Source term Exchange

The source term is delayed due to a formation time $\tau \sim 1 \text{ fm/c}$

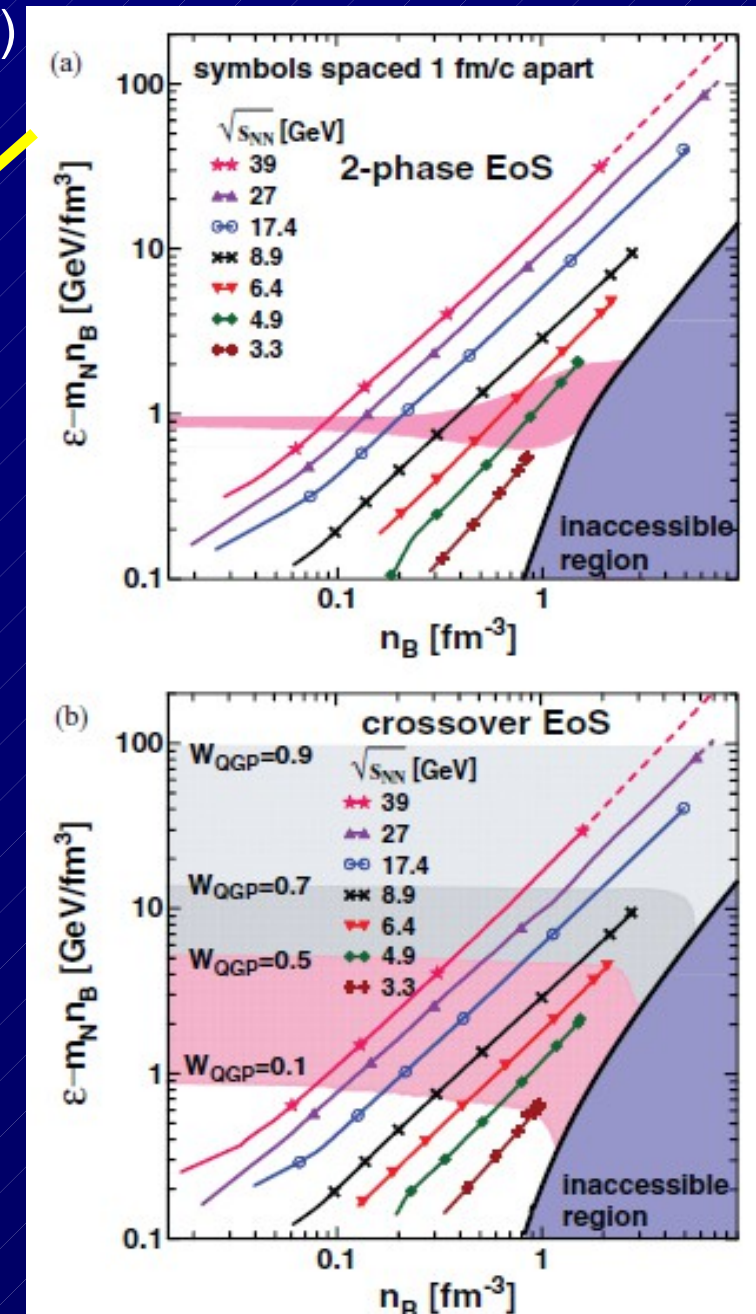
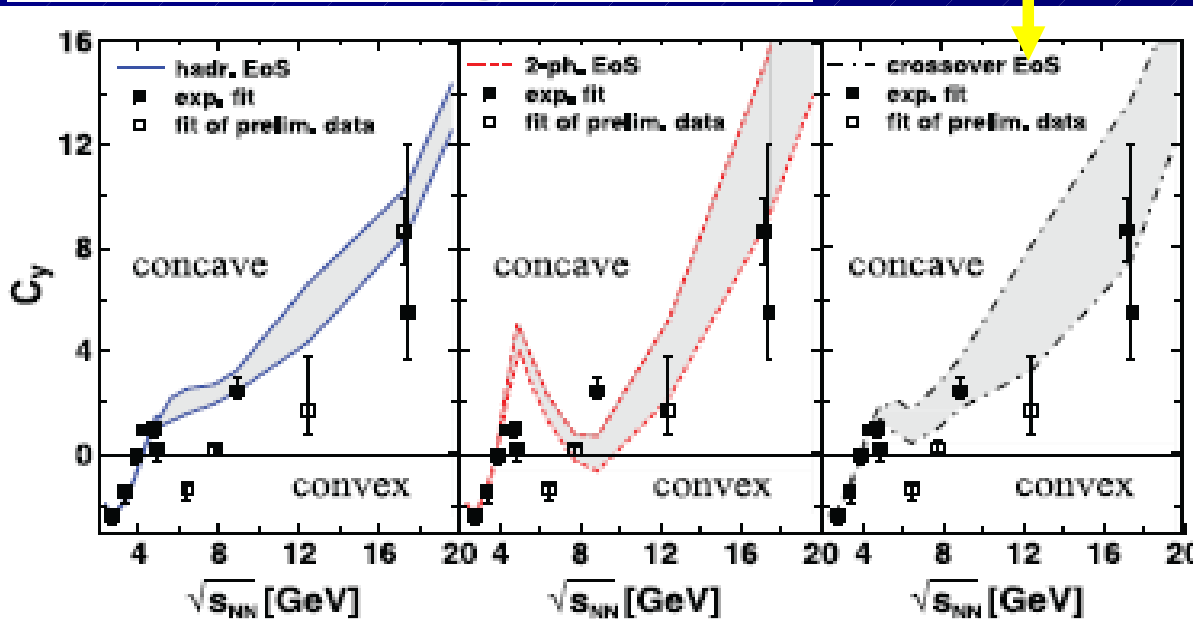
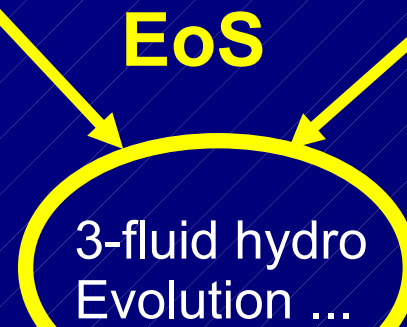
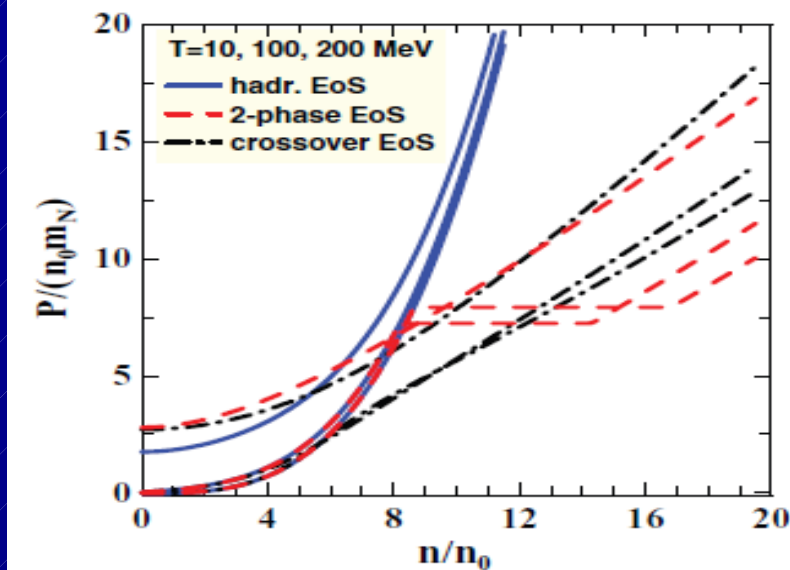
Total energy-momentum conservation:

$$\partial_\mu (T_p^{\mu\nu} + T_t^{\mu\nu} + T_f^{\mu\nu}) = 0$$

<http://theory.gsi.de/~ivanov/mfd/>

Net proton rapidity distribution – test case for a 1st order PT signal

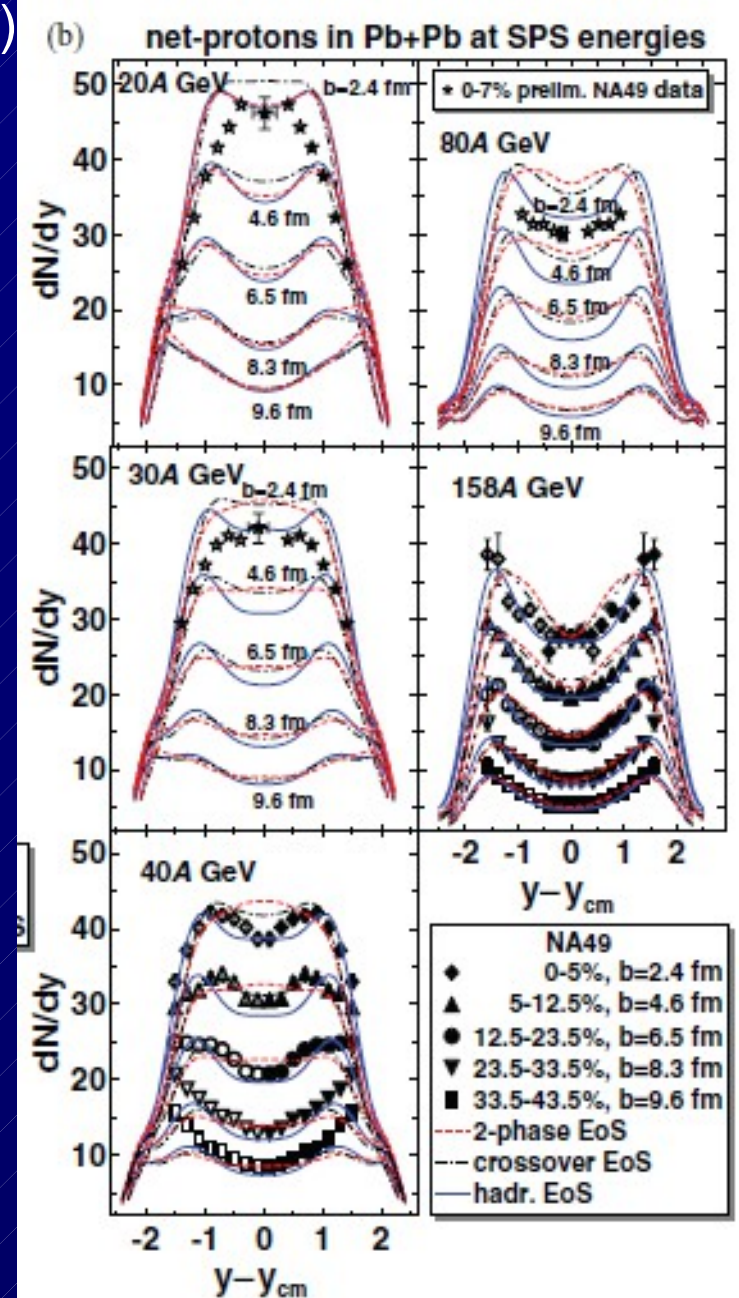
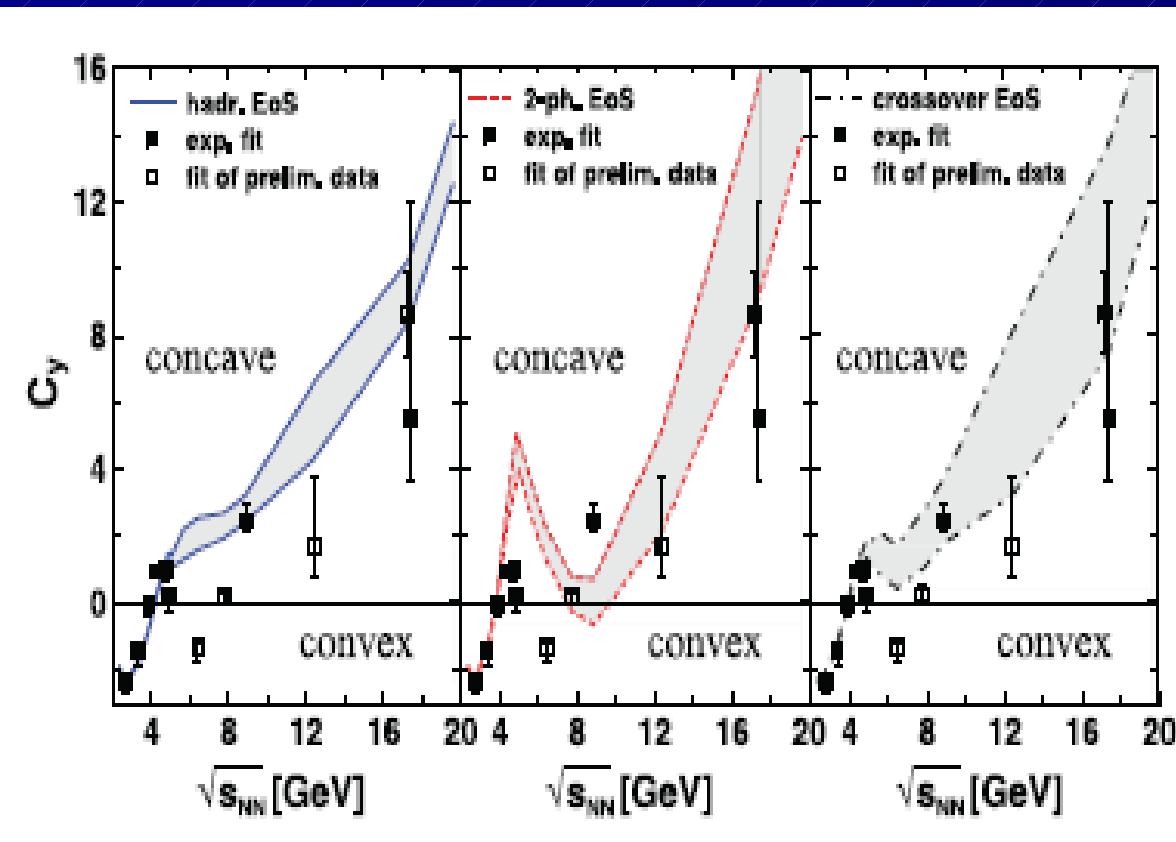
Theory: Yu.B. Ivanov, Phys. Rev. C 87, 064904 (2013)



Net proton rapidity distribution – test case for a 1st order PT signal

Theory: Yu.B. Ivanov, Phys. Rev. C 87, 064904 (2013)

$$C_y = \left(y_{\text{c.m.}}^3 \frac{d^3 N}{dy^3} \right)_{y=y_{\text{c.m.}}} / \left(y_{\text{c.m.}} \frac{dN}{dy} \right)_{y=y_{\text{c.m.}}} \\ = (y_{\text{c.m.}}/w_s)^2 (\sinh^2 y_s - w_s \cosh y_s).$$



Net proton rapidity distribution – test case for a 1st order PT signal

Event set:

40k AuAu @ $\sqrt{s}_{NN} = 9$ GeV [0-5%]

The most reliable region

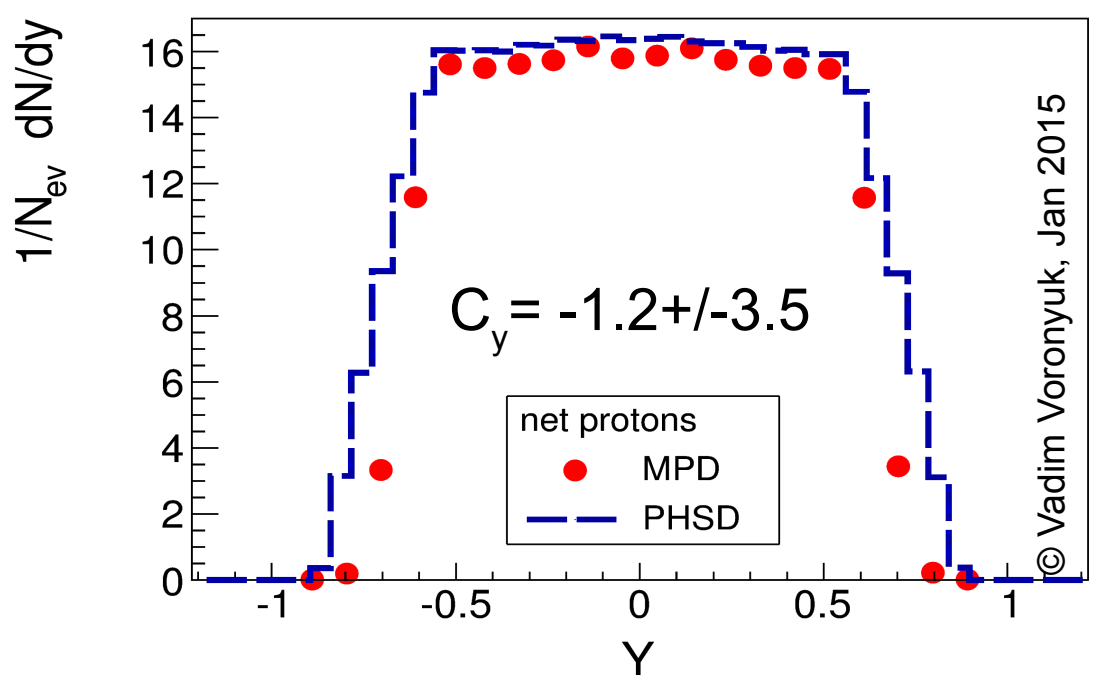
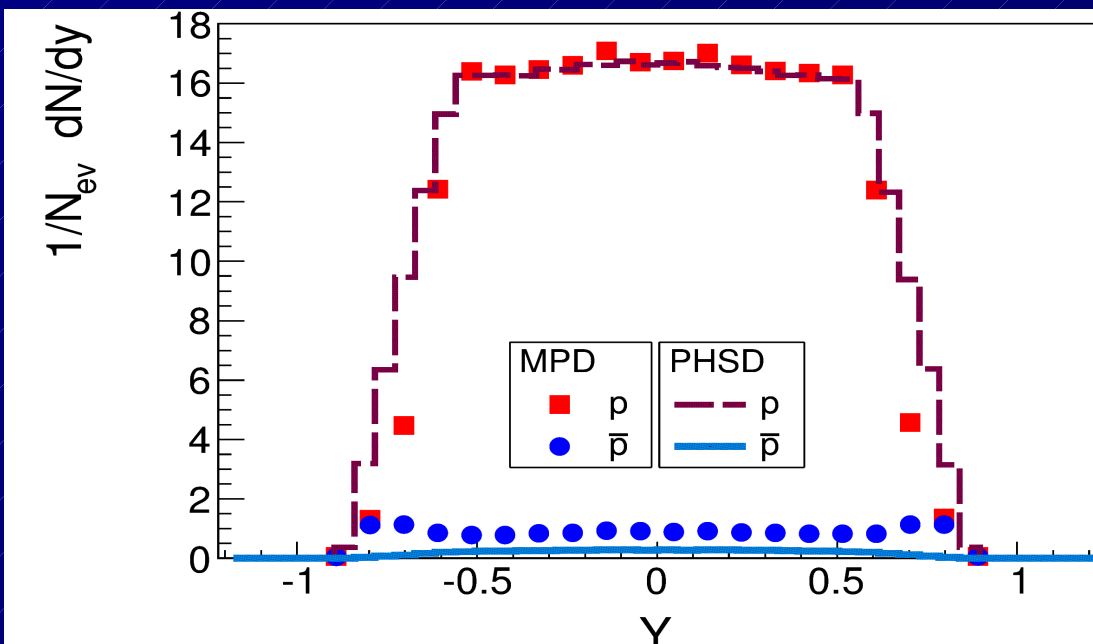
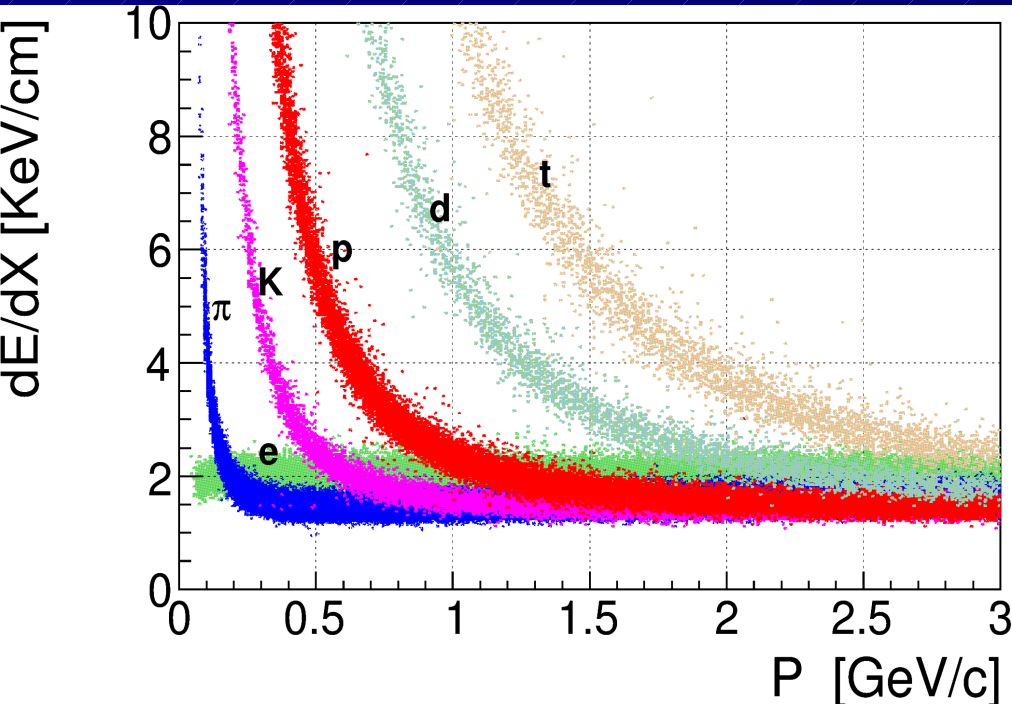
$|\eta| < 1.2 ; 0.4 < p_t$ [GeV/c] < 0.8

Result:

PHSD input → GEANT+MPD
detector reproduces the rapidity distribution !
(previous concerns not confirmed !!)

Signal:

$$C_y = \left(y_{cm}^3 \frac{d^3 N}{dy^3} \right)_{y=0} / \left(y_{cm} \frac{dN}{dy} \right)_{y=0}$$



Net proton rapidity distribution – test case for a 1st order PT signal

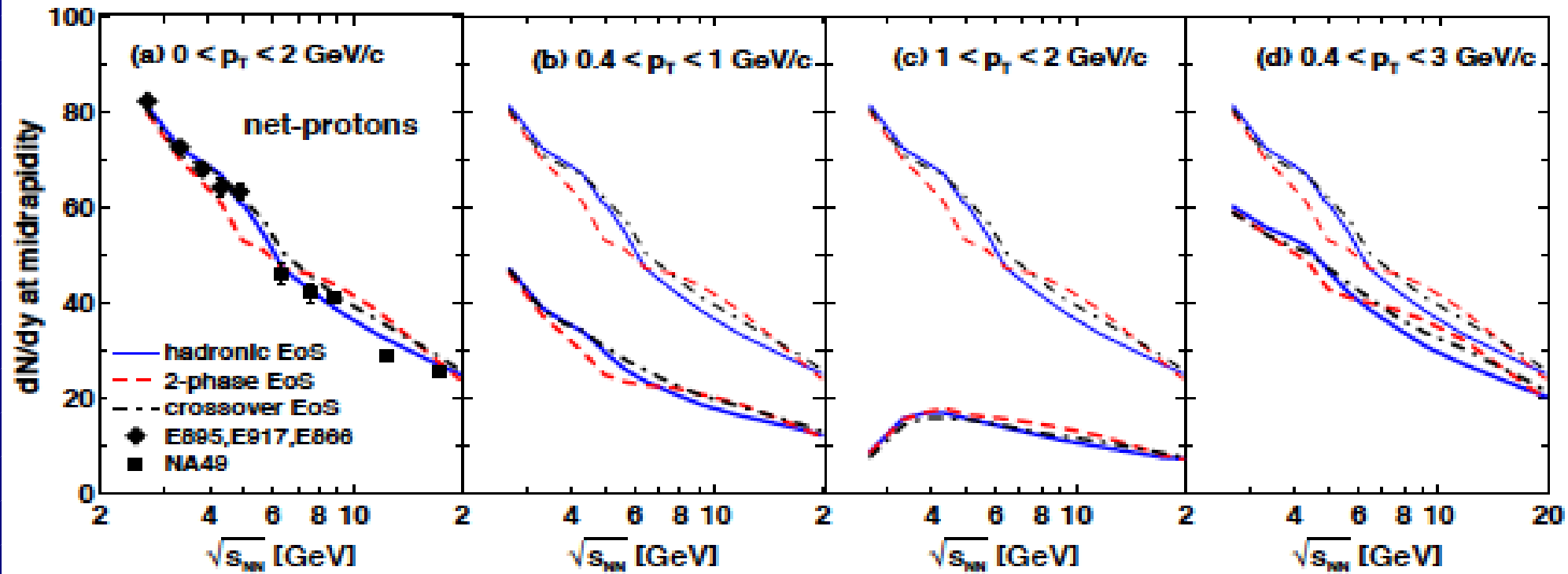
Investigation of p_T cuts:

Yu. Ivanov & D. Blaschke, arxiv:1504.03992

$$C_y = \left(y_{\text{beam}}^3 \frac{d^3 N}{dy^3} \right)_{y=0} / \left(y_{\text{beam}} \frac{dN}{dy} \right)_{y=0}$$

$$= (y_{\text{beam}}/w_s)^2 (\sinh^2 y_s - w_s \cosh y_s).$$

- i. $0 < p_T < 2 \text{ GeV}/c$ and a very unrestrictive constraint to the rapidity range $|y| < 0.7 y_{\text{beam}}$, where y_{beam} is the beam rapidity in the collider mode, which is practically equivalent to the full acceptance;
- ii. $0.4 < p_T < 1 \text{ GeV}/c$ and $|y| < 0.5$, the expected MPD acceptance [17];
- iii. $1 < p_T < 2 \text{ GeV}/c$ and $|y| < 0.5$, an acceptance range where low-momentum particles witnessing collective behaviour are largely eliminated;
- iv. $0.4 < p_T < 3 \text{ GeV}/c$ and $|y| < 0.5$, the range of the STAR acceptance [18].



Net proton rapidity distribution – test case for a 1st order PT signal

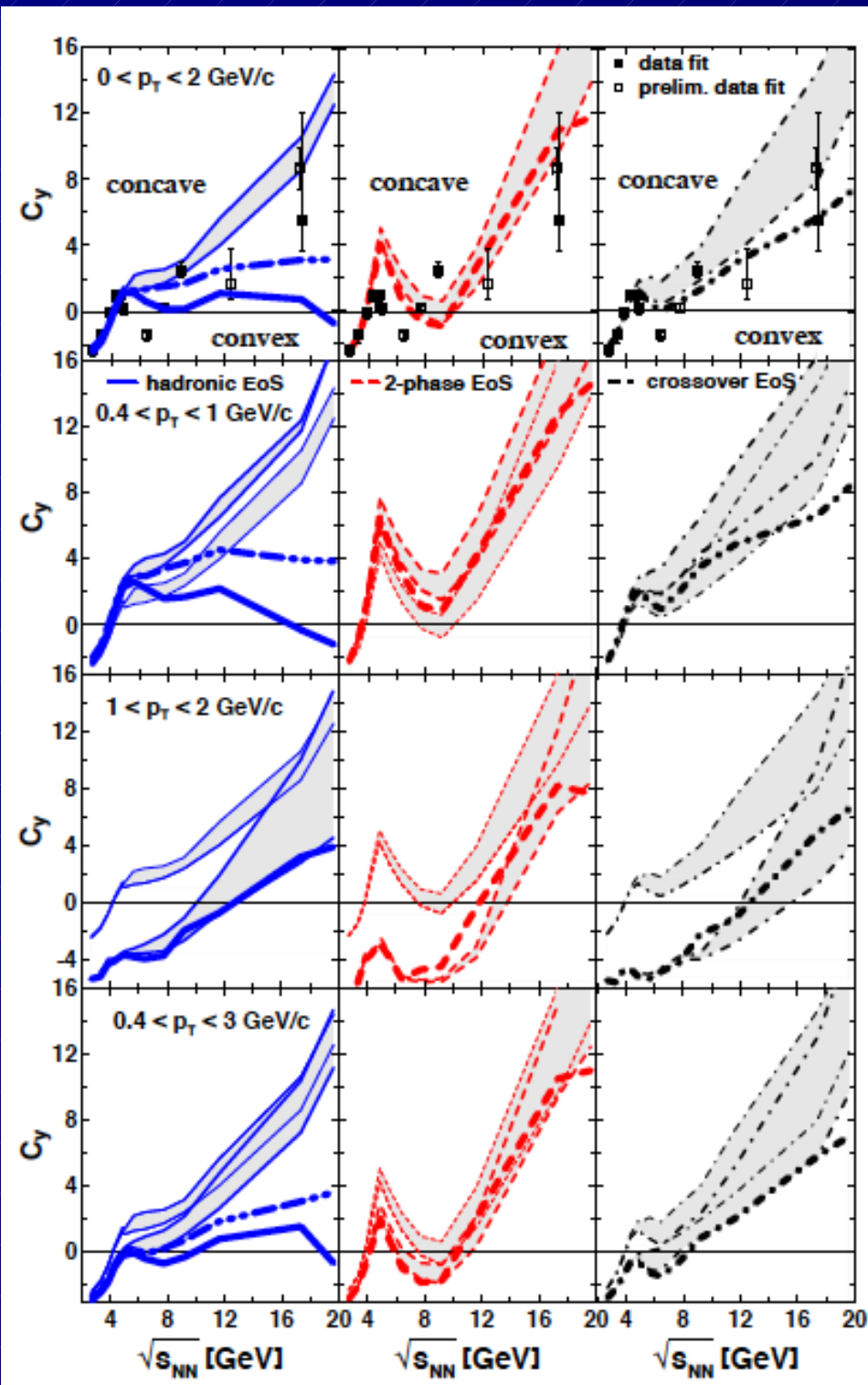
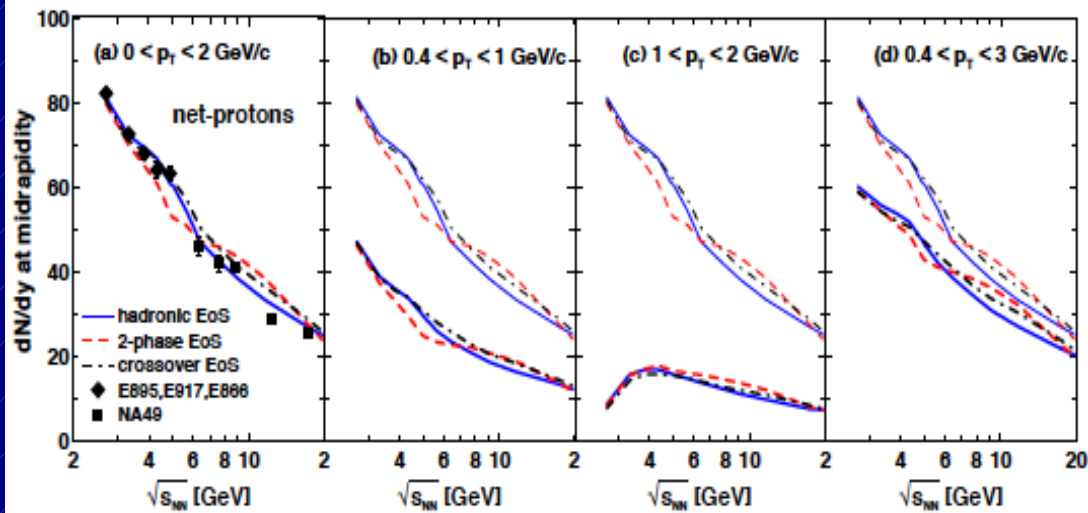
Investigation of p_T cuts:

Yu. Ivanov & D. B., PRC 92, 024916 (2015)

$$C_y = \left(y_{\text{beam}}^2 \frac{d^3 N}{dy^3} \right)_{y=0} / \left(y_{\text{beam}} \frac{dN}{dy} \right)_{y=0}$$

$$= (y_{\text{beam}}/w_s)^2 (\sinh^2 y_s - w_s \cosh y_s).$$

- “wiggle” formed in the nonequilibrium compression stage of the collision, where p_T only in 3FH
- robust against serious p_T cuts
- at high p_T (1 - 2 GeV/c) in convex region
- at low p_T (0.2 - 1 GeV/c) in concave region
- required accuracy in C_y determination: ΔC_y < 2



Net proton rapidity distribution – test case for a 1st order PT signal

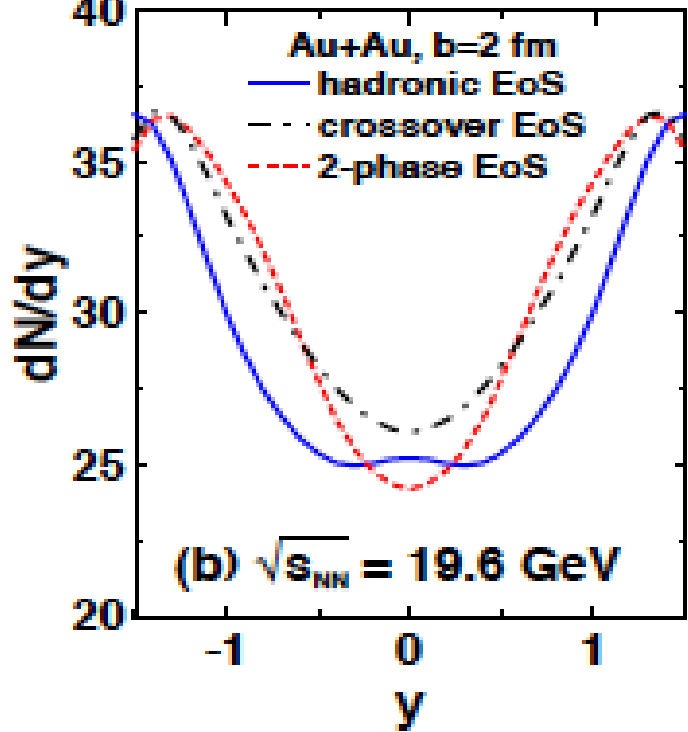
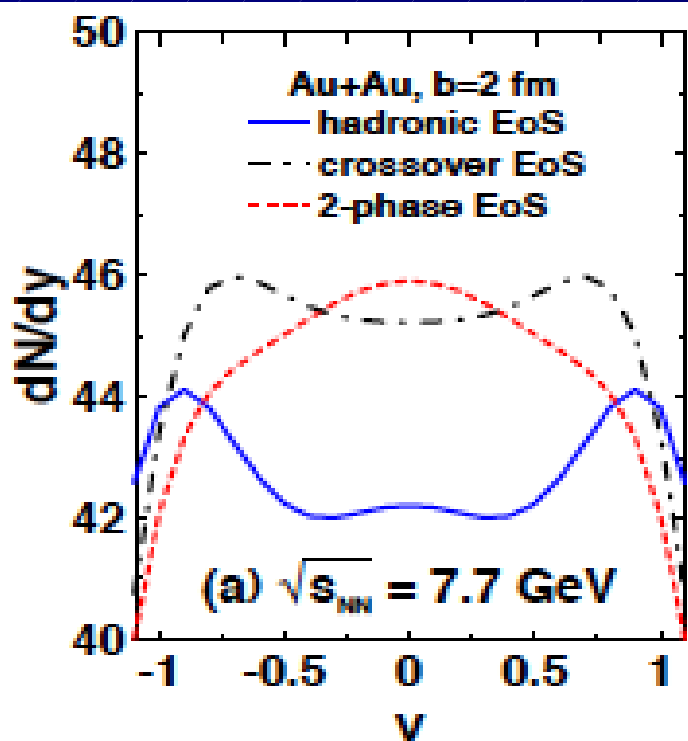
Investigation of p_T cuts:

Yu. Ivanov & D. Blaschke, arxiv:1504.03992

$$\frac{dN}{dy} = a \left(\exp \left\{ -(1/w_s) \cosh(y - y_s) \right\} + \exp \left\{ -(1/w_s) \cosh(y + y_s) \right\} \right),$$

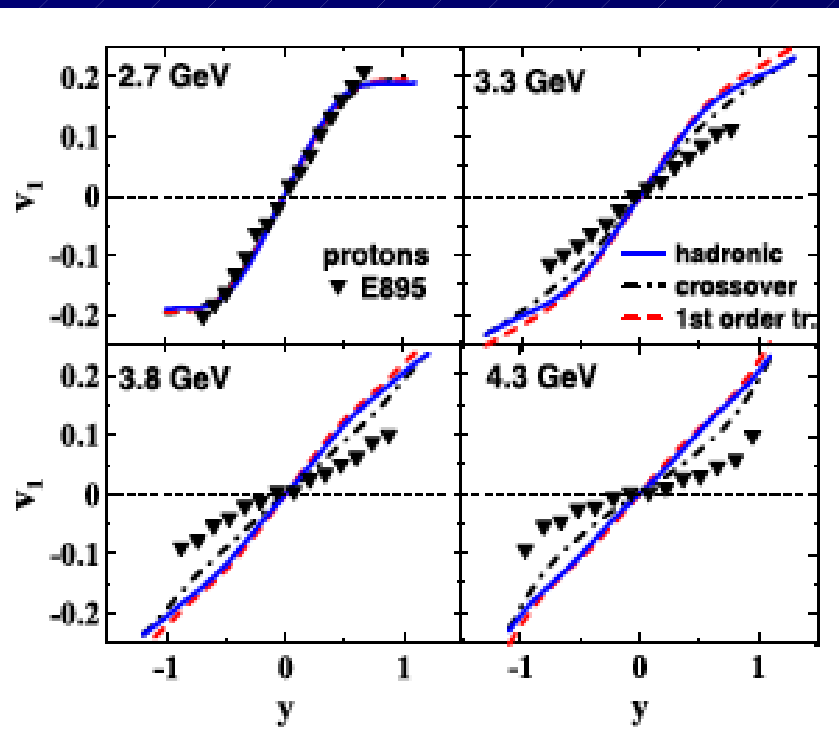
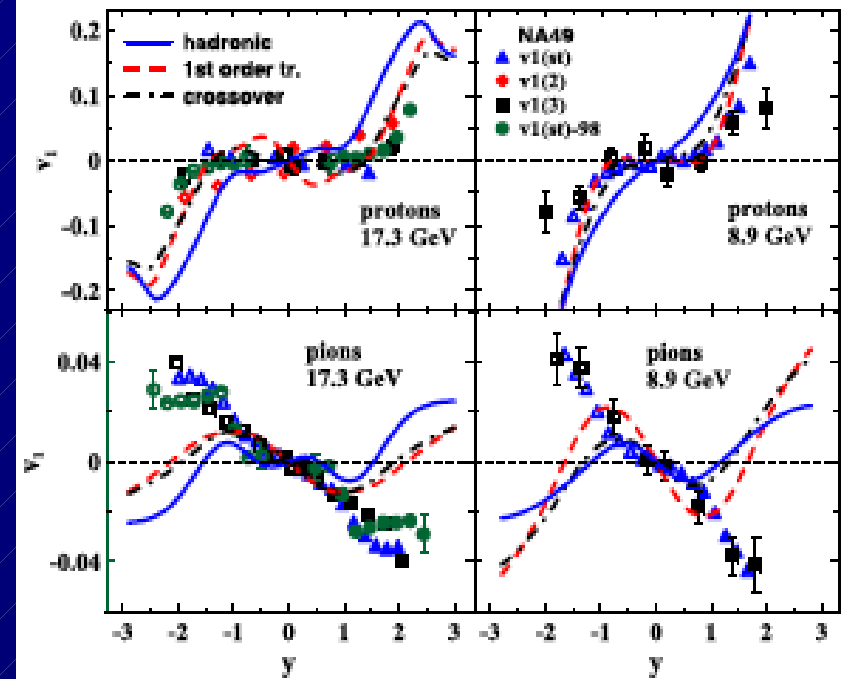
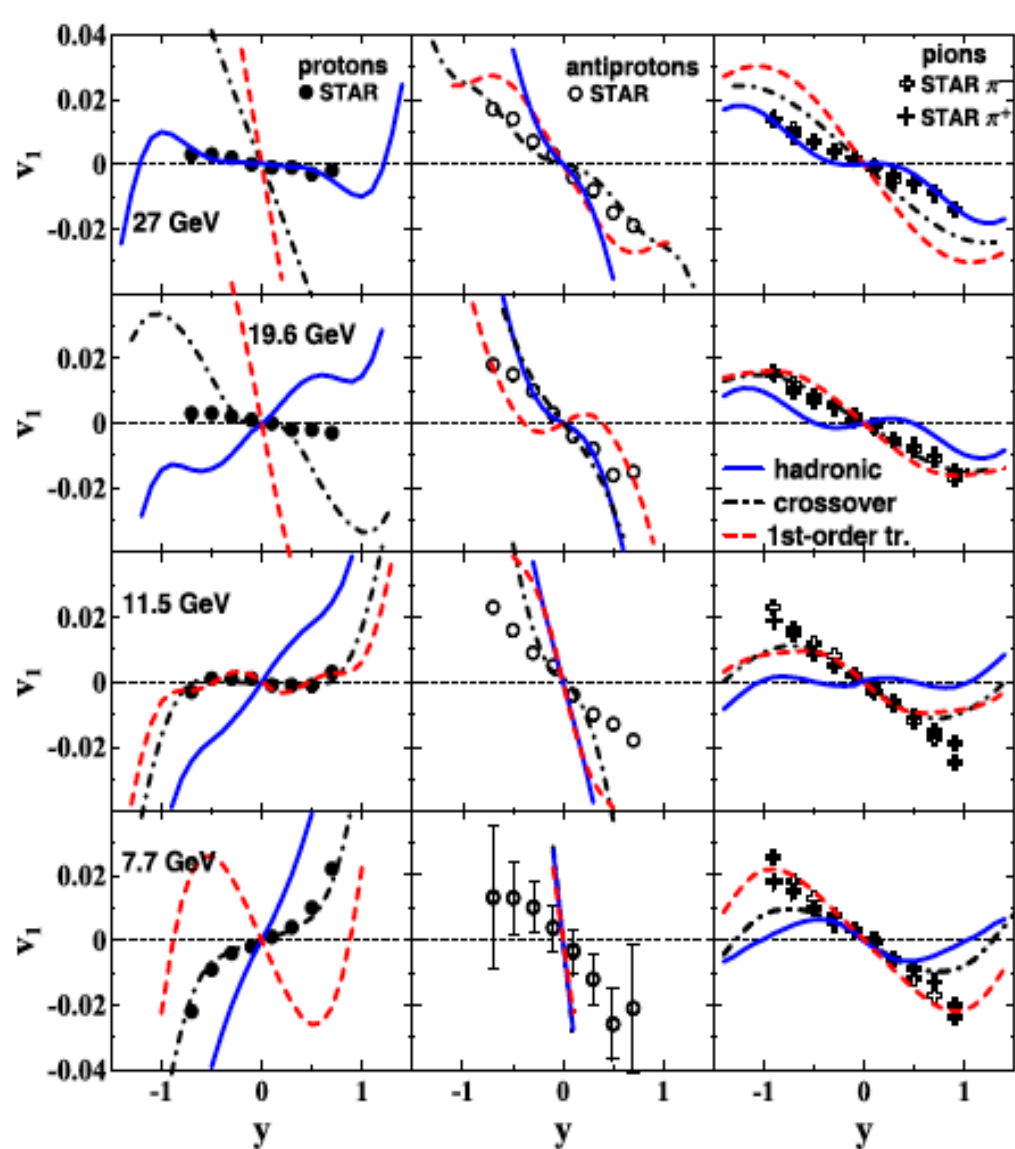
$$C_y = \left(y_{beam}^3 \frac{d^3 N}{dy^3} \right)_{y=0} / \left(y_{beam} \frac{dN}{dy} \right)_{y=0} \\ = (y_{beam}/w_s)^2 (\sinh^2 y_s - w_s \cosh y_s).$$

- “wiggle” formed in the nonequilibrium compression stage of the collision, where p_T only in 3FH
- robust against serious p_T cuts
- at high p_T (1 - 2 GeV/c) in convex region
- at low p_T (0.2 - 1 GeV/c) in concave region
- required accuracy in C_y determination: ΔC_y < 2



Directed flow indicates a cross-over Deconfinement transition ...

Ivanov & Soldatov, Phys. Rev. C 91 (2015)



3+1D viscous hydro-cascade model (Yu. Karpenko, FIAS)

3+1D viscous hydro+cascade model was applied for A+A collisions at RHIC Beam Energy Scan energies ($\sqrt{s} = 7.7 - 39$ GeV), and for SPS energy points

Cascade-hydro-cascade approach:

Initial state: UrQMD cascade

S.A. Bass et al., Prog. Part. Nucl. Phys. 41 255-369, 1998

Hydrodynamic phase: numerical 3+1D hydro solution via original relativistic viscous hydro code

Iu. Karpenko, P. Huovinen, M. Bleicher, arXiv:1312.4160

Hydro starts at $\tau = \sqrt{t^2 - z^2} = \tau_0$ (red curve): $\tau_0 = \frac{2R}{\gamma v_z}$

$\{T^{0\mu}, N_b^0, N_q^0\}$ of fluid = averaged $\{T^{0\mu}, N_b^0, N_q^0\}$ of particles

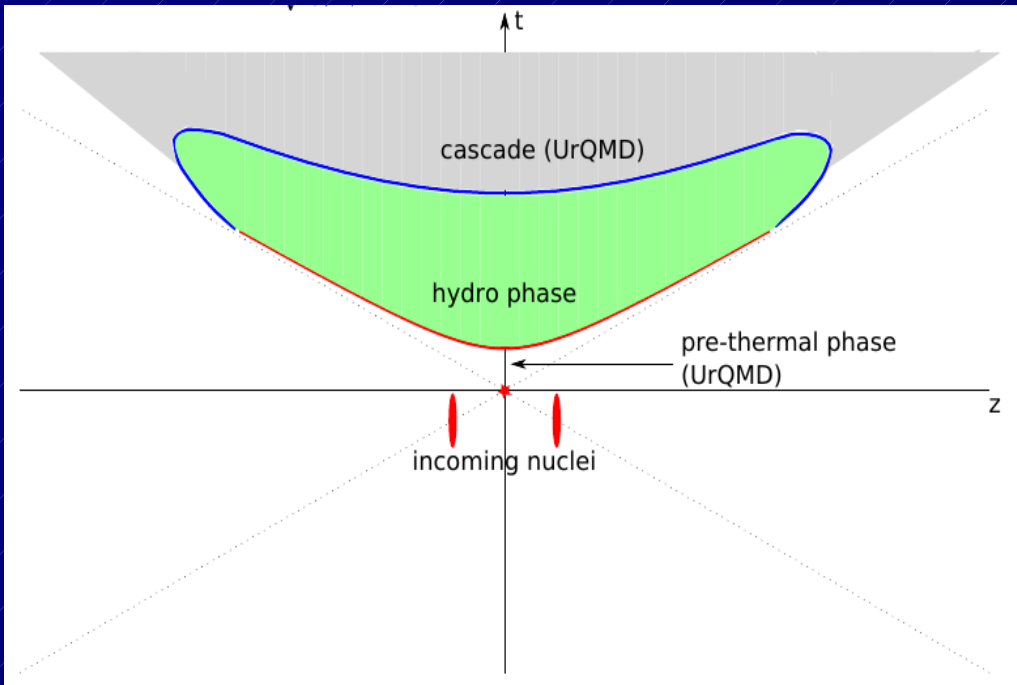
Fluid→particle transition

$\varepsilon = \varepsilon_{sw} = 0.5$ GeV/fm³ (blue curve):

$\{T^{0\mu}, N_b^0, N_q^0\}$ of hadron-resonance gas = $\{T^{0\mu}, N_b^0, N_q^0\}$ of fluid

Hadronic cascade: UrQMD

P. Huovinen, H. Petersen: "Particilization in hybrid models", Eur. Phys. J. A48 (2012) 171; arxiv:1206.3371



Equations of state for hydrodynamic phase

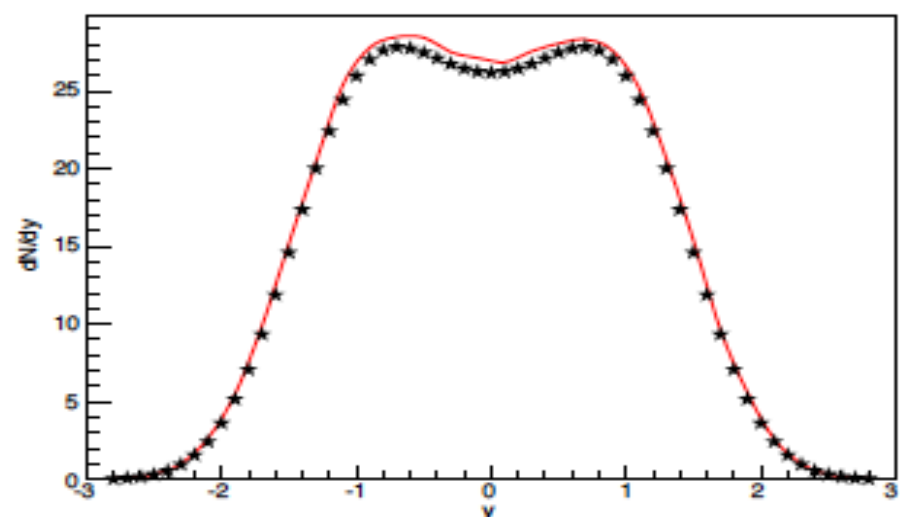
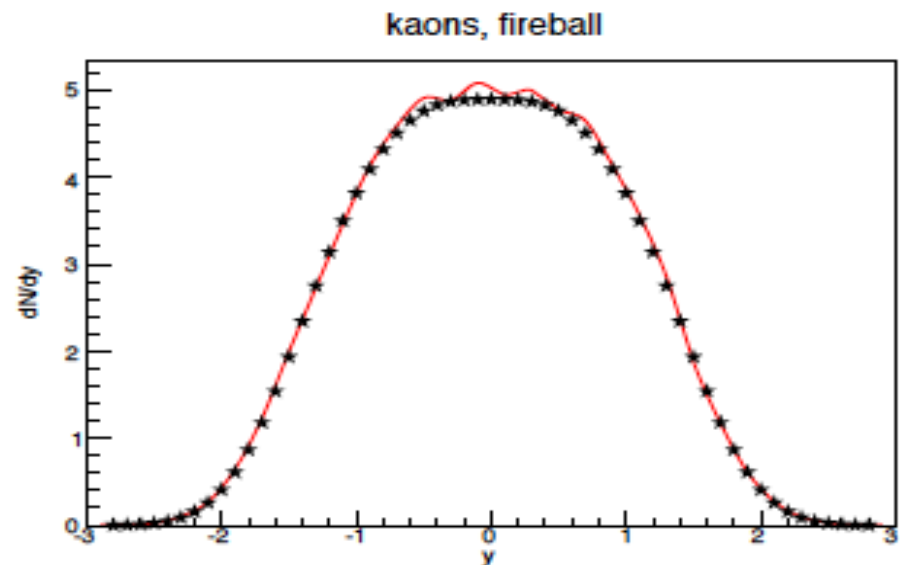
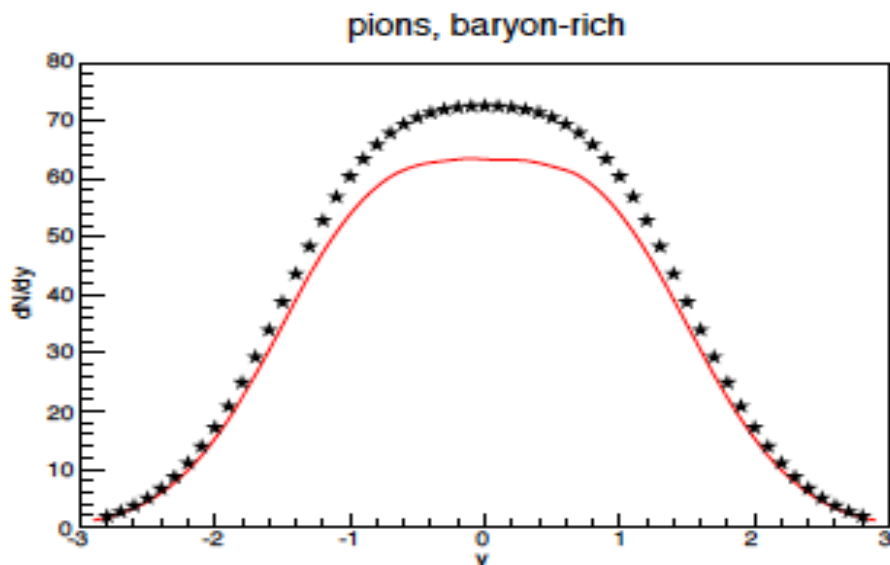
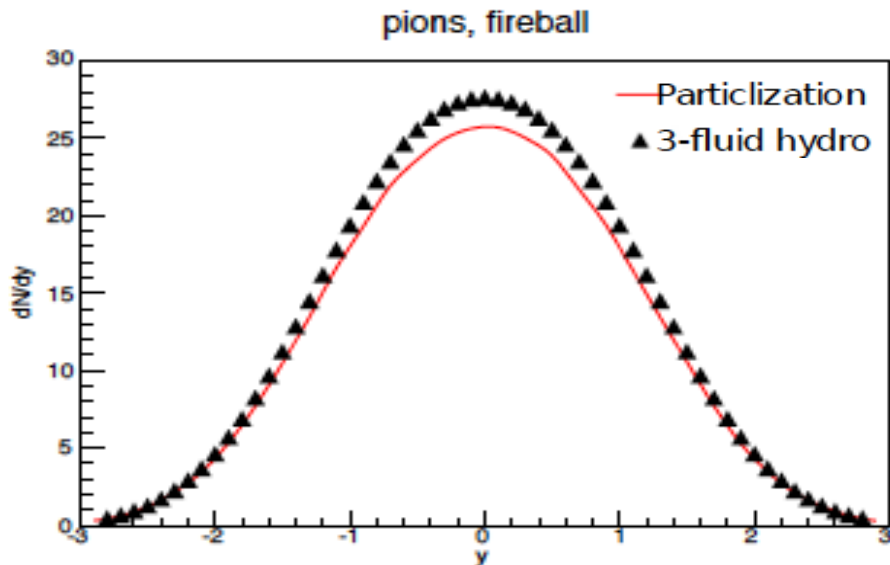
- Chiral model
 - ▶ coupled to Polyakov loop to include the deconfinement phase transition
 - ▶ good agreement with lattice QCD data at $\mu_B = 0$, also applicable at finite baryon densities
 - ▶ (current version) has **crossover type PT** between hadron and quark-gluon phase at all μ_B
- Hadron resonance gas + Bag Model (a.k.a. EoS Q)
 - ▶ hadron resonance gas made of u, d quarks including repulsive meanfield
 - ▶ the phases matched via Maxwell construction, resulting in **1st order PT**

J. Steinheimer, S. Schramm and H. Stocker, J. Phys. G 38, 035001 (2011);
P.F. Kolb, J. Sollfrank, and U. Heinz, Phys. Rev. C 62, 054909 (2000).

Preview: Particilization of 3-fluid Hydrodynamics model

Yu. Karpenko & Yu. Ivanov: May 2014 - May 2015

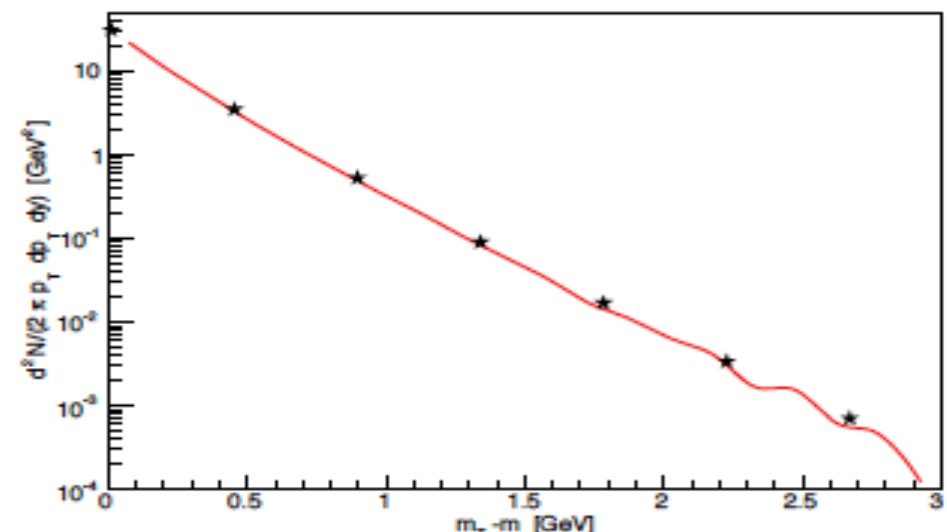
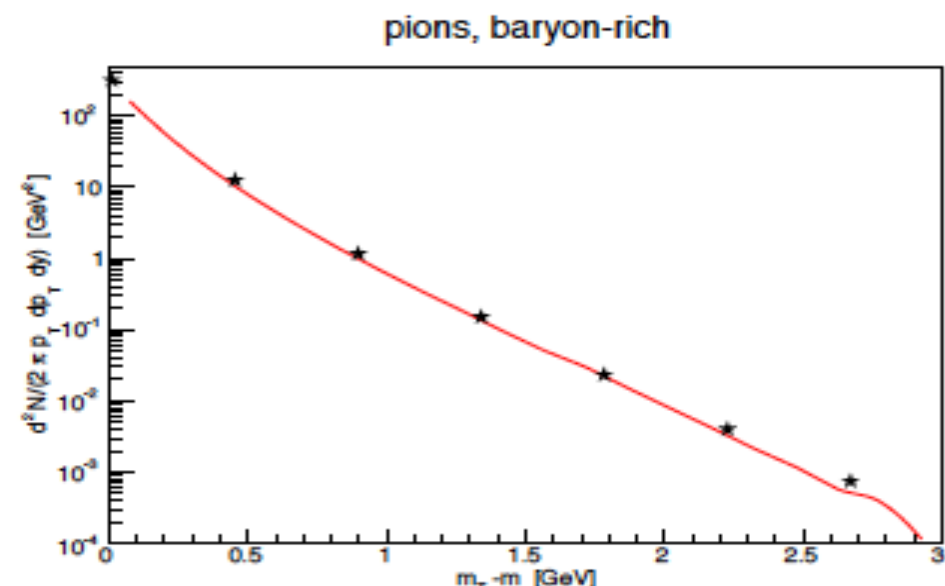
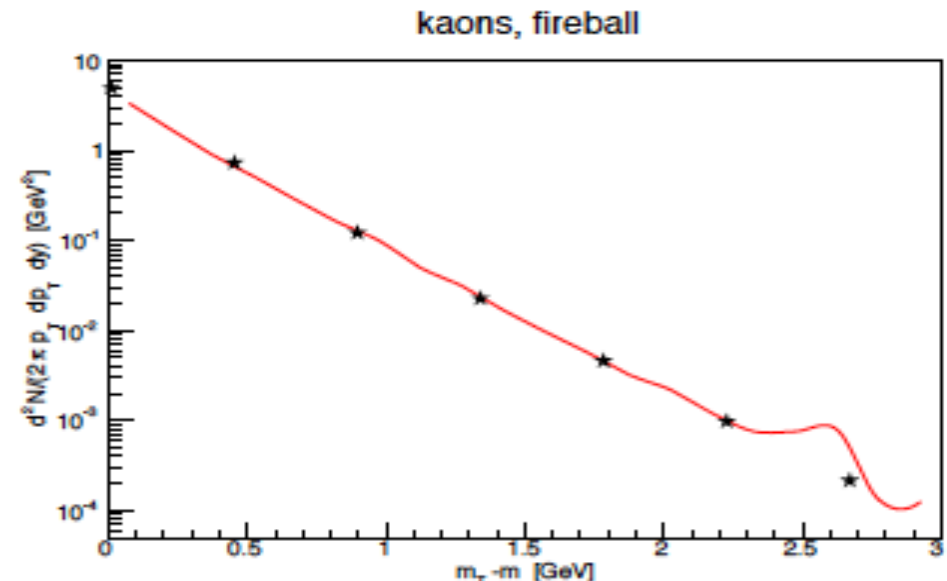
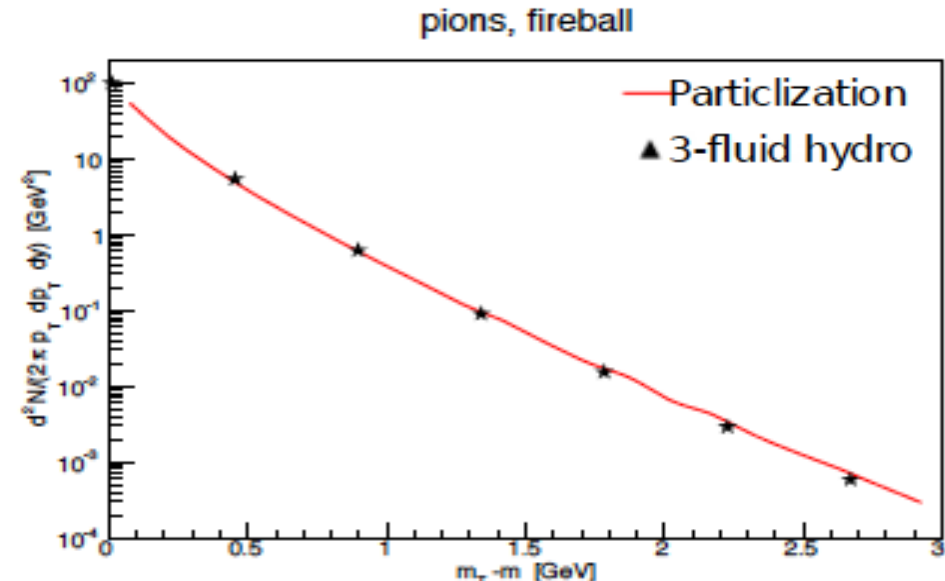
Rapidity distribution



Preview: Particilization of 3-fluid Hydrodynamics model

Yu. Karpenko & Yu. Ivanov: May 2014 - May 2015

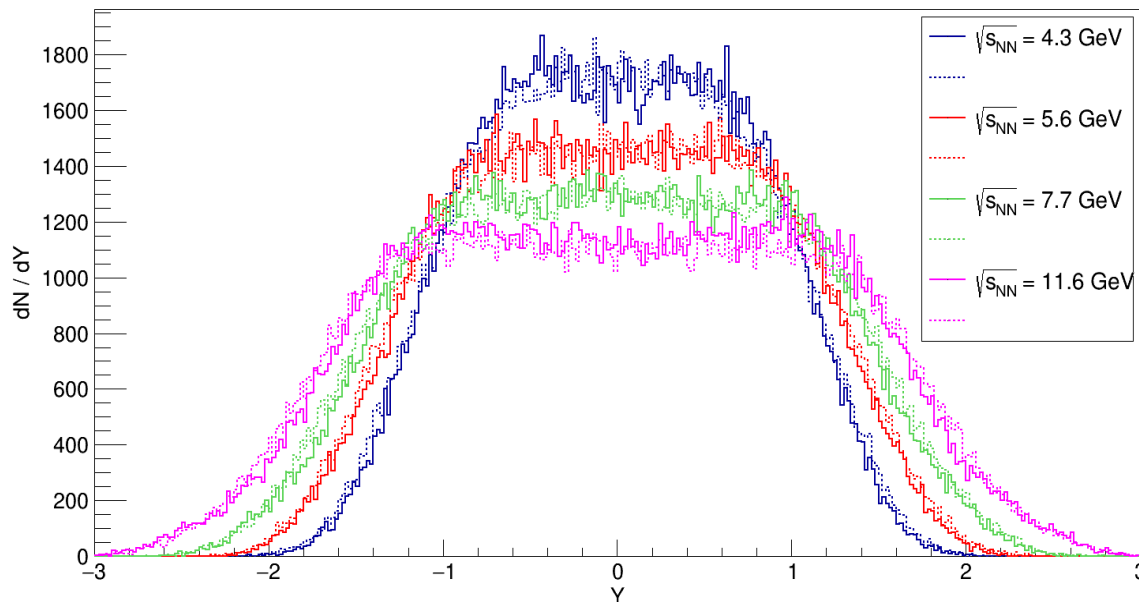
P_T / m_T distribution



Baryon stopping signal for first order phase transition ?

Baryon stopping signal for first order phase transition ?

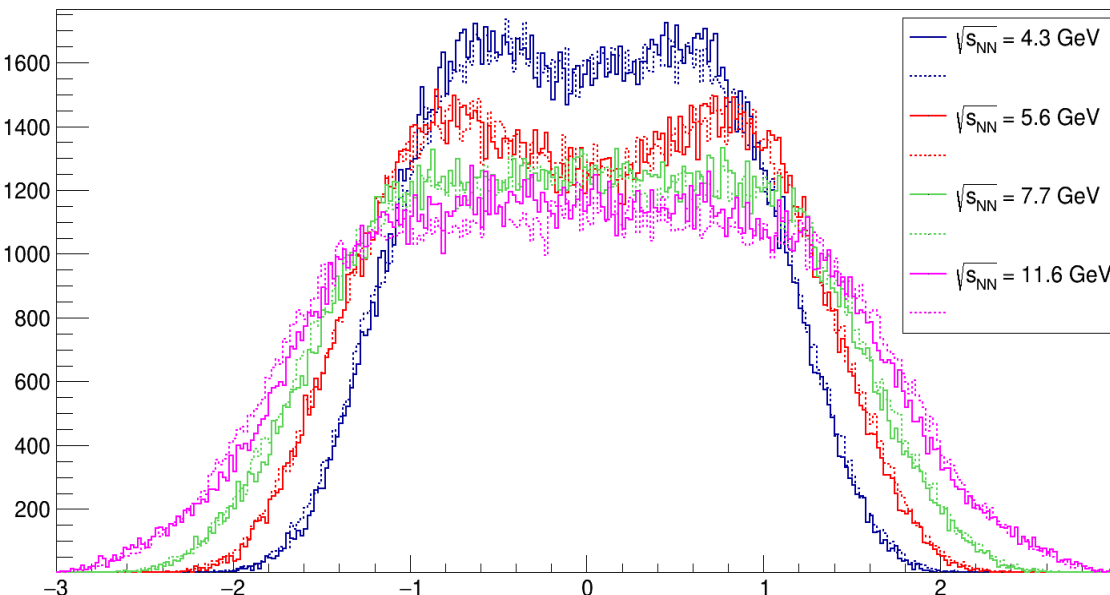
i1, EoS - crossover, solid line - 3FD, dashed line - 3FD + UrQMD



EoS: Crossover

Impact parameter: $b=2$ fm

i1, EoS - 1PT, solid line - 3FD, dashed line = 3FD + UrQMD



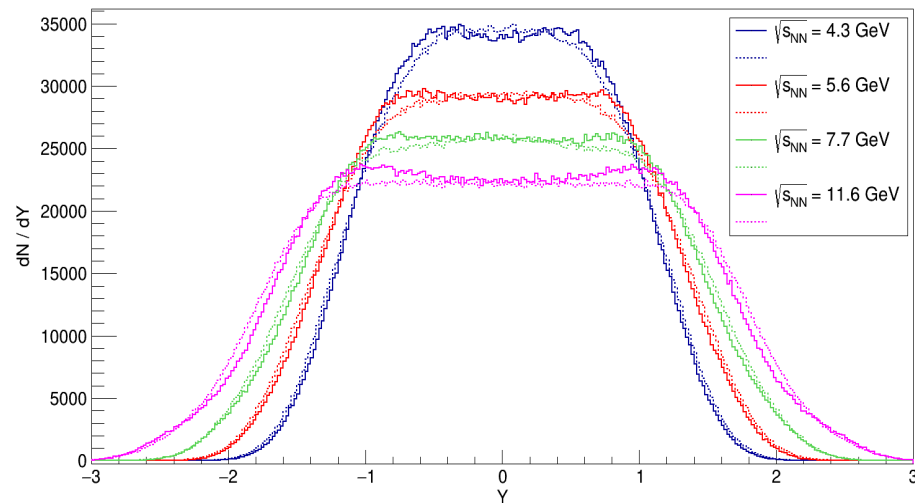
EoS: First order PT

Impact parameter: $b=2$ fm

Baryon stopping signal for first order phase transition ?

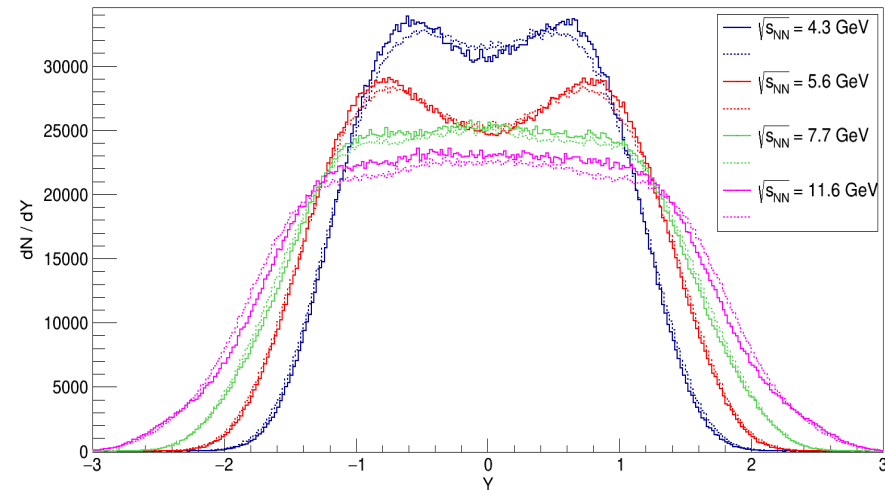
EoS: Crossover

$b = 2 \text{ fm}$, EoS - crossover, 3FD (solid line) , 3FD + UrQMD (dashed line)



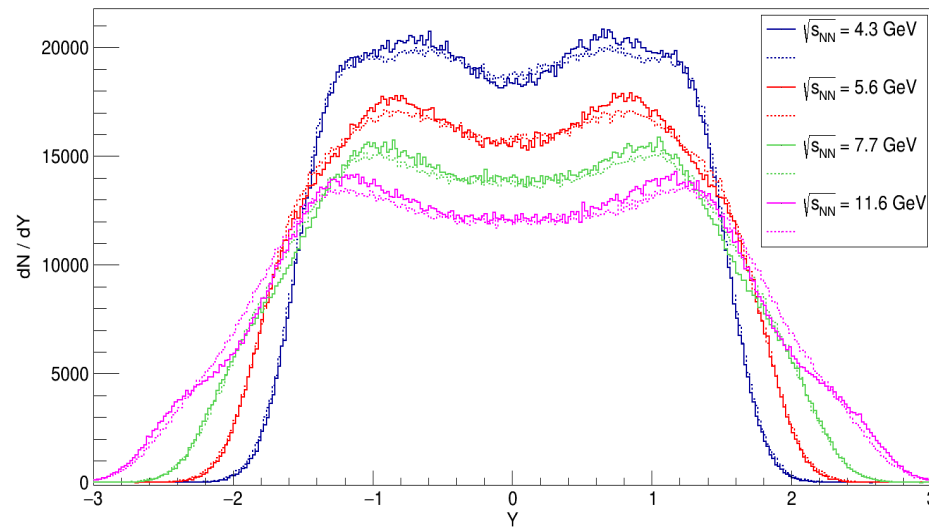
EoS: First order PT

$b = 2 \text{ fm}$, EoS - 1PT, 3FD (solid line), 3FD+ UrQMD (dashed line)

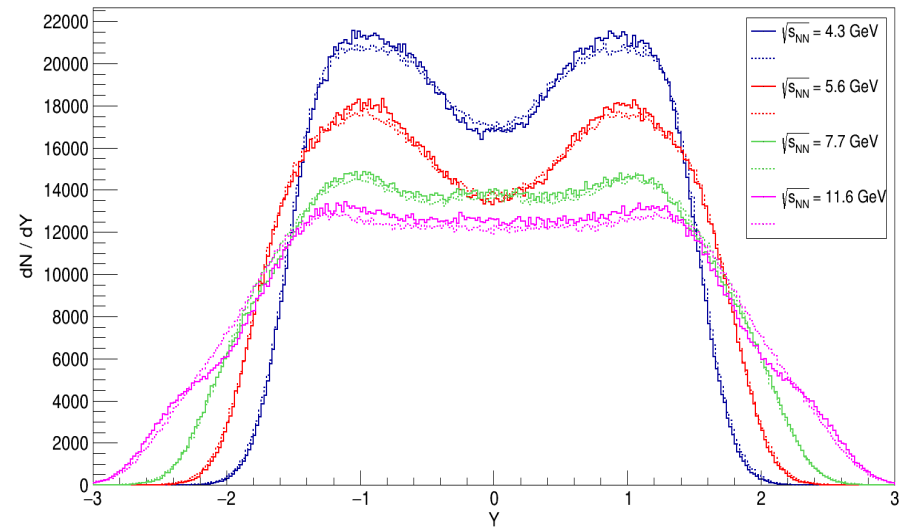


i1:
 $b=2 \text{ fm}$

$b = 6 \text{ fm}$, EoS - crossover, 3FD (solid line), 3FD + UrQMD (dashed line)

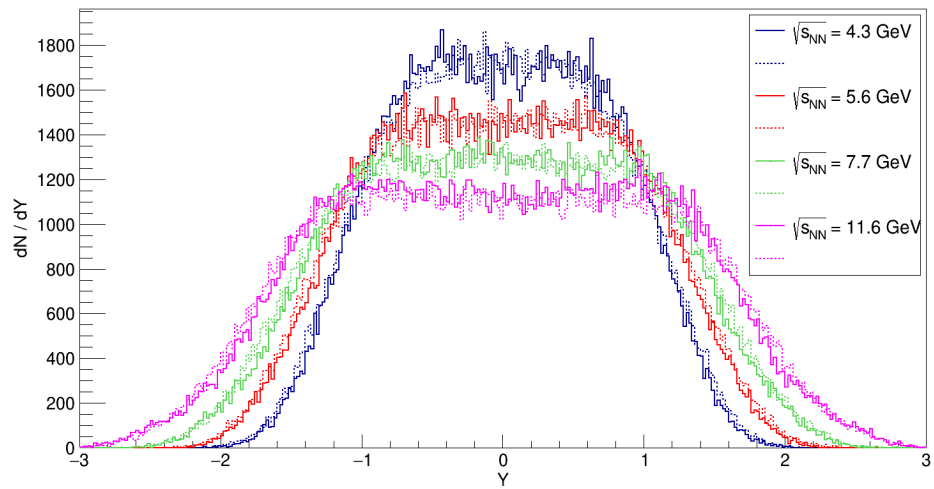


$b = 6 \text{ fm}$, EoS - 1PT, 3FD (solid line), 3FD + UrQMD (dashed line)

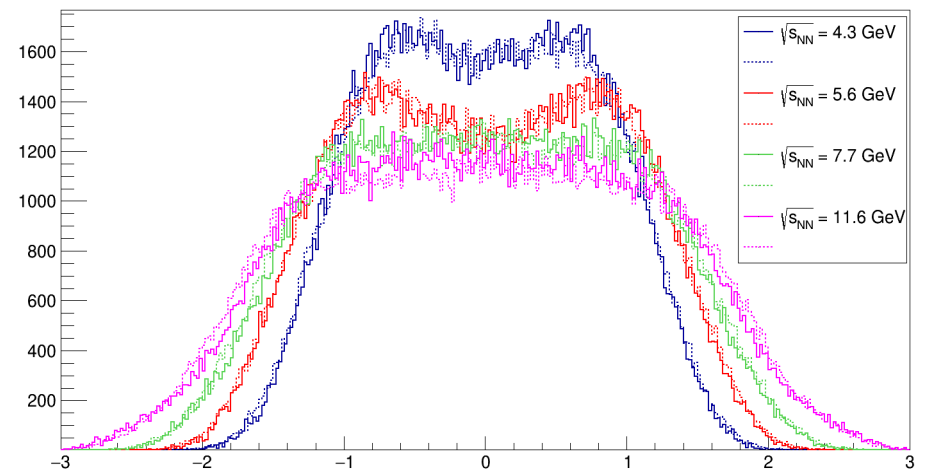


i3:
 $b=6 \text{ fm}$

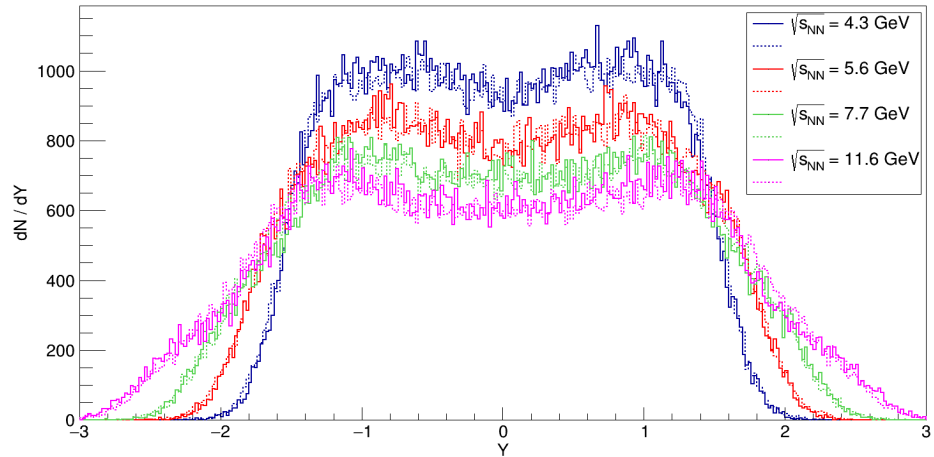
i1, EoS - crossover, solid line - 3FD, dashed line - 3FD + UrQMD



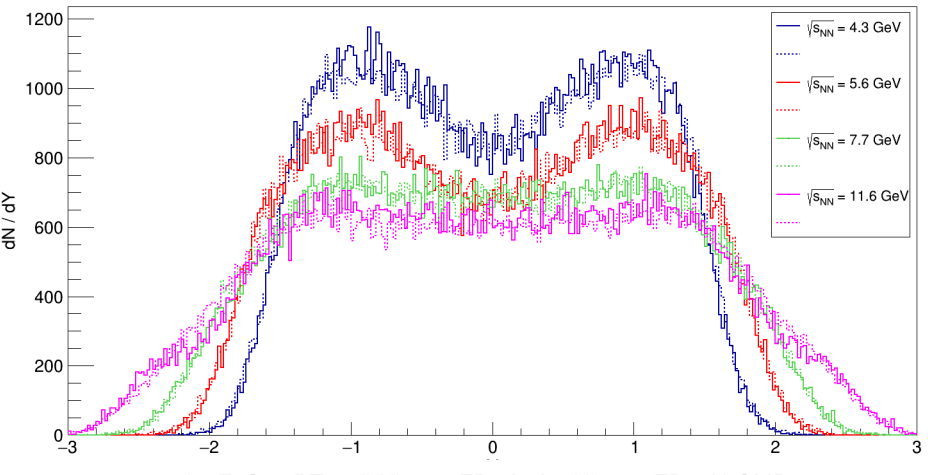
i1, EoS - 1PT, solid line - 3FD, dashed line = 3FD + UrQMD



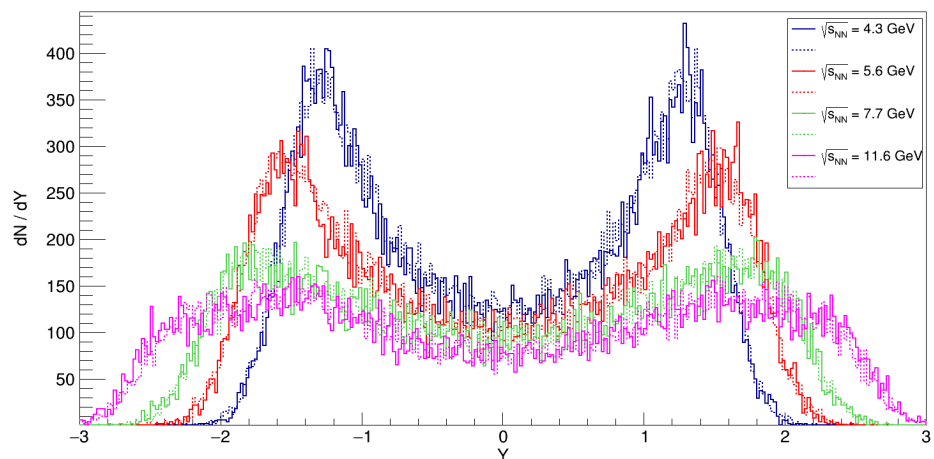
i3, EoS - crossover, solid line - 3FD, dashed line - 3FD + UrQMD



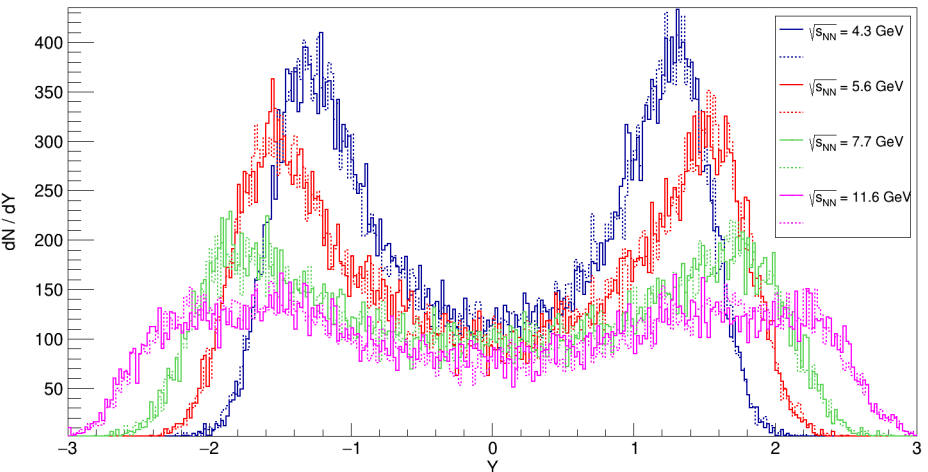
i3, EoS- 1PT, solid line - 3FD, dashed line - 3FD + UrQMD



i5, EoS - crossover, solid line - 3FD, dashed line - 3FD + UrQMD

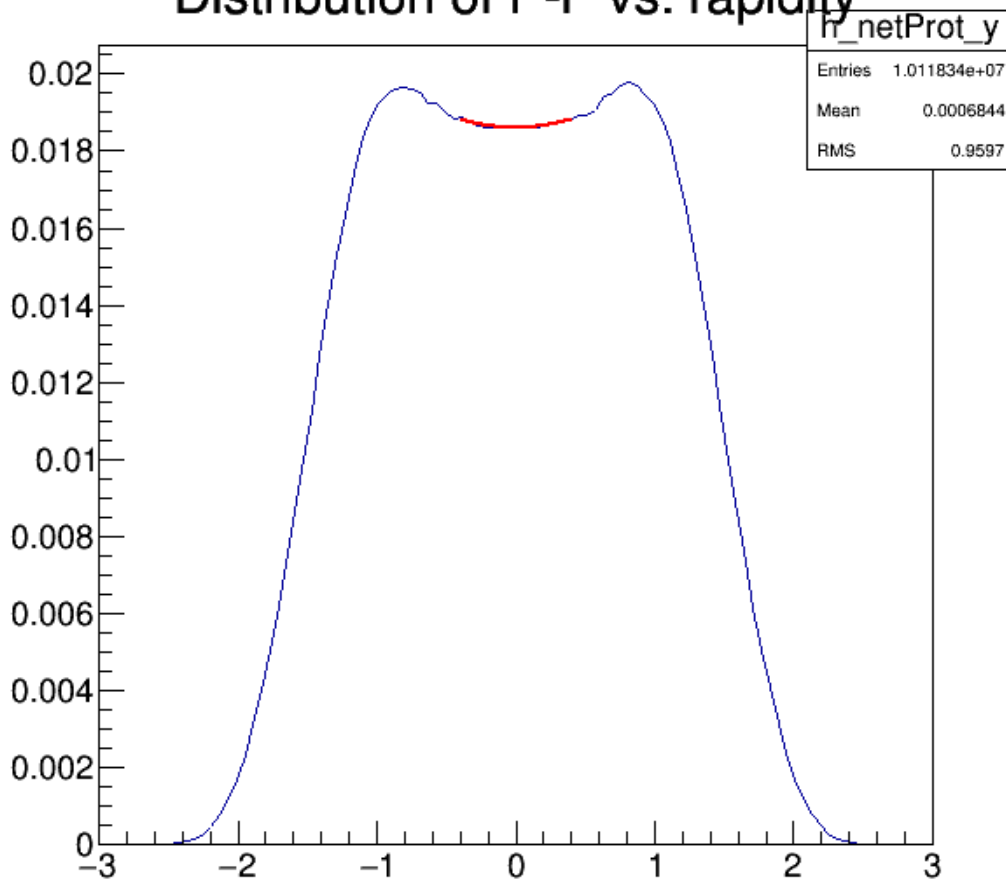


i5, EoS - 1PT, solid line - 3FD, dashed line - 3FD + UrQMD

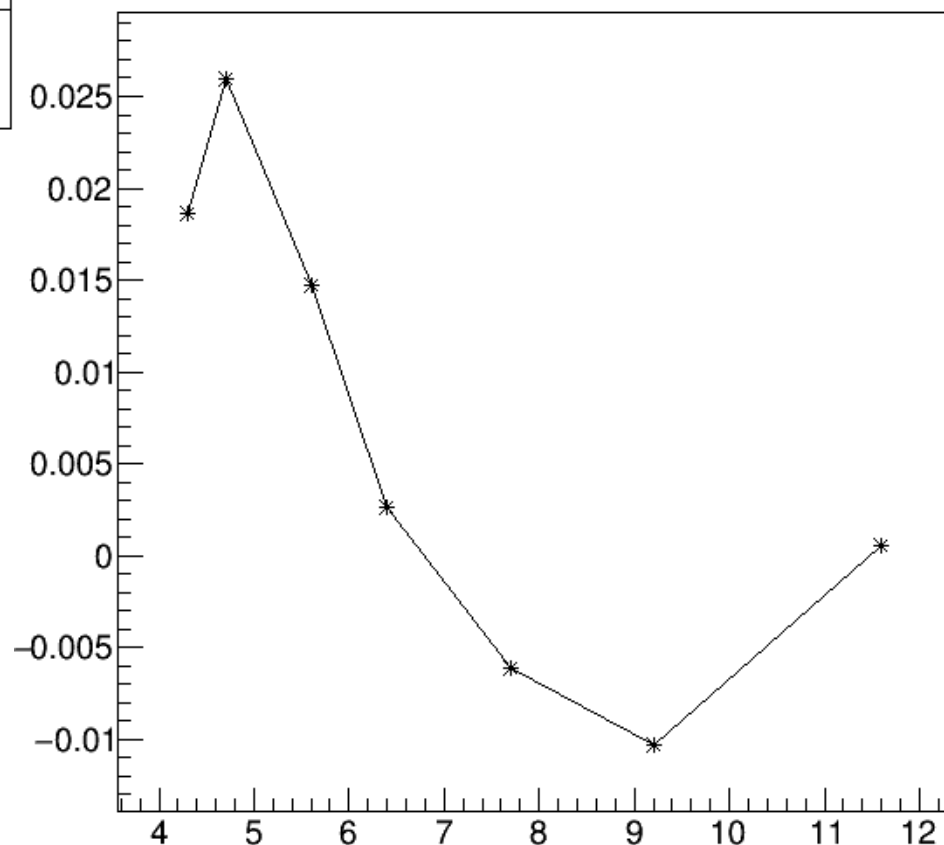


Baryon stopping signal: extract the curvature at midrapidity !

Distribution of $P - \bar{P}$ vs. rapidity



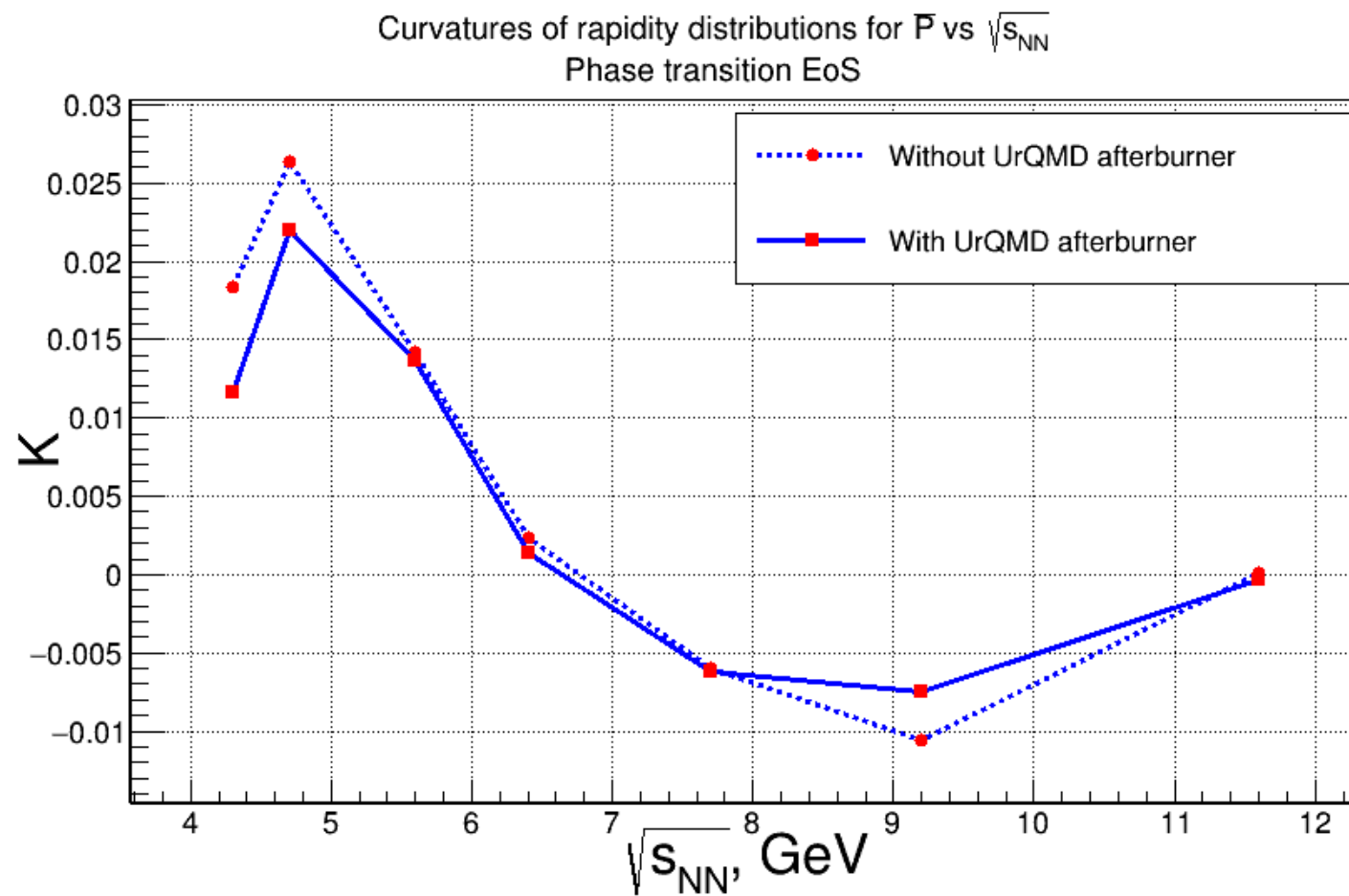
Curvatures of rapidity distributions for \bar{P} vs $\sqrt{s_{NN}}$



“Wiggle” in the excitation function (energy scan) confirmed !

Particilization of 3FH works satisfactorily → join with UrQMD “afterburner”

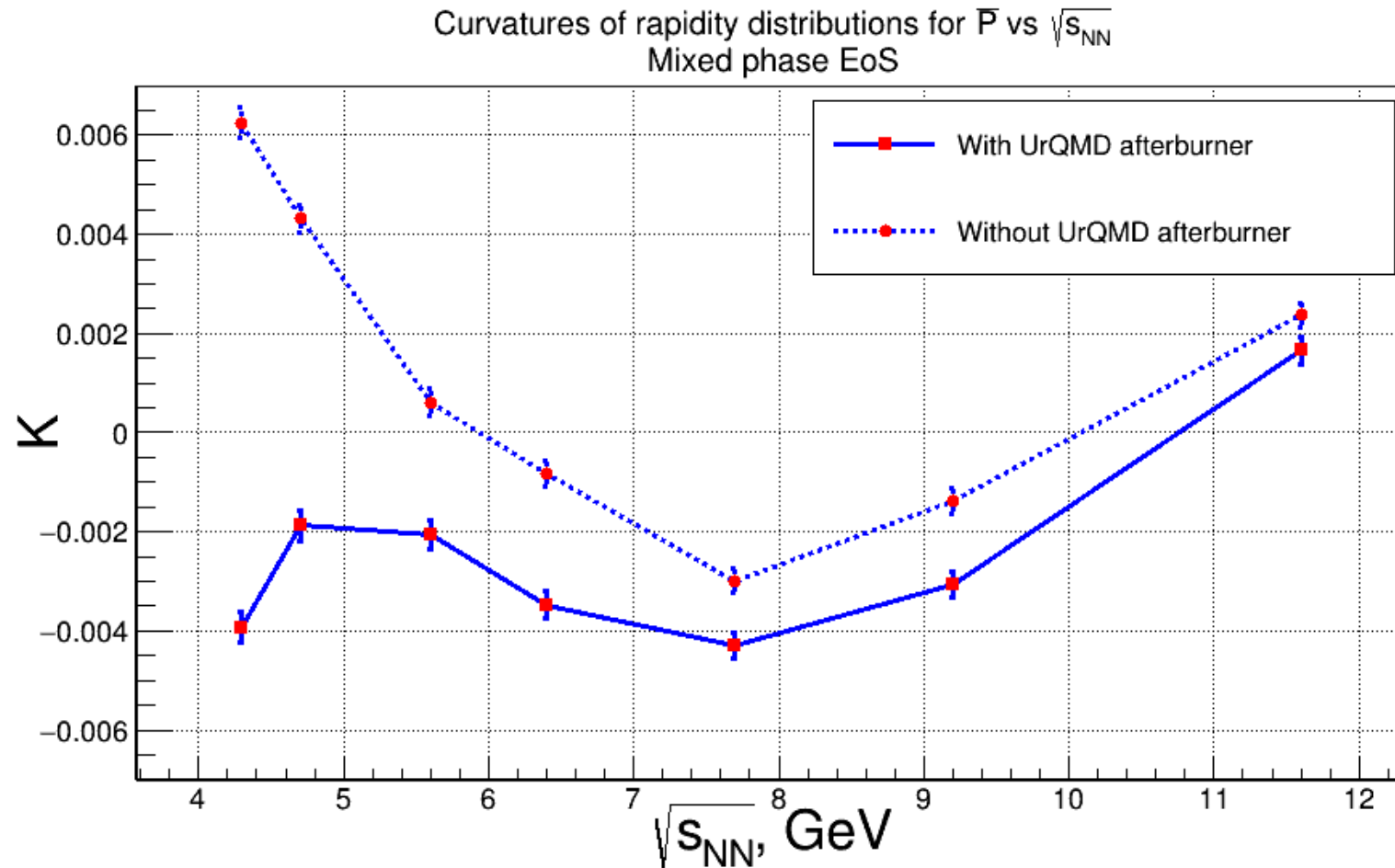
Baryon stopping signal: effect of UrQMD afterburner !



“Wiggle” in the excitation function (energy scan) confirmed !

UrQMD afterburner almost no effect on the “wiggle” for the 2PT EoS

Baryon stopping signal: effect of EoS & UrQMD afterburner !

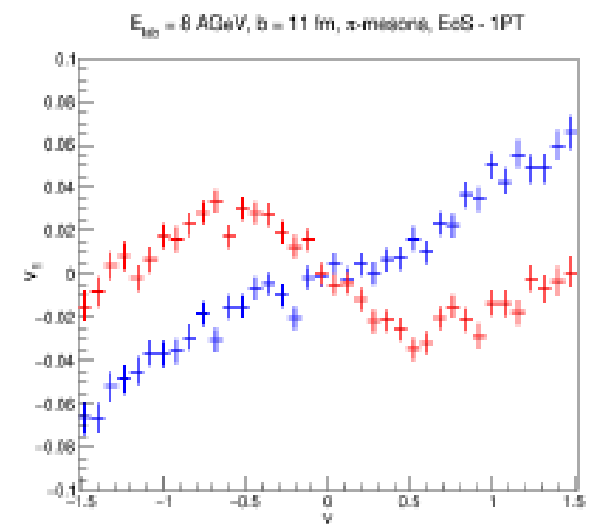
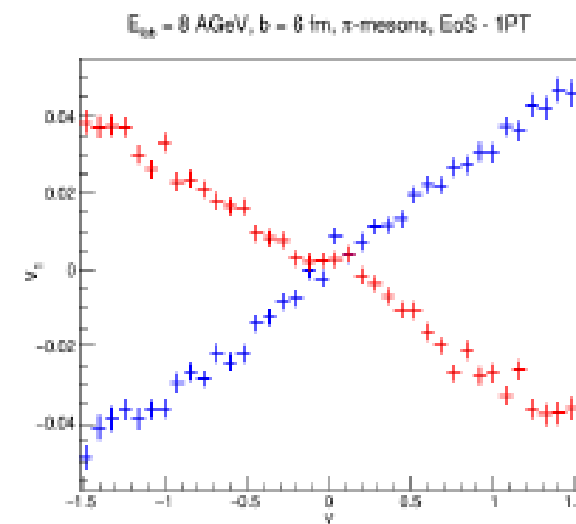
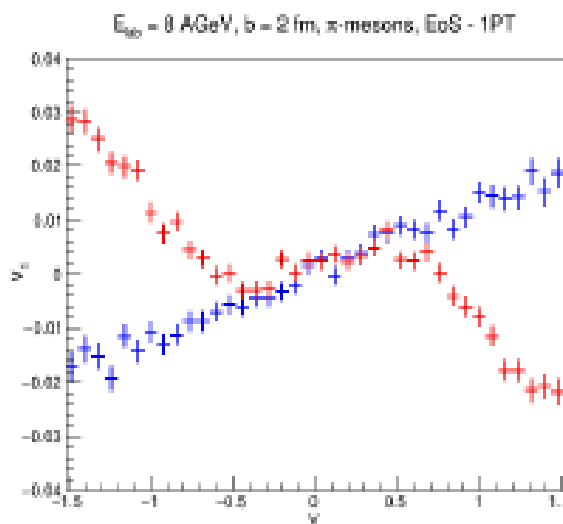
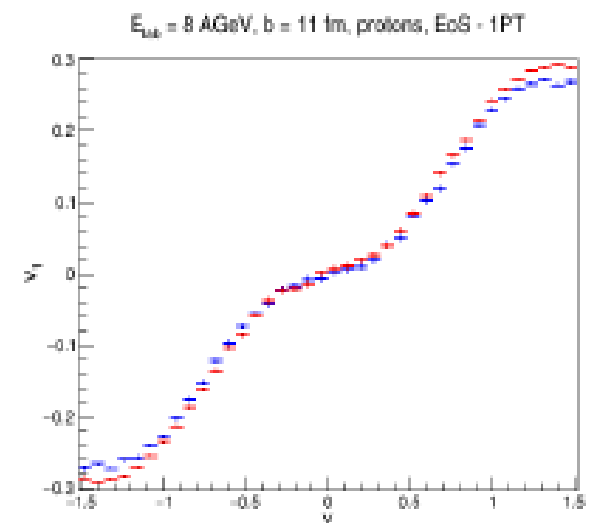
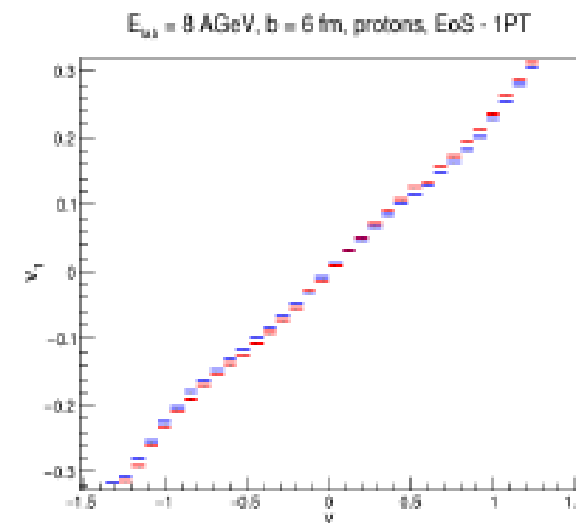
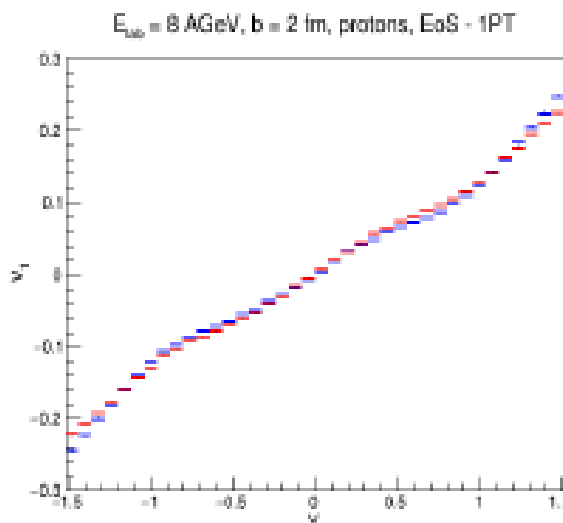


“Wiggle” in the excitation function (energy scan) confirmed !

UrQMD afterburner smoothes the “wiggle” for the crossover EoS !

What about flow? First results (v1)

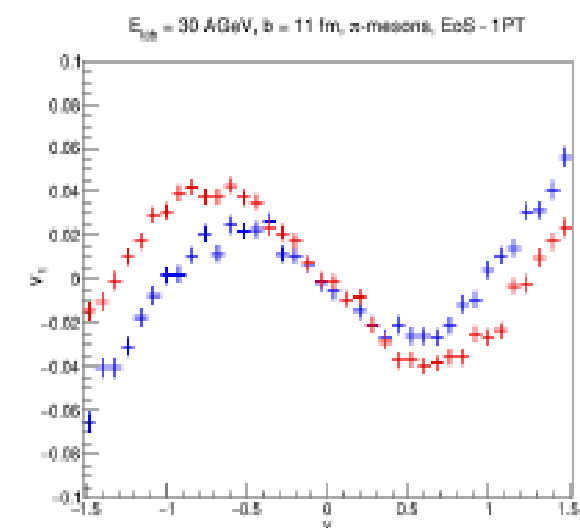
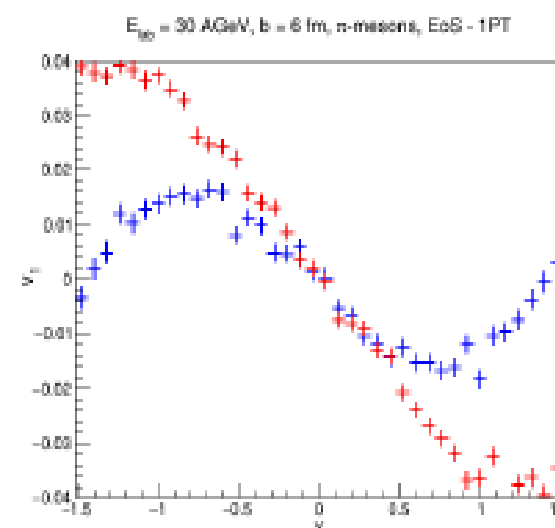
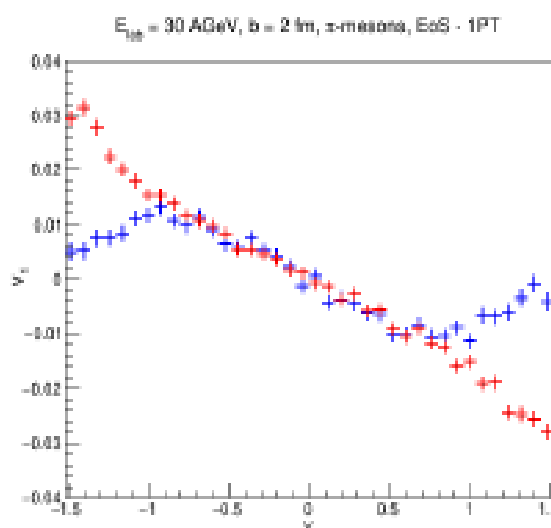
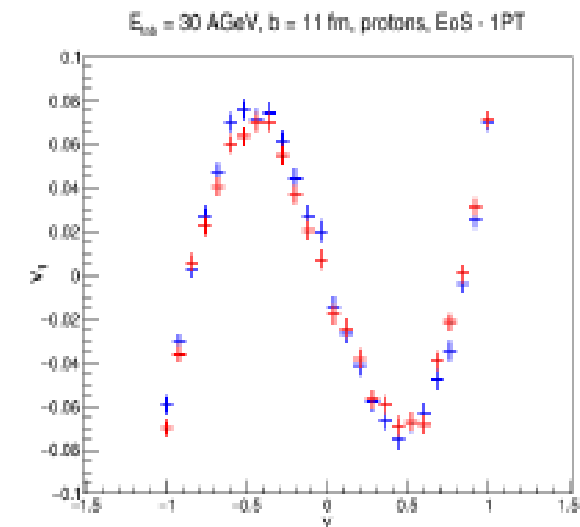
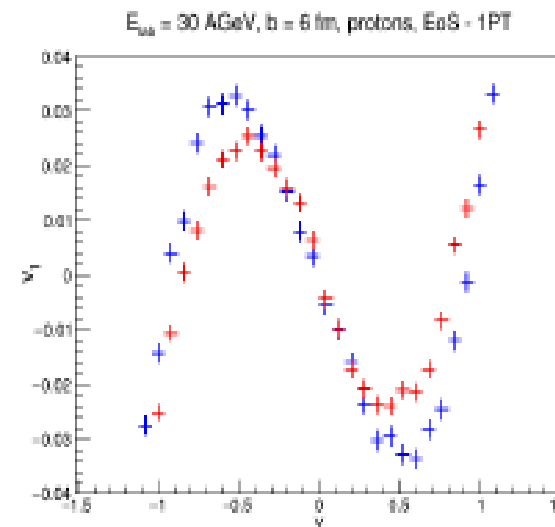
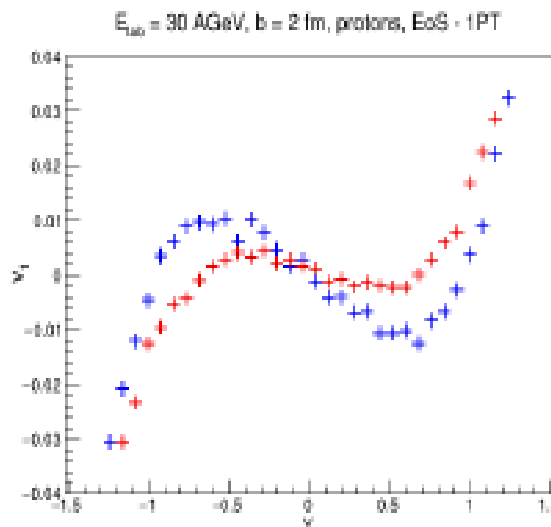
$E_{\text{lab}} = 8 \text{ AGeV}$



Blocking of pions by hadronic rescattering (red plusses), upper w/o UrQMD !

What about flow? First results(v1)

$E_{\text{lab}} = 30 \text{ AGeV}$



Antiflow of protons \rightarrow pions follow !

Further developments:

- MPD Detector simulation (Oleg Rogachevsky et al.)**
- New 2-phase EoS (Wroclaw group, see talk Bastian)**

A new class of 2-phase EoS: Motivation from Astrophysics

Modern 2-phase EoS in Astrophysics of Compact Stars

1. Pauli blocking effect → Excluded volume

Well known from modeling dissociation of clusters in the supernova EoS:

- excluded volume: Lattimer-Swesty (1991), Shen-Toki-Oyematsu-Sumiyoshi (1996), ...
- Pauli blocking: Roepke-Grigo-Sumiyoshi-Shen (2003), Typel et al. PRC 81 (2010)
- excl. Vol. vs. Pauli blocking: Hempel, Schaffner-Bielich, Typel, Roepke PRC 84 (2011)

Here: nucleons as quark clusters with finite size --> excluded volume effect !

Available volume fraction: $\Phi = V_{\text{av}}/V = 1 - v \sum_{i=n,p} n_i, \quad v = \frac{1}{2} \frac{4\pi}{3} (2r_{\text{nuc}})^3 = 4V_{\text{nuc}}$

Equations of state for T=0 nuclear matter: $p_{\text{tot}}(\mu_n, \mu_p) = \frac{1}{\Phi} \sum_{i=n,p} p_i + p_{\text{mes}},$

$$p_i = \frac{1}{4} \left(E_i n_i - m_i^* n_i^{(s)} \right),$$

$$n_i = \frac{\Phi}{3\pi^3} k_i^3,$$

$$n_i^{(s)} = \frac{\Phi m_i^*}{2\pi^2} \left[E_i k_i - (m_i^*)^2 \ln \frac{k_i + E_i}{m_i^*} \right],$$

$$E_i = \sqrt{k_i^2 + (m_i^*)^2} = \mu_i - V_i - \frac{v}{\Phi} \sum_{j=p,n} p_j,$$

$$\epsilon_{\text{tot}}(\mu_n, \mu_p) = -p_{\text{tot}} + \sum_{i=n,p} \mu_i n_i,$$

Effective mass: $m_i^* = m_i - S_i.$

Scalar meanfield: $S_i \sim n_i^{(s)}$

Vector meanfield: $V_i \sim n_i$

Modern 2-phase EoS in Astrophysics of Compact Stars

2. Stiff quark matter at high densities

S. Benic, Eur. Phys. J. A 50, 111 (2014)

$$\mathcal{L} = \bar{q}(i\partial - m)q + \mu_q \bar{q}\gamma^0 q + \mathcal{L}_4 + \mathcal{L}_8 , \quad \mathcal{L}_4 = \frac{g_{20}}{\Lambda^2}[(\bar{q}q)^2 + (\bar{q}i\gamma_5\tau q)^2] - \frac{g_{02}}{\Lambda^2}(\bar{q}\gamma_\mu q)^2 ,$$

$$\mathcal{L}_8 = \frac{g_{40}}{\Lambda^8}[(\bar{q}q)^2 + (\bar{q}i\gamma_5\tau q)^2]^2 - \frac{g_{04}}{\Lambda^8}(\bar{q}\gamma_\mu q)^4 - \frac{g_{22}}{\Lambda^8}(\bar{q}\gamma_\mu q)^2[(\bar{q}q)^2 + (\bar{q}i\gamma_5\tau q)^2]$$

Meanfield approximation: $\mathcal{L}_{\text{MF}} = \bar{q}(i\partial - M)q + \tilde{\mu}_q \bar{q}\gamma^0 q - U ,$

$$M = m + 2\frac{g_{20}}{\Lambda^2}\langle\bar{q}q\rangle + 4\frac{g_{40}}{\Lambda^8}\langle\bar{q}q\rangle^3 - 2\frac{g_{22}}{\Lambda^8}\langle\bar{q}q\rangle\langle q^\dagger q\rangle^2 ,$$

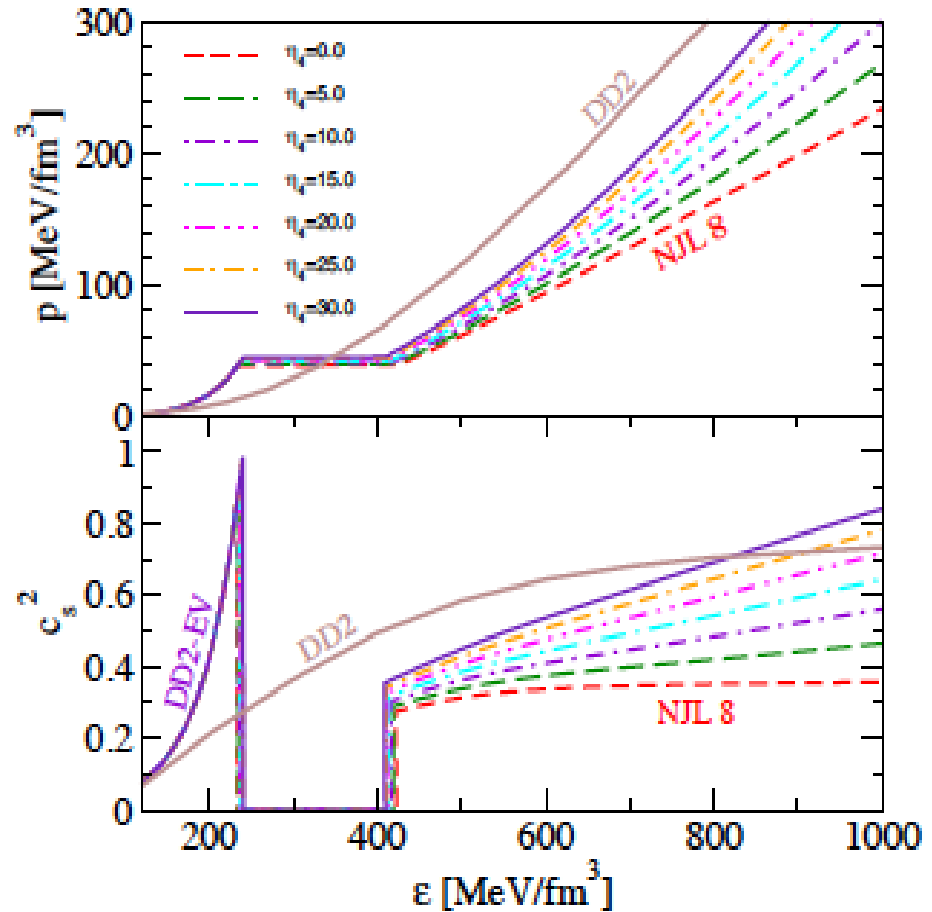
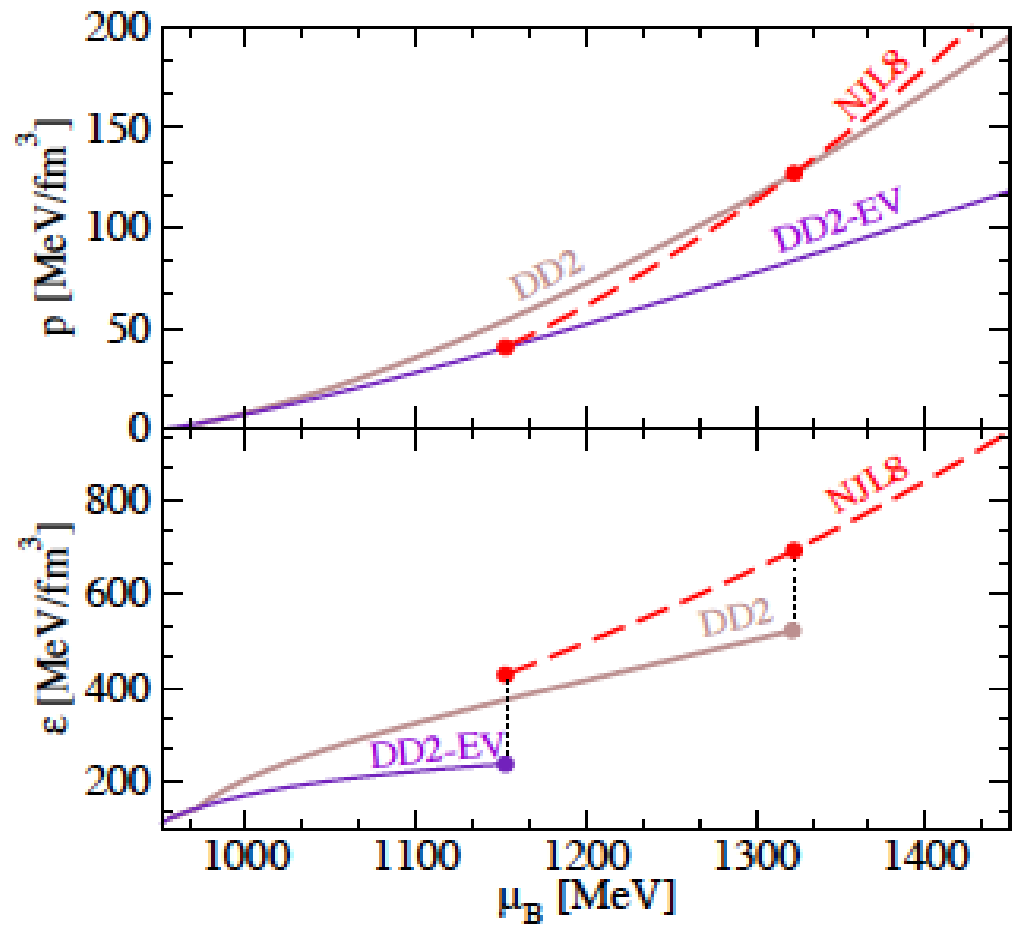
$$\tilde{\mu}_q = \mu_q - 2\frac{g_{02}}{\Lambda^2}\langle q^\dagger q\rangle - 4\frac{g_{04}}{\Lambda^8}\langle q^\dagger q\rangle^3 - 2\frac{g_{22}}{\Lambda^8}\langle\bar{q}q\rangle^2\langle q^\dagger q\rangle ,$$

$$U = \frac{g_{20}}{\Lambda^2}\langle\bar{q}q\rangle^2 + 3\frac{g_{40}}{\Lambda^8}\langle\bar{q}q\rangle^4 - 3\frac{g_{22}}{\Lambda^8}\langle\bar{q}q\rangle^2\langle q^\dagger q\rangle^2 - \frac{g_{02}}{\Lambda^2}\langle q^\dagger q\rangle^2 - 3\frac{g_{04}}{\Lambda^8}\langle q^\dagger q\rangle^4 .$$

Thermodynamic Potential:

$$\Omega = U - 2N_f N_c \int \frac{d^3 p}{(2\pi)^3} \left\{ E + T \log[1 + e^{-\beta(E - \tilde{\mu}_q)}] + T \log[1 + e^{-\beta(E + \tilde{\mu}_q)}] \right\} + \Omega_0$$

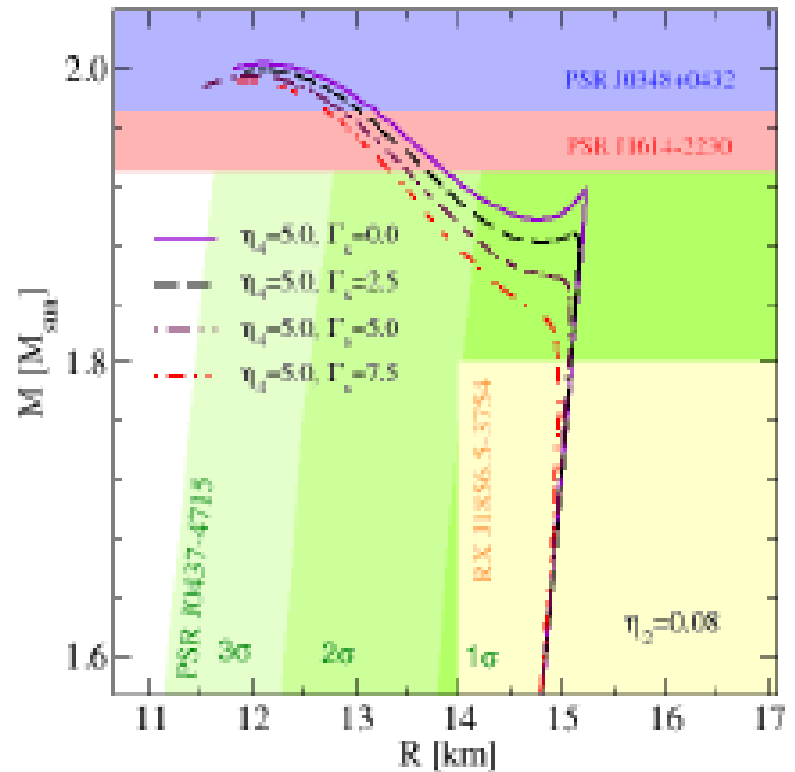
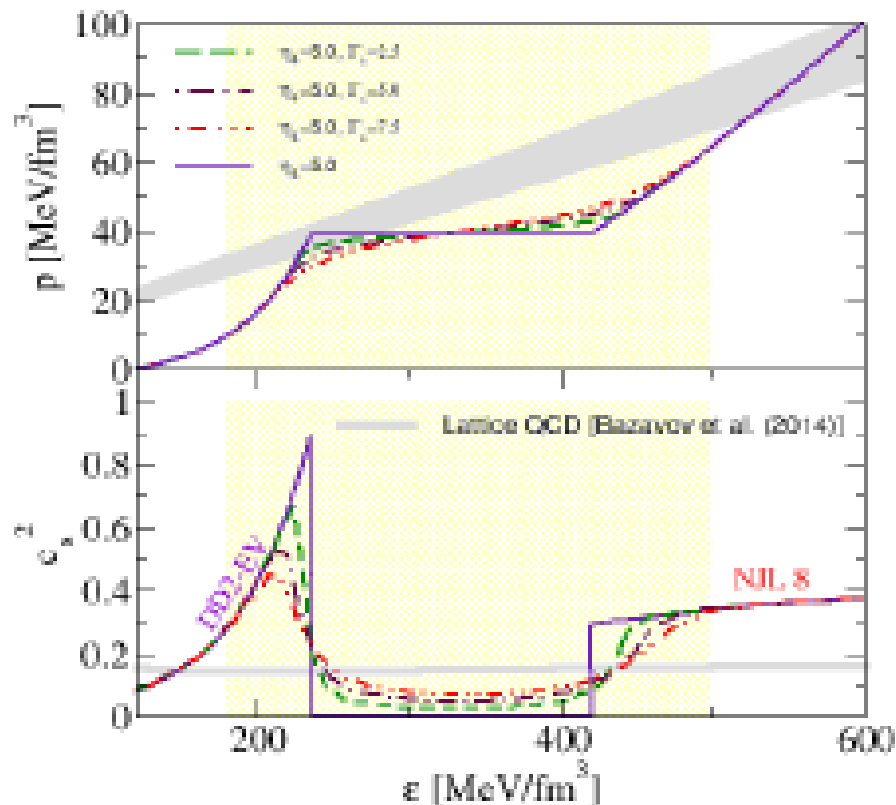
Modern 2-phase EoS in Astrophysics of Compact Stars



Here: Stiffening of dense hadronic matter by excluded volume in density-dependent RMF
Stiffening of dense quark matter by higher order quark vector current interactions (η_4)

Modern 2-phase EoS in Astrophysics of Compact Stars

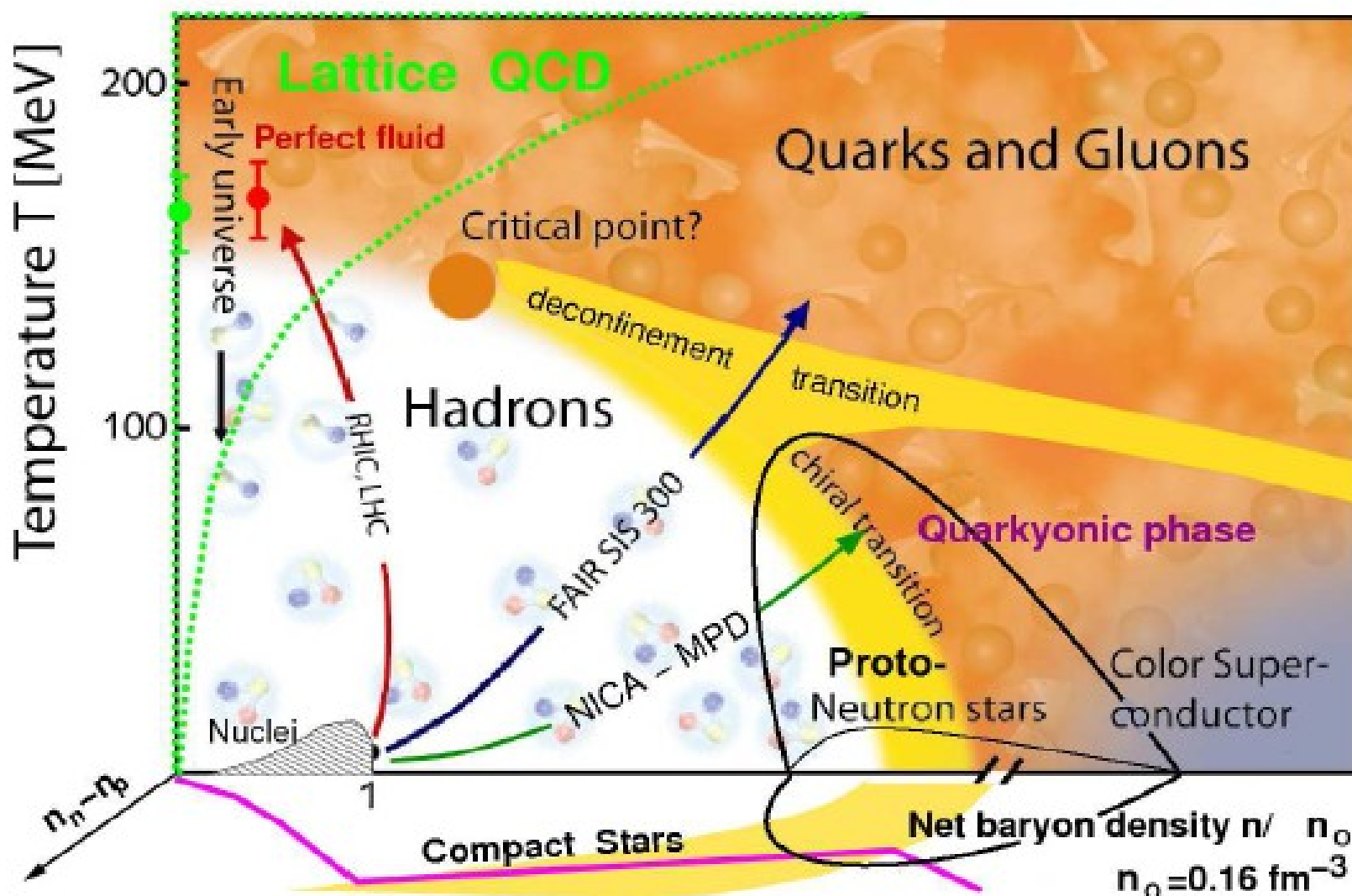
Estimate effects of structures in the phase transition region (“pasta”)



High-mass Twins relatively robust against “smoothing” the Maxwell transition construction

D. Alvarez-Castillo, D.B., arxiv:1412.8463

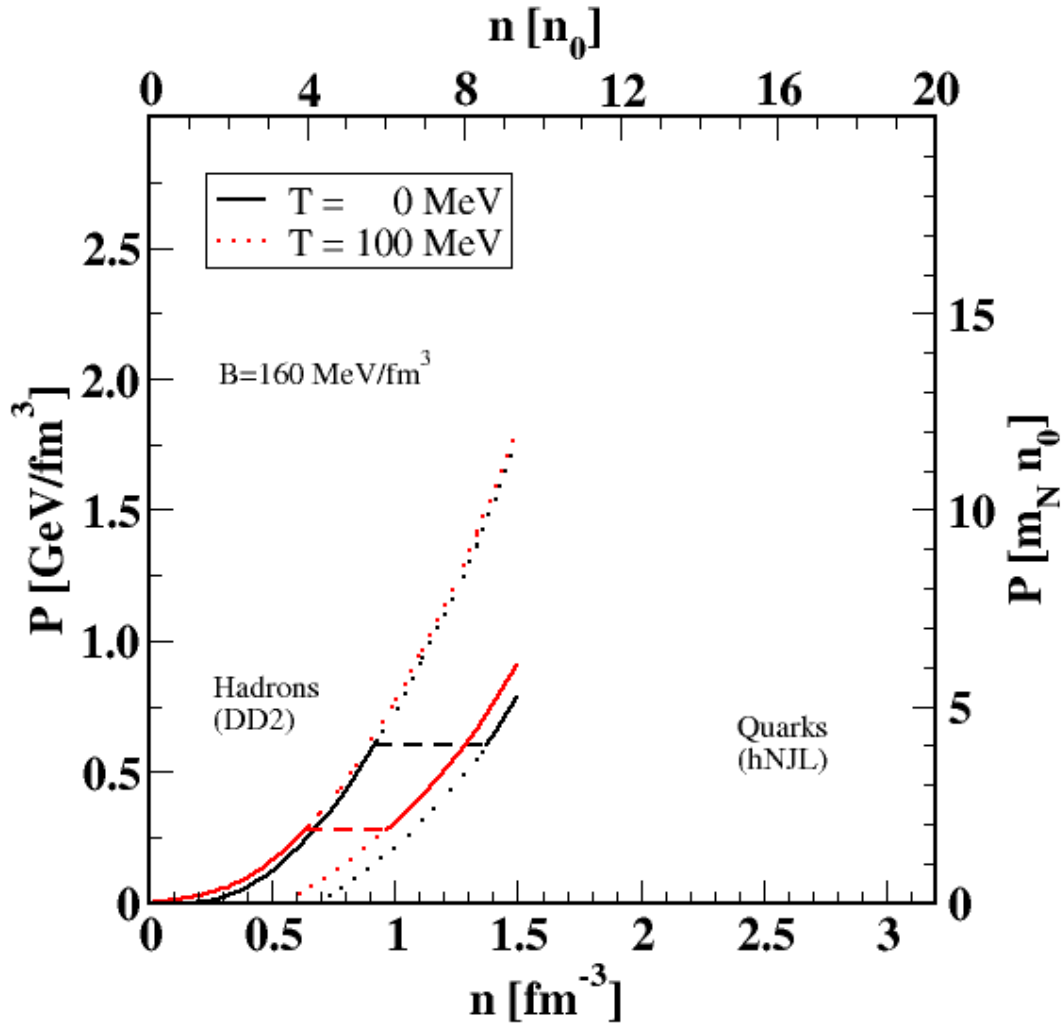
Support a CEP in QCD phase diagram with Astrophysics?



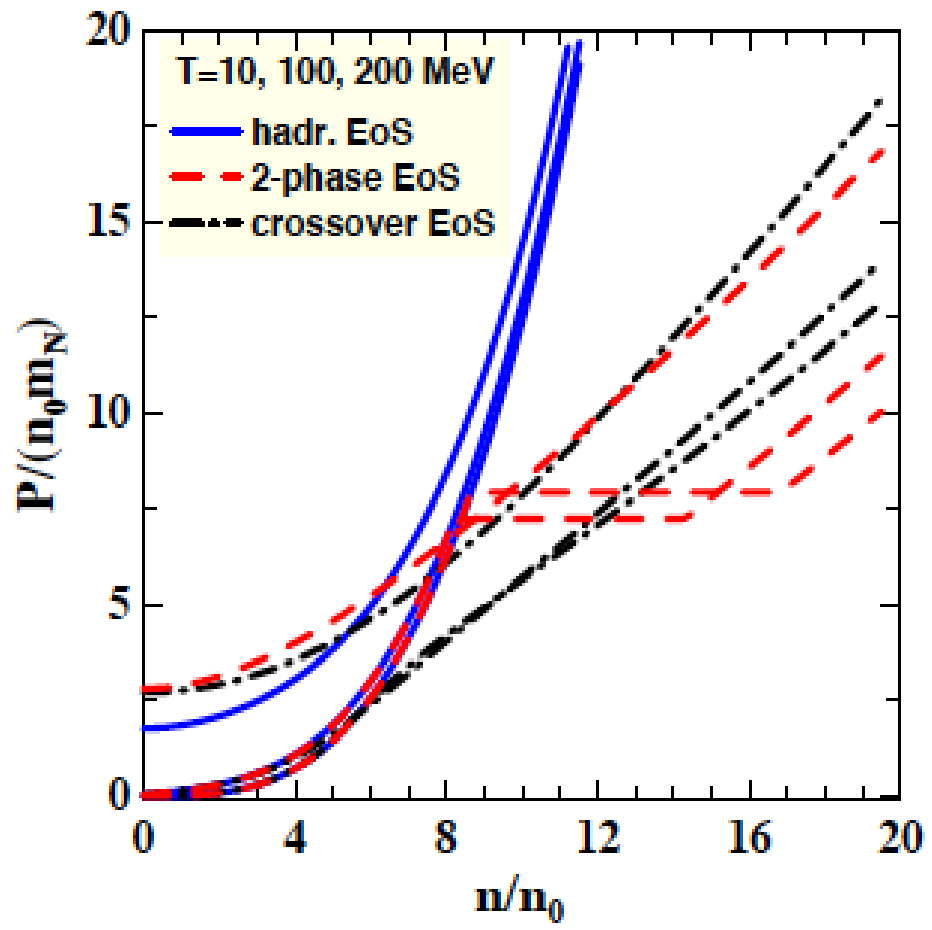
NICA White Paper, <http://theor.jinr.ru/twiki-cgi/view/NICA/WebHome>

Crossover at finite T (Lattice QCD) + First order at zero T (Astrophysics) = Critical endpoint exists!

Comparison 2-phase EoS

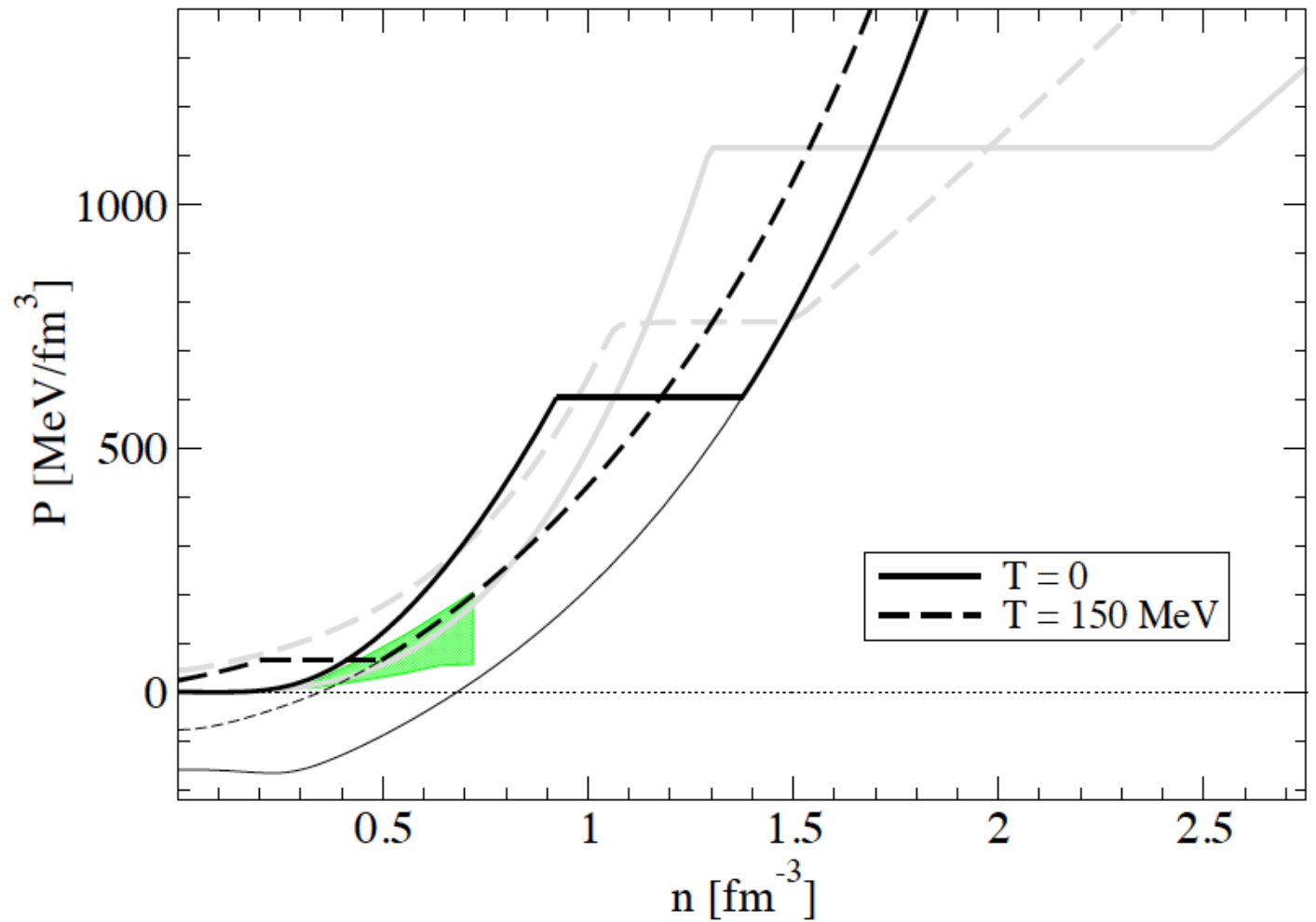


N.-U. Bastian, D. Blaschke (S. Benic, S. Typel),
In progress (2015)



A. Khvorostukhin et al. EPJC 48 (2006) 531
Yu. Ivanov, D. Blaschke, arxiv:1504.03992

Comparison 2-phase EoS



Grey: Ivanov (2010)

Black: DD2 vs. HNJLb

$B=160$ MeV/fm 3

Summary / Outlook:

- Baryon stopping signal (“wiggle”) remains a robust signal for 1st order PT also under severe cuts in transverse momentum !
- Discrimination between hadronic phase and crossover transition ambiguous
- Position of the “wiggle” in the beam energy scan is EoS dependent – new EoS ?!
- Particlization of 3-Fluid Hydrodynamics model works !
- UrQMD “afterburner” works too !

- Detector simulation in progress
- Systematic study of modern 2-phase EoS (Bayesian analysis) in progress



Critical Point and Onset of Deconfinement 2016

and

Working Group Meeting of COST Action MP1304

Wrocław, Poland

May 30th - June 4th, 2016



Int. Advisory Comm.
F. Becattini (Florence)
D. Blaschke (Dubna)
Xin Dong (Berkeley)
M. Gaździcki (Frankfurt)
L. McLerran (Upton)
E. Laermann (Bielefeld)
J. Mitchell (Upton)
K. Rajagopal (Boston)
J. Randrup (Berkeley)
D. Röhrich (Bergen)
P. Senger (Darmstadt)
P. Seyboth (Munich)
E. Shuryak (Stony Brook)
A. Sorin (Dubna)
M Stephanov (Chicago)
J. Stroth (Genf)
Nu Xu (Berkeley)
Dacui Zhou (Wuhan)

Organization Comm.

D. Blaschke (Wroclaw)
J. Margueron (Lyon)
K. Redlich (Wroclaw)
L. Turko (Wroclaw)
C. Sasaki (Wroclaw)

Local Org. Comm.

T. Fischer (Wroclaw)
T. Klähn (Wroclaw)
Pok Man Lo (Wroclaw)
M. Marczenko (Wroclaw)
M. Naskrét (Wroclaw)

Website:

ift.uni.wroc.pl/~cpod2016

Email:

cpod2016@ift.uni.wroc.pl



Uniwersytet
Wrocławski

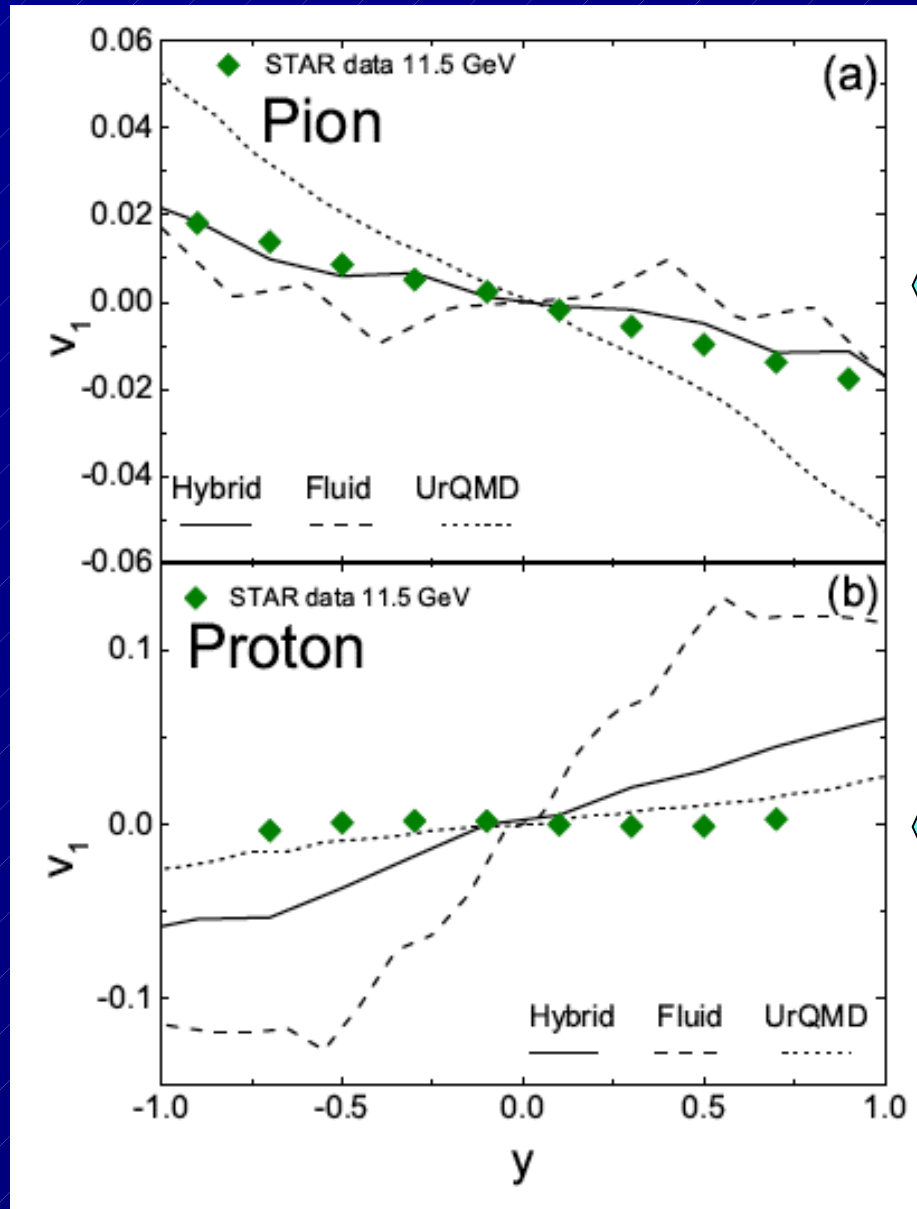


Springer

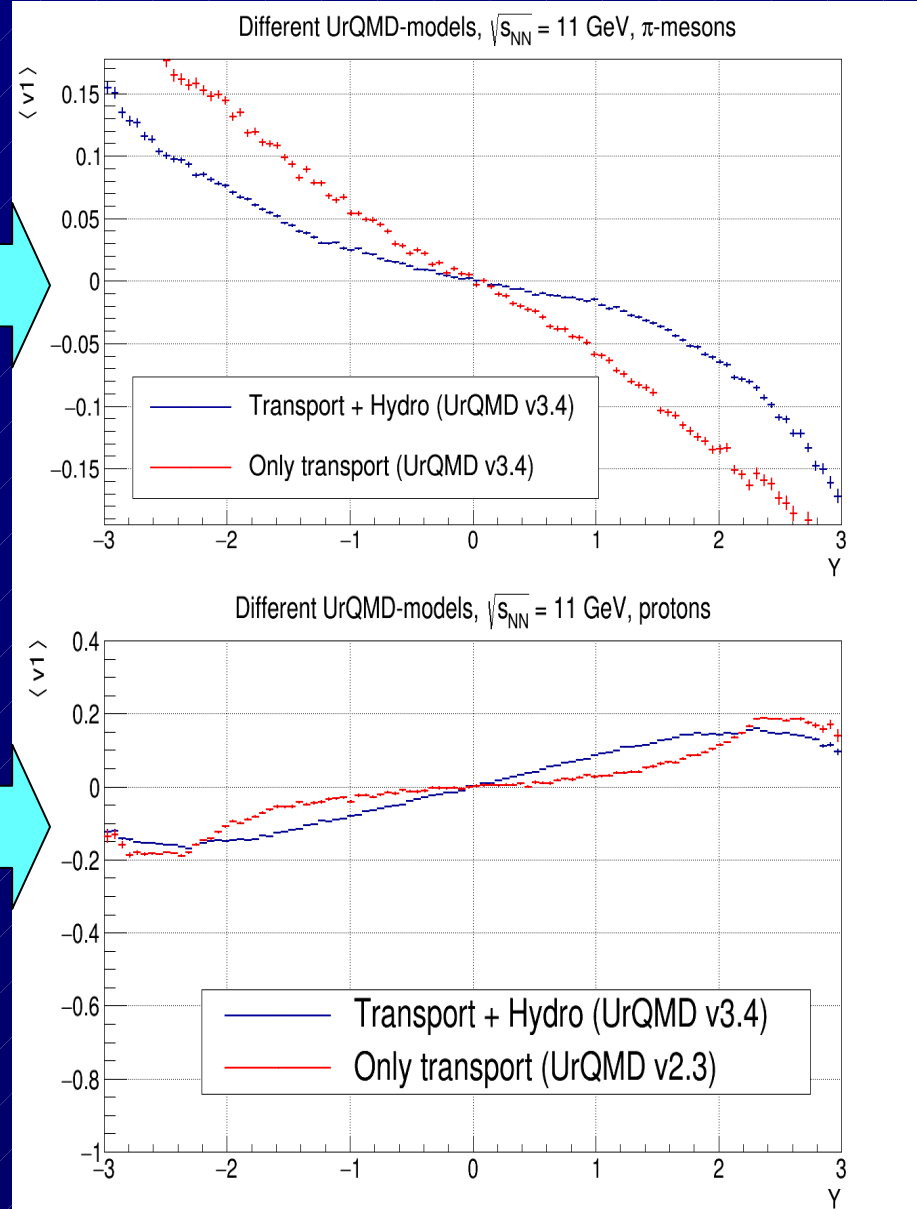


Additional Slides

Further results of test simulations – flow observables



Reproduced!

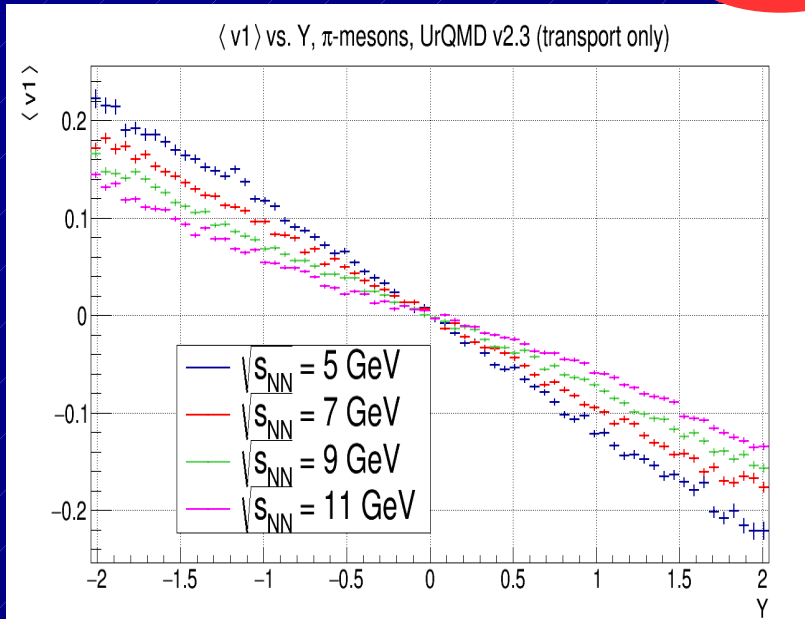


Further results of test simulations – flow observables

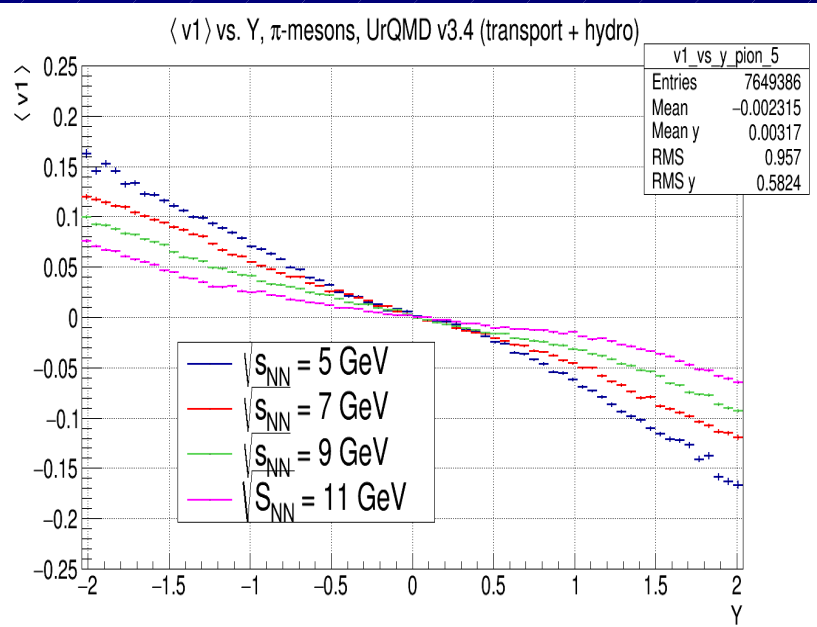
NICA energy scan: UrQMD

$\langle v_1 \rangle$

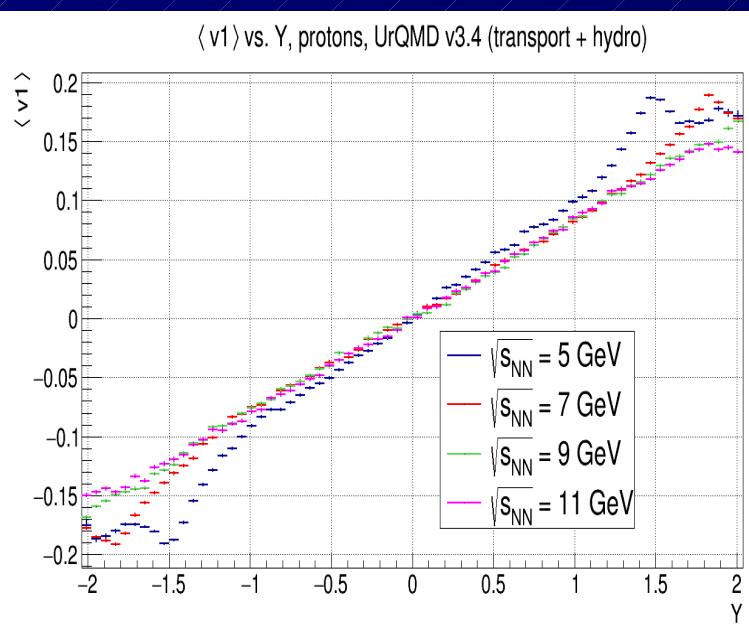
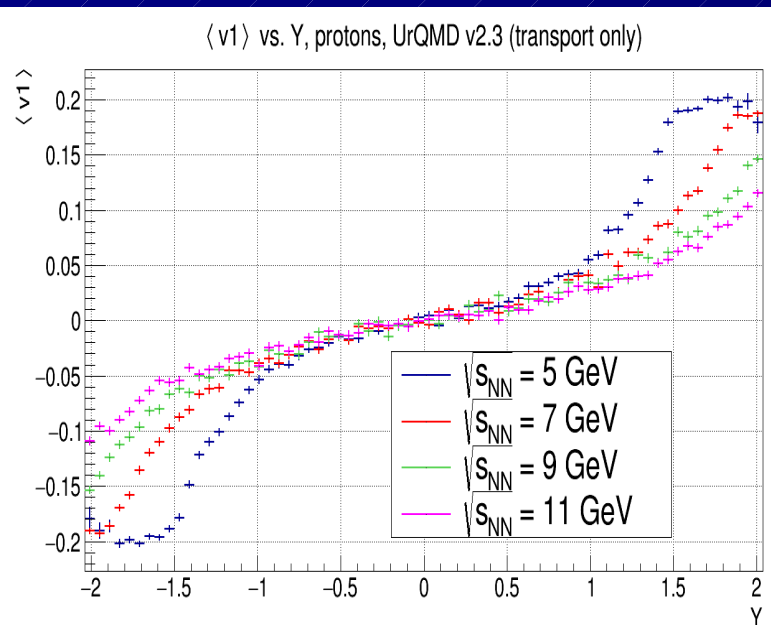
Pions



UrQMD + hydro (1st order PT)



Protons

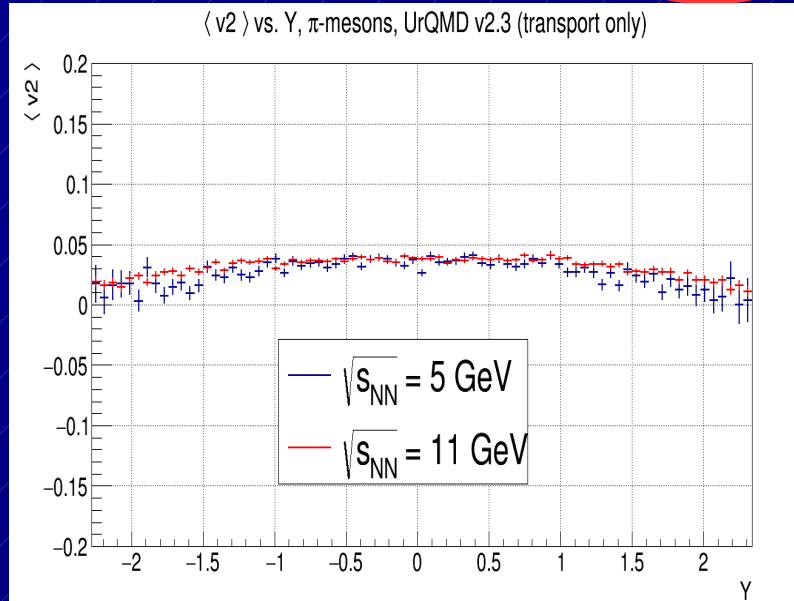


Further results of test simulations – flow observables

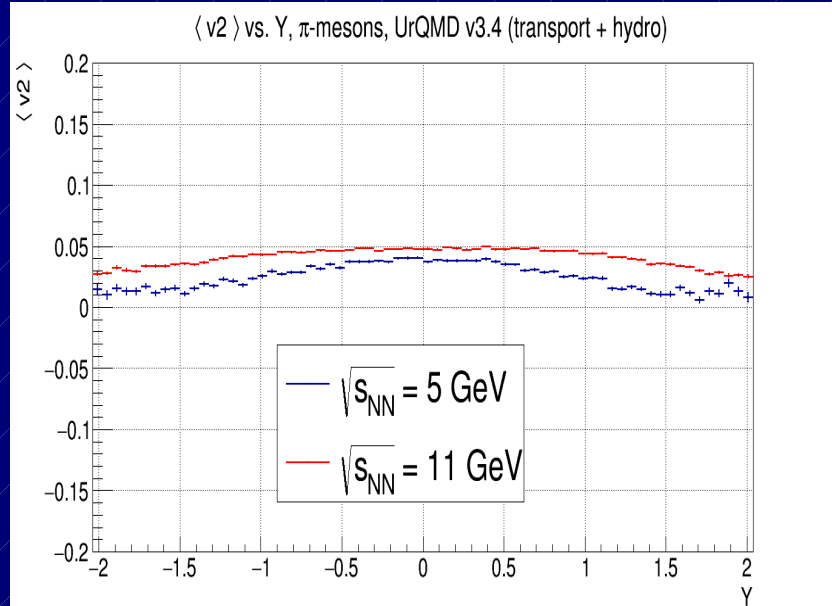
NICA energy scan: UrQMD

$\langle v_2 \rangle$

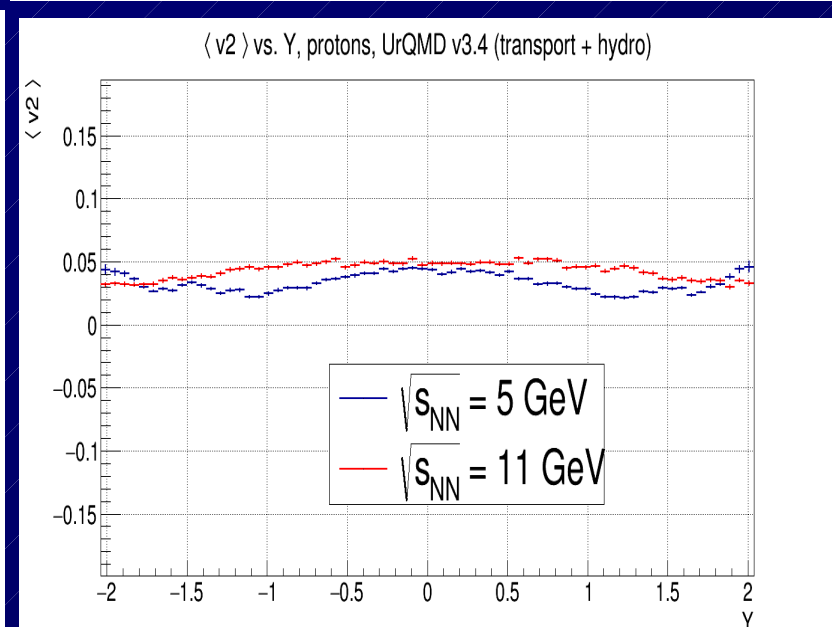
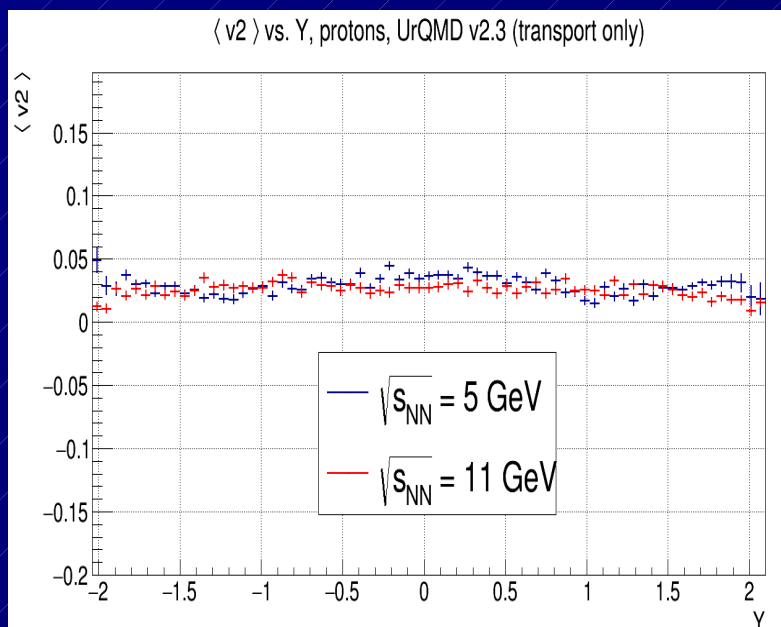
Pions



UrQMD + hydro (1st order PT)



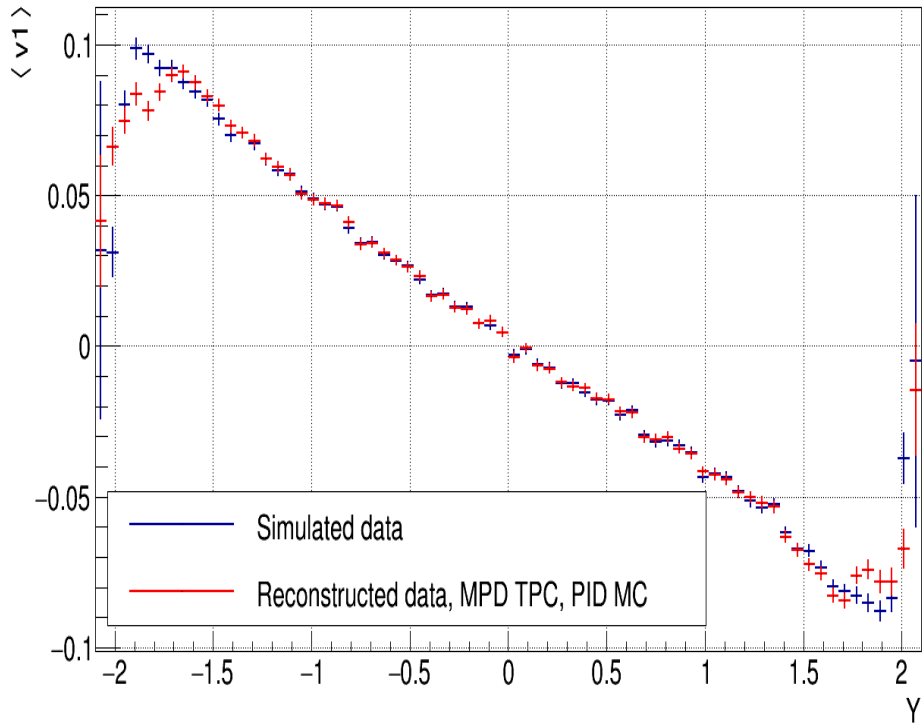
Protons



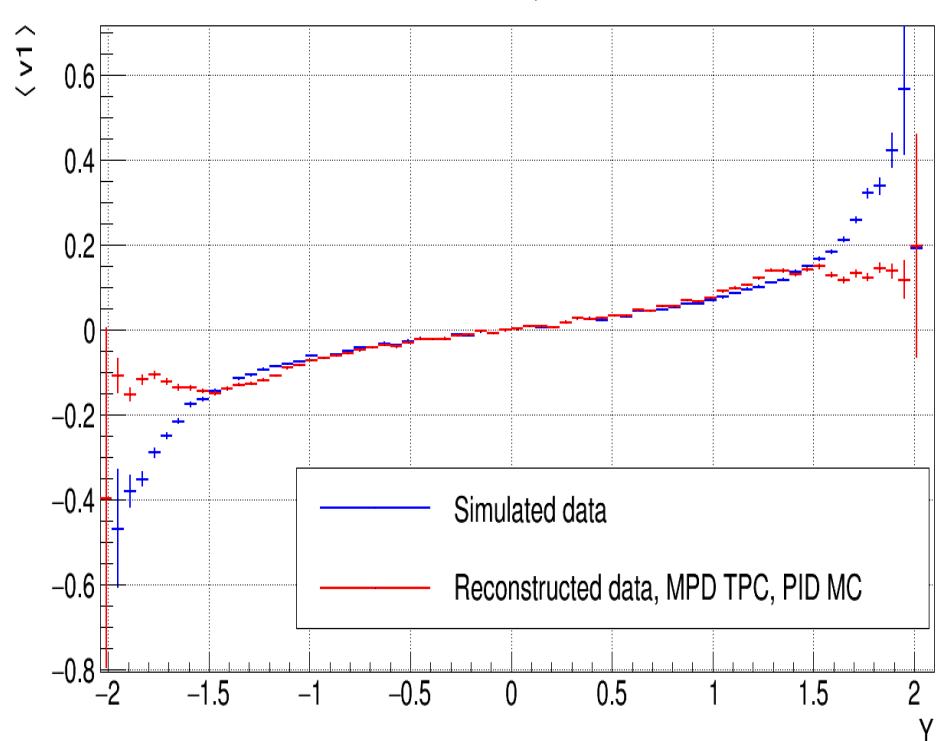
Further results of test simulations – flow observables

Detector Simulation with GEANT : Excellent reproduction of simulation results !

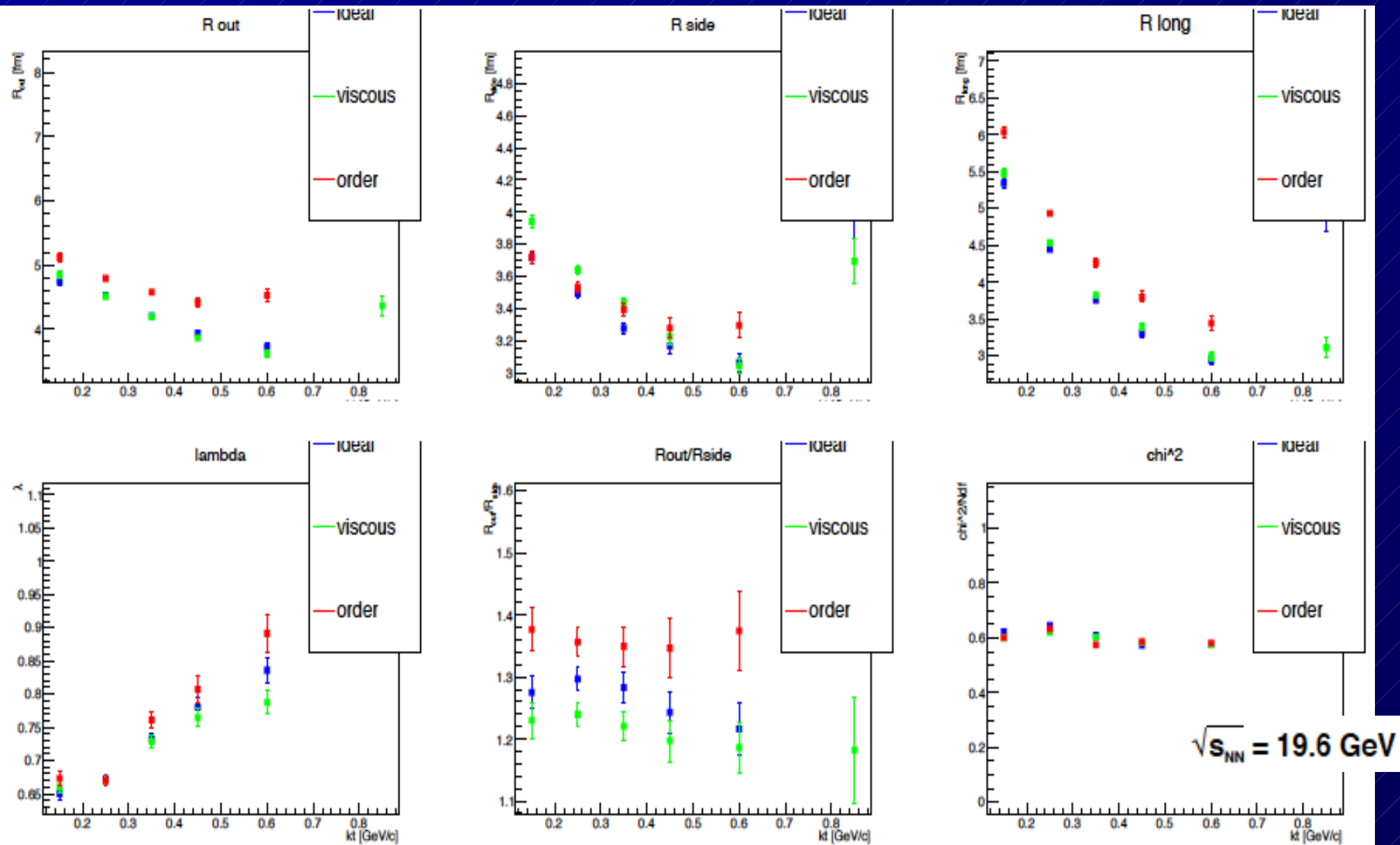
$\langle v_1 \rangle$ vs. Υ , π -mesons, $\sqrt{s_{NN}} = 9$ GeV

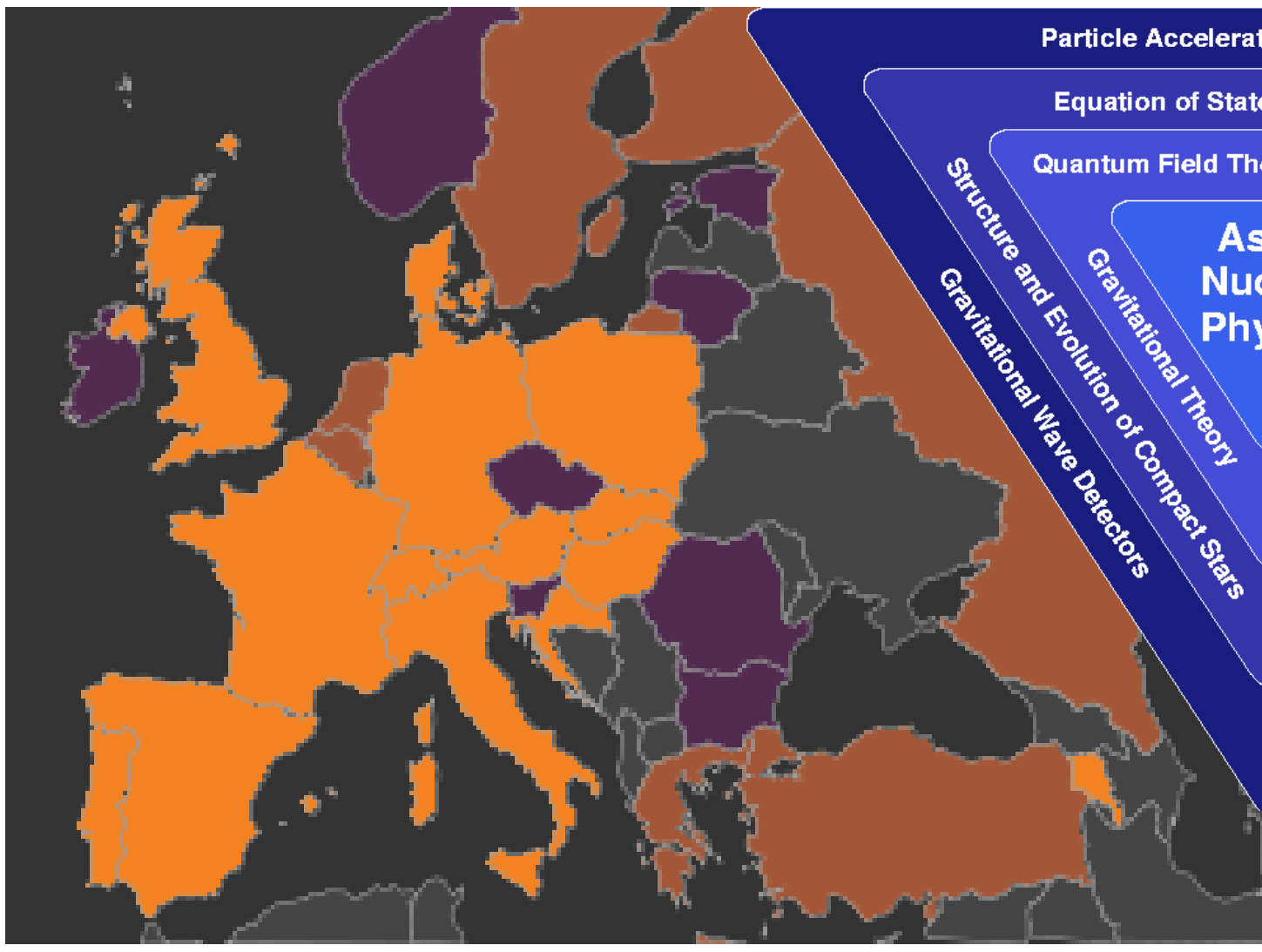


$\langle v_1 \rangle$ vs. Υ , protons, $\sqrt{s_{NN}} = 9$ GeV



Further results of test simulations – HBT radii





Particle Accelerators and Detectors

Equation of State – Phase Diagram

Quantum Field Theory of Dense Matter

Astro– Nuclear– Physics

Structure and Evolution
Gravitational Wave Detectors
Gravitational Theory
Gravitational Evolution of Compact Stars

Astrophysics

Particle Production under Extreme Conditions
Radio- and optical Telescopes; X-ray-, Gamma- Satellites

**28 member
countries !!
(MP1304)**

New
comp
star !



Kick-off: Brussels, November 25, 2013



Critical Point and Onset of Deconfinement 2016

and

Working Group Meeting of COST Action MP1304

Wrocław, Poland

May 30th - June 4th, 2016



Website:

ift.uni.wroc.pl/~cpod2016

Email:

cpod2016@ift.uni.wroc.pl



Uniwersytet
Wrocławski



International advisory committee:

- Francesco Becattini (Florence)
David Blaschke (Wrocław and Dublin)
Xin Dong (Berkeley)
Marek Gaździcki (Frankfurt)
Larry McLerran (Upton)
Edwin Laermann (Bielefeld)
Jeffery Mitchell (Upton)
Krishna Rajagopal (Boston)
Jørgen Randrup (Berkeley)
Dieter Röhrich (Bergen)
Peter Senger (Darmstadt)
Peter Seyboth (Munich)
Edward Shuryak (Stony Brook)
Alexander Sorin (Dubna)
Misha Stephanov (Chicago)
Joachim Stroth (Genf)
Nu Xu (Berkeley)
Daicui Zhou (Wuhan)

Organization committee:

- David Blaschke (Wrocław and Dublin)
Jérôme Margueron (Lyon)
Krzysztof Redlich (Wrocław)
Ludwik Turko (Wrocław)

Local organization committee:

- Tobias Fischer (Wrocław)
Thomas Klaehn (Wrocław)
Pok Man Lo (Wrocław)
Michał Marczenko (Wrocław)
Michał Naskręt (Wrocław)
Chihiro Sasaki (Wrocław)